A Comparison of CDMA and Frequency Hopping in a Cellular Environment

Thesis by

Michael I. Mandell

In Partial Fulfillment of the Requirements

for the Degree of

Doctor of Philosophy

California Institute of Technology

Pasadena, California

1993

(Submitted November 25, 1992)

in memory of my grandfather

Mr. Alex Lankin

Acknowledgments

I don't think that it is truly possible to express in words alone my gratitude and appreciation to the many individuals that have helped and supported me both throughout my career and throughout my life. I consider myself very fortunate to have had Professor Robert J. McEliece as my thesis advisor. Since the day I began this research project, he has always been available to offer advice and encouragement and has generously provided me with all the resources and support necessary to proceed with this research in a timely manner. In addition, he has been an invaluable source of technical knowledge and insight, and has certainly helped inspire many of the ideas expressed in this paper.

I would also like to thank GTE Laboratories and the Air Force Office of Scientific Research for their support of this research. In particular, I wish to express my gratitude towards Dr. John Ketchum and Dr. Mark Wallace, of GTE Laboratories, for having helped inspire this topic of research and also for having provided numerous useful comments and criticisms at several points throughout the last few years.

I also wish to express my gratitude towards those individuals that were willing to be members of my thesis defense committee. These are: Professor Robert J. McEliece, Professor Edward C. Posner, Dr. Marvin K. Simon, Professor Yasser Abu-Mostafa, and Professor Joel Franklin.

Several of the ideas in this thesis have been influenced through discussions with the many friends that I have met here at Caltech. Before I began this research, Kumar Sivarijan is one individual who helped me to get interested in problems related to cellular telephony in the first place. Kumar is a former student of Professor McEliece who was finishing his thesis on frequency assignment algorithms during my first year at Caltech. More recently, I have had the pleasure of working closely with Michihiro Izumi on many of the problems considered in this paper. Michihiro and I have had many valuable technical discussions over the last year, and he has been working to expand upon and generalize many of the ideas presented here. It is also appropriate to mention Petros Mouchtaris and John Murphy. These former Caltech classmates not only listened and discussed many of my technical ideas with me, but have also been very good friends. I also wish to express my gratitude to

my friends that have stood by me and encouraged me since long before I came to Caltech. My years as an undergraduate at The University of Michigan, and even back at Oak Park High School, would not have been the same without the friendship of Gorman Leung, Richard Moceri, Nguyet Nguyen, Ava Udvadia, Mark Fogarasi, and Margaret Yellin. It is not possible to mention all my friends and all the people that have in some way influenced this work, and I apologize to those individuals whose names are omitted.

Finally, I must thank my family for their love and devoted support throughout my life. My parents and grandparents have always been there for me and supported me in every way possible. My siblings and cousins have always given me their encouragement and support. As I mentioned previously, I don't think that it is possible to express my gratitude and appreciation in words alone. I can only hope that the friendship, encouragement, and support that I offer in return is received with equal gratitude and appreciation.

Abstract

This paper compares the performances of Direct Sequence Code Division Multiple Access (CDMA) and Frequency Hopping (FH) schemes in a cellular multiuser environment. Our multiuser channel model incorporates the effects of propagation, frequency selective fading, and interference among users in the presence of a constrained system bandwidth. This channel model is applicable for cellular mobile communications, as well as other forms of personal communications. The CDMA and FH systems are compared using BPSK modulation. The main point of contrast between these systems is that the orthogonal hopping patterns in a FH system result in a decreased additive interference power, however, the frequency spreading nature of CDMA results in both the ability to combat fading, and the ability to effectively use low rate codes. An information-theoretic analysis is presented, and shows that the system capacity is larger for CDMA than for FH. Hence, with sufficient coding the CDMA system can achieve a higher level of performance than the FH system. However, it is unclear what level of complexity would be required to achieve such performance, and what effect such complexity would have on the practicality of the system. Finally, through the use of simulation, the performances of several simple coding schemes are measured and compared to the theoretical limits. These simple coding schemes perform far below the theoretical limits and also display a tradeoff in performance where the FH system performs better at high levels of traffic, and the CDMA system performs better at low levels of traffic.

* This work is supported by a grant from GTE Laboratories and AFOSR Grant 91-0037.

Table of Contents

1. Introduction

In this paper, we compare the performances of Direct Sequence Code Division Multiple Access (CDMA) and Frequency Hopping (FH) in a cellular, multiuser environment. Currently, there is much debate in this field as to what is the best access scheme to use. This problem is complicated by the fact that the cellular channel has many nonideal characteristics that make it difficult to model mathematically. Irregularities in terrain, as well as the elements of an urban environment (such as skyscrapers, bridges, and tunnels) produce a channel with complex multipath fading and shadowing characteristics. In this paper, we take a step back from this problem and attempt to approach it from the point of view of simply comparing CDMA and FH systems. Rather that try to model all the complicated characteristics of the cellular mobile channel, we adopt a rather simplified channel model and analyze the problem from a more "academic" perspective as opposed to an industrial one. The analysis includes many idealizations, and emphasis is placed on trying to find analytic solutions whenever possible. Nevertheless, irrespective of whatever simplifying assumptions are made, these assumptions are applied equally to the analysis of both the CDMA and FH systems. In this sense we have maintained a fair comparison. While these results may not be directly applicable to system engineers building cellular systems, we feel that this is a good theoretical background to the problem and perhaps will give some additional insight into the problem.

We begin in chapter 2 by considering the uncoded performance of these systems in the absence of fading. The geometrical structure of the system is taken to be a grid of hexagonal cells with each cell divided into three 120° sectors. We assume that there is a fixed system bandwidth, B, and a fixed data rate, R, at which each user communicates. Furthermore, we restrict our attention to the reverse link performance (user to cell site) using Binary Phase Shift Keying (BPSK) modulation. In the CDMA system users are assumed to have random, mutually independent, PN sequences. In the FH system, on the other hand, hopping patterns are assumed to be orthogonal among the users in a sector and otherwise random. We define the normalized traffic of a system, p, to be the number of users per sector, N_s, divided by the ratio of B to R. System performance is measured by computing the probability of bit error as a function of the normalized traffic. We observe that, in the absence

of fading and coding, each user of the FH system sees less interference power than in the CDMA system. This is because of the orthogonality of users in each sector of the FH system. We also observe that the distribution of the additive interference in the FH system is quite different in shape from the Gaussian distribution in the CDMA system. This results in a tradeoff in performance; the FH system performs better at higher levels of traffic with relatively high probability of bit error, and the CDMA system performs better at lower levels of traffic with relatively low probability of bit error.

Next, we focus our attention in chapter 3 on the nature of the frequency selective fading of the channel. We develop a general channel model based on the model described in ([1], pg. 705). This channel model is then applied to both the FH and CDMA systems, and the analysis of chapter 2, in the absence of coding, is carried out accounting for these additional parameters. We find that the FH system still sees less interference power than the CDMA system. However, it is susceptible to frequency selective fades, whereas the wideband nature of CDMA offers a level of resistance to such fading. Again, a tradeoff in performance exists where the FH system performs better at higher levels of traffic with relatively high probability of bit error, and the CDMA system performs better at lower levels of traffic with relatively low probability of bit error. We also observe that the distribution of the additive interference in the FH system is considerably smoothed out by the fading and results in a system performance not much different than if the additive noise had a Gaussian distribution at the same power level.

In chapter 4, we consider the use of coding and show that using a code of rate r_{code} at a level of normalized traffic p, each codeword symbol sees a channel similar to the uncoded channel, but with an effective coded normalized traffic, $\bar{p}$, given by p/r_{code}. In other words, if a rate 1/2 code were used, each codeword symbol would see a channel that appears to have twice as many interfering users than there actually are, and thus, a correspondingly higher level of interference power. For the FH system, the requirement that the users in a sector maintain orthogonality restricts the value of $\bar{p}$ to be less than one. For the CDMA system, however, there is no corresponding restriction on $\bar{p}$. Assuming that there is no cooperation among the users in the system on the level of coding, we

apply an information-theoretic analysis to the system models that we have developed. The capacity of the system is defined to be the largest possible value of normalized traffic, p, for which each user in the system can communicate reliably at rate R. The capacity of FH and CDMA are computed and we find that the CDMA system has a larger capacity. This is due to the fact that the requirement, $\bar{p} \leq 1$, for the FH system does not allow for the effective use of very low code rates. It turns out that, from an information-theoretic viewpoint, the ability of CDMA to use low rate codes is an advantage over the lower interference power in the FH system. Having thus obtained this information-theoretic channel model, we consider the effects on capacity of fading versus nonfading channels; soft decision versus hard decision decoding; and BPSK versus multilevel modulation.

The information-theoretic results of the previous chapter give the best possible system performance that can be achieved using arbitrarily complicated coding schemes. Unfortunately, arbitrarily complex codes include arbitrarily long block lengths, and thus, arbitrarily long delays. In chapter 5, we investigate the performance of specific coding schemes and the effects of a finite, controlled, delay using interleaving. These results are obtained primarily through simulation. We begin by looking at repetition codes and then consider binary block codes. For a specific code, it is possible to measure the performance for infinite interleaving and zero interleaving. To evaluate the performance using infinite interleaving, it is assumed that each codeword symbol sees independent channel statistics. On the other hand, the performance using zero interleaving is evaluated by assuming that each codeword symbol sees an identical, 100% correlated, channel. Finally, making some assumptions about the vehicle speed and transmitter frequency, we evaluate performance using a finite amount of interleaving delay by taking into account the actual amount of correlation among channel samples as seen from one codeword symbol to the next. We have evaluated the performance of several repetition codes as well as an (8,4) biorthogonal block code. These coding schemes perform far below information-theoretic capacity, and yield performance curves for FH and CDMA that cross with FH performing better at higher levels of traffic with relatively high probability of bit error, and the CDMA performing better at lower levels of traffic with relatively low probability of bit error.

Chapter 6 is not closely related to the rest of this paper. Here we look at the information-

theoretic problem of interference channels when there is no assumption that users do not cooperate on the level of coding. Very few results in the area of multiuser information theory are known. Some examples are shown of relatively simple two-user systems where the capacity region is currently unknown.

In chapter 7, we try to see what conclusions one can reach from the results of the previous sections. We have seen that an information-theoretic capacity can by defined, and that using BPSK in a fading environment CDMA has a larger capacity than FH. However, for the codes we have simulated it is unclear which system performs better because the performance curves cross. We conclude with some ideas on how this research can be further improved and expanded upon.

2. Nonfading Channel

2.1 Introduction

In this chapter, we compute the average probability of bit error for FH and CDMA using Binary Phase Shift Keying (BPSK) modulation over a nonfading channel. We assume that there is a fixed system bandwidth, B, and a fixed data rate, R, at which each user communicates. A sectored hexagonal cell system is used as shown in figure 2.1. Each cell is divided into 3 sectors labeled 0,1, and 2 as shown. The 3-tuple (i, j, s) refers to sector s of cell (i, j). In appendix A.1, some basic properties of this cellular geometry are derived. We consider the reverse link, mobile to base.

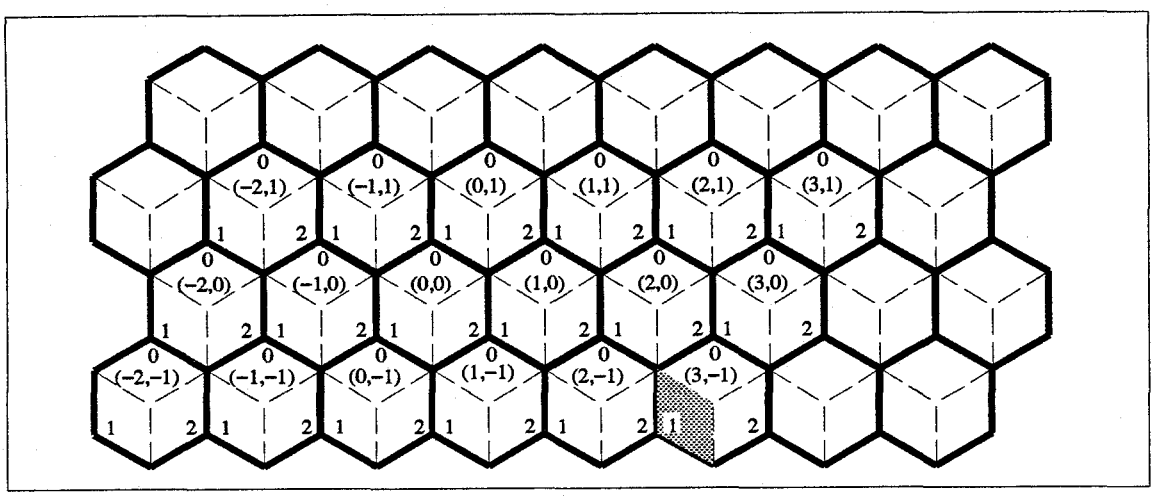

Figure 2.1: *Sectored hexagonal grid. The shaded sector is sector 1 of cell (3,-1).*

We begin with some basic assumptions regarding system operation that apply to both FH and CDMA throughout this paper.

(1) Power control is maintained such that each mobile is received at its corresponding base station at the same power level. Without loss of generality, we assume that this power level is unity.

(2) R^{-4} propagation loss in power.

(3) $G(\phi) =$ antenna gain at angle ϕ.

(4) Uniformly distributed users.

(5) Background noise is negligible and only interference from other users is considered.

(6) The effects of co-channel interference are not considered.

(7) Total system bandwidth $\gg$ data rate at which each user communicates.

Next, we define some parameters that apply to both FH and CDMA throughout this paper. Let

$B =$ Total system bandwidth (Hz),

$R =$ Rate at which each user communicates (bps),

$N_s =$ Number of users per sector,

$N = B/R$ is the total number of available frequency channels in a FH system and also the spread factor, or processing gain, ([2], pg. 5) in a CDMA system,

$p = N_s/N$ is the normalized traffic,

$T_b = 1/R$ is the bit time,

$T_c = 1/B$ is the chip time in a CDMA system.

$\Delta = (i, j, s)$ represents sector s of cell (i, j),

$\bar{0} = (0, 0, 0)$ represents sector 0 of cell $(0, 0)$.

Remark. For simplicity, we are assuming that a digital source at rate W (bps) can be transmitted using BPSK in a bandwidth of W (Hz). However, since this is assumed for both the FH and CDMA systems, there is no loss of generality from the standpoint of comparison between systems.

2.2 Analysis of FH System

We begin by computing the probability of bit error for a FH system and a nonfading channel. In the FH system, the total system bandwidth, B, is divided into N frequency channels, each having bandwidth R. The frequency hopping is assumed to be slow in the sense that the time between successive hops is larger than the bit time, T_b. We assume random orthogonal hopping patterns among the users in each sector. That is, on each hop the $N(N-1)(N-2)\ldots(N-N_s+1)$ possible assignments of distinct frequency channels to the N_s users in a sector are equally likely. Note that inherent in this assumption is that synchronization of hopping times is maintained among the users in a sector. Also note that the assumption of orthogonality implies $N_s \leq N$, hence the normalized

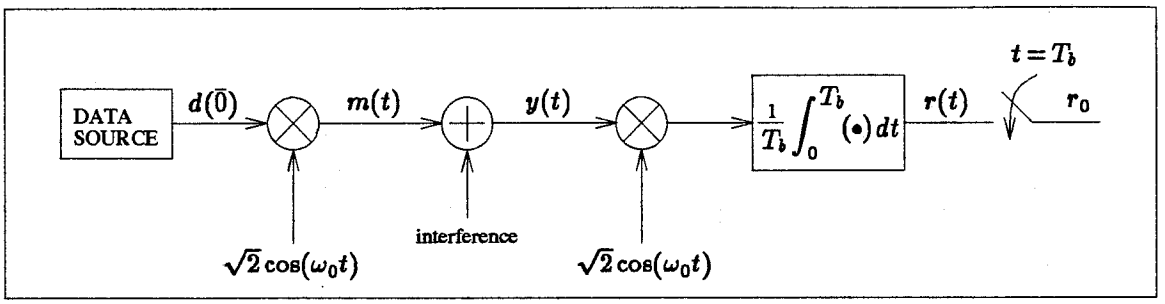

Figure 2.2: *Equivalent BPSK system using FH for communication from a single user in sector* $\bar{0}$ *transmitting on a channel at frequency* ω_0 *to the corresponding base-station receiver.*

traffic satisfies

$$p \leq 1. \tag{2.1}$$

Similar systems have been considered in [3] and [4].

Figure 2.2 shows a BPSK system for a single user in sector $\bar{0}$ transmitting on a channel at frequency ω_0. Since hopping patterns are orthogonal within each sector, interference is due to the users in other sectors. To analyze this system, it is useful to define the following random variables. For each sector Δ, let

$\chi(\Delta) = \begin{cases} 1 & \text{if there is a user in sector } \Delta \text{ at } \omega_0 \text{ (prob } p\text{)}, \\ 0 & \text{otherwise (prob } 1-p\text{)}, \end{cases}$

$d(\Delta) =$ data bit of user in sector Δ that is transmitting on the channel at frequency ω_0 (± 1 equally likely),

$\theta(\Delta) =$ relative phase of user in sector Δ that is transmitting on the channel at frequency ω_0 (uniformly distributed on interval 0 to 2π),

$\bar{r}(\Delta) =$ random position uniformly distributed over sector Δ,

$P(\bar{r}(\Delta)) =$ relative power received by antenna in sector $\bar{0}$ from an interfering user at position $\bar{r}$ in sector Δ.

Consider the transmission of a single bit through the system. For $t \in (0, T_b)$,

$$y(t) = \sqrt{2}\, d(\bar{0}) \cos(\omega_0 t) + \sum_{\Delta \neq \bar{0}} \chi(\Delta) \sqrt{2P(\bar{r}(\Delta))}\, d(\Delta) \cos(\omega_0 t + \theta(\Delta)). \tag{2.2}$$

The sample at the output of the receiver, r_0, is thus given by

$$r_0 = \underbrace{d(\bar{0})}_{r_{\text{signal}}} + \underbrace{\sum_{\Delta \neq \bar{0}} \chi(\Delta)\sqrt{P(\bar{r}(\Delta))}\, d(\Delta)\cos(\theta(\Delta))}_{r_{\text{noise}}}, \tag{2.3}$$

which is composed of a signal part due to the transmitted data bit, and a noise part due to other interfering users in the system. The random variable r_{noise}, given by

$$r_{\text{noise}} = \sum_{\Delta \neq \bar{0}} \chi(\Delta)\sqrt{P(\bar{r}(\Delta))}\, d(\Delta)\cos(\theta(\Delta)), \tag{2.4}$$

is a sum of independent random variables each having mean zero. Thus,

$$\text{Mean}(r_{\text{noise}}) = 0, \tag{2.5}$$

$$\begin{aligned} \text{Var}(r_{\text{noise}}) &= \text{E}\{r_{\text{noise}}^2\}, \\ &= \sum_{\Delta \neq \bar{0}} \underbrace{\text{E}\{\chi^2(\Delta)\}}_{p} \text{E}\{P(\bar{r}(\Delta))\} \underbrace{\text{E}\{\cos^2(\theta(\Delta))\}}_{\frac{1}{2}}, \\ &= \frac{p}{2} \sum_{\Delta \neq \bar{0}} \text{E}\{P(\bar{r}(\Delta))\}, \\ &= \frac{1}{2} ap, \end{aligned} \tag{2.6}$$

where the interference parameter, a, is defined as

$$a = \sum_{\Delta \neq \bar{0}} \text{E}\{P(\bar{r}(\Delta))\}. \tag{2.7}$$

This parameter a is of central importance in our analysis. $P(\bar{r}(\Delta))$ is a function of the random variable $\bar{r}(\Delta)$. Thus, the expectation in equation (2.7) is over the probability distribution of $\bar{r}(\Delta)$. In appendix A.2, a is computed numerically for a uniform distribution on $\bar{r}(\Delta)$, and an antenna gain $G(\phi)$ that is constant over a 120° beam width and 20db below this at other angles. We find $a = 0.46$. Note that for non-uniform traffic, $\bar{r}(\Delta)$ has a non-uniform distribution, and the expectation in (2.7) is over an arbitrary probability distribution on $\bar{r}(\Delta)$. Hence, it is straightforward to extend these results to the case of non-uniform traffic. The value of a is a measure of interference inherent in the system and plays an important role in the analysis of both FH and CDMA systems. Note that the

value of a depends on 4 things:

(1) cellular geometry (sectored hexagonal grid),

(2) propagation loss (R^{-4}),

(3) antenna gain (constant over a 120° beam width and 20db below this at other angles),

(4) distribution of traffic (uniform).

The random variable r_{noise}, is a sum of a large number of independent random variables, but unfortunately the random variables in this sum are not identically distributed. Thus, the Central Limit Theorem cannot be applied here to conclude that r_{noise} is approximately Gaussian. If r_{noise} were in fact Gaussian, since the mean and variance of r_{noise} have been computed, we could write the marginal probability of bit error, P_b, as

$$P_b[\text{No Fading, Gaussian}] = \frac{1}{2}\text{erfc}\left(\sqrt{\frac{1}{ap}}\right). \tag{2.8}$$

This is equivalent to the result given in ([1], pg. 717) for communication over a nonfading Gaussian channel. Figure 2.3 shows plots of the probability of bit error versus the normalized traffic by simulating the exact distribution of r_{noise} and also the result of equation (2.8) for Gaussian noise. We see that these curves differ by many orders of magnitude so that in general the additive noise in the FH system in the absence of fading is very different from Gaussian and yields a much higher probability of bit error.

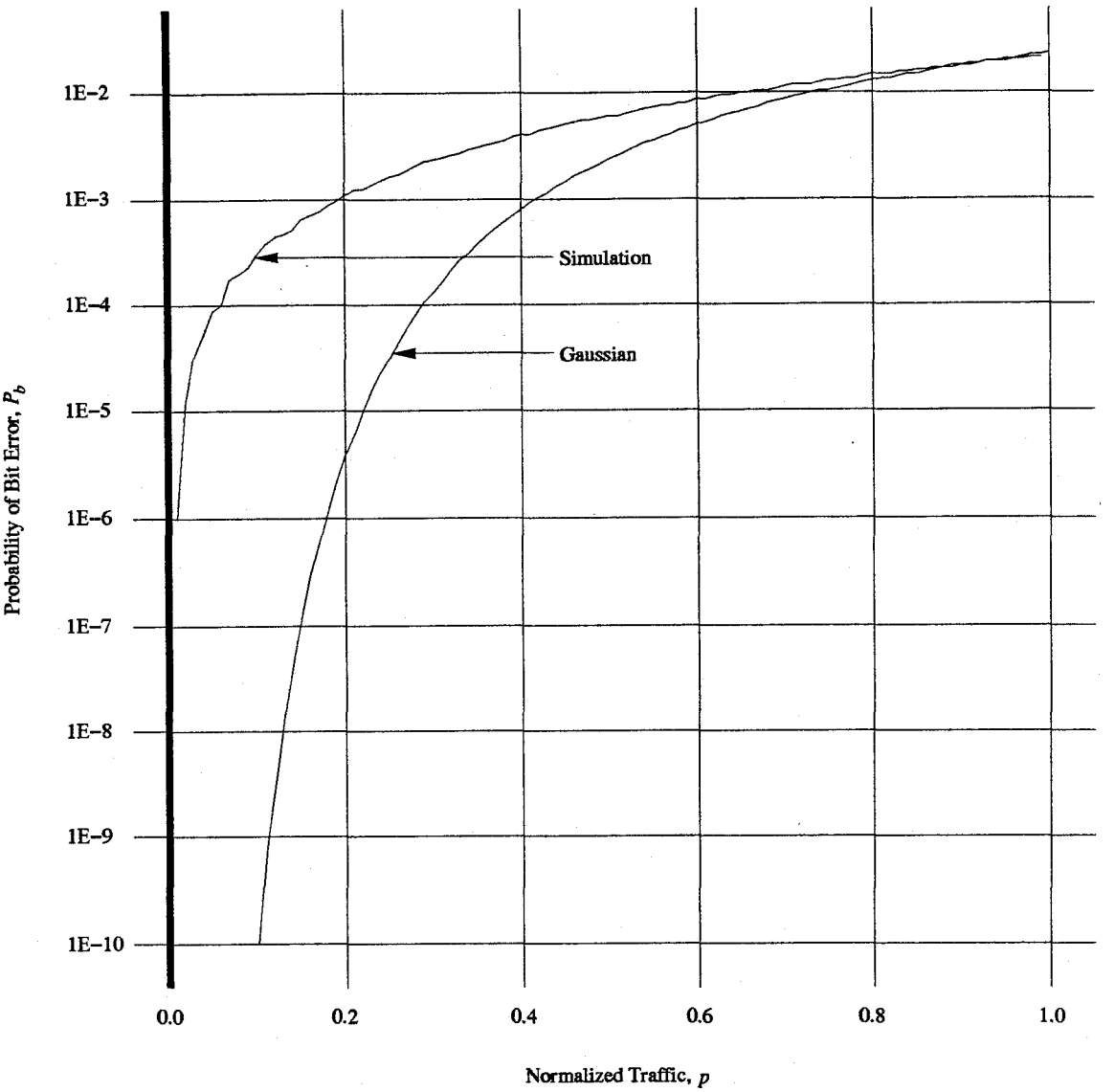

Figure 2.3: *Probability of bit error versus normalized traffic for FH system in a nonfading environment. Curves are shown for the exact distribution of additive noise, determined by simulation, and for Gaussian additive noise.*

2.3 Analysis of CDMA System

Next, we compute the probability of bit error for a CDMA system and a nonfading channel. Each of the N_s users in a sector are indexed by a number $k \in [0, N_s - 1]$. Figure 2.4 shows a CDMA system for user 0 in sector $\bar{0}$. The transmitter multiplies the data signal by a pseudorandom (PN) sequence and the result is used to modulate a sinusoidal carrier ([2], pg. 5). Since the PN sequence generates a symbol every T_c seconds, the signal of each user is spread over the entire system bandwidth, B. It is assumed that each user has a random PN sequence, and that PN sequences are mutually independent. Note that the CDMA spread factor, $N = B/R$, is equivalent to the number of available frequency channels in the FH system, and is assumed to be large. To analyze this system, it is useful to define the following random variables. For each user in the system, let

$d_k(\Delta) =$ data bit of user $k \in [0, N_s - 1]$ in sector Δ (± 1 equally likely),

$c_k(\Delta, m) =$ mth chip ($m \in [0, N - 1]$) in PN sequence for user k in sector Δ (± 1 equally likely),

$\theta_k(\Delta) =$ relative phase of user k in sector Δ (uniformly distributed on interval 0 to 2π),

$\bar{r}_k(\Delta) =$ position of user k in sector Δ,

$P(\bar{r}_k(\Delta)) =$ relative power received by antenna in sector $\bar{0}$ from an interfering user at position $\bar{r}_k$ in sector Δ.

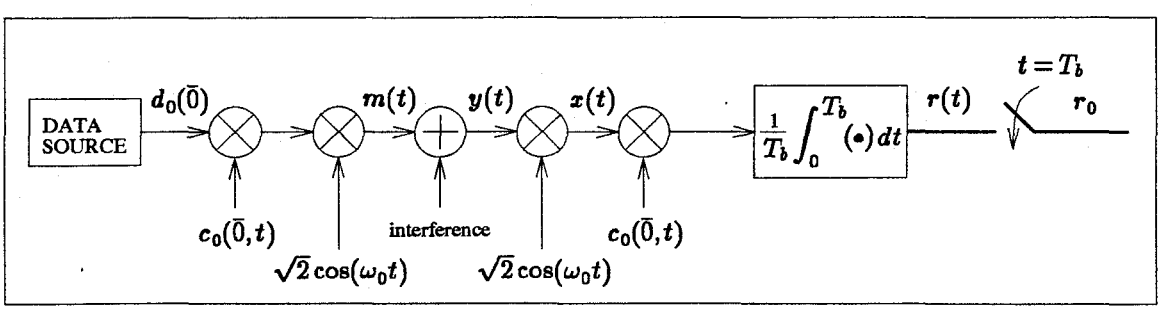

Figure 2.4: *Equivalent BPSK system using CDMA for communication from user 0 in sector $\bar{0}$ to the corresponding base-station receiver. The value of ω_0 is taken to be the center frequency of the system bandwidth B.*

Consider the transmission of a single bit through the system. For $t \in (0, T_b)$, the PN sequences are given by

$$c_k(\Delta, t) = c_k(\Delta, m), \quad \text{where} \quad mT_c < t < (m+1)T_c. \tag{2.9}$$

The receiver input, $y(t)$, is given by

$$y(t) = \sqrt{2}\, d_0(\bar{0}) c_0(\bar{0}, t) \cos(\omega_0 t) + \sum_{(\Delta,k)\neq(\bar{0},0)} \sqrt{2P(\bar{r}_k(\Delta))}\, d_k(\Delta) c_k(\Delta, t) \cos(\omega_0 t + \theta_k(\Delta)). \tag{2.10}$$

Performing the demodulation of $y(t)$ by multiplication by $\sqrt{2}\cos(\omega_0 t)$ and neglecting second harmonics of ω_0 gives

$$x(t) = d_0(\bar{0}) c_0(\bar{0}, t) + \sum_{(\Delta,k)\neq(\bar{0},0)} \sqrt{P(\bar{r}_k(\Delta))}\, d_k(\Delta) c_k(\Delta, t) \cos(\theta_k(\Delta)). \tag{2.11}$$

The sample at the output of the receiver, r_0, is thus given by

$$r_0 = \underbrace{d_0(\bar{0})}_{r_{\text{signal}}} + \underbrace{\sum_{(\Delta,k)\neq(\bar{0},0)} \sqrt{P(\bar{r}_k(\Delta))}\, d_k(\Delta) \cos(\theta_k(\Delta)) \frac{T_c}{T_b} \sum_{m=0}^{N-1} c_k(\Delta, m)\, c_k(\bar{0}, m)}_{r_{\text{noise}}}, \tag{2.12}$$

which, like the corresponding sample in the FH system given by equation (2.3), is composed of a signal part due to the transmitted data bit, and a noise part due to other interfering users in the system. The random variable r_{noise} is given by

$$r_{\text{noise}} = \sum_{(\Delta,k)\neq(\bar{0},0)} \sqrt{P(\bar{r}_k(\Delta))} \cos(\theta_k(\Delta)) \frac{T_c}{T_b} \sum_{m=0}^{N-1} d_k(\Delta)\, c_k(\Delta, m)\, c_k(\bar{0}, m). \tag{2.13}$$

Let

$$b_k(\Delta, m) = \frac{d_k(\Delta)\, c_k(\Delta, m)\, c_k(\bar{0}, m) + 1}{2} = \begin{cases} 1 & \text{prob} = 0.5, \\ 0 & \text{prob} = 0.5, \end{cases} \tag{2.14}$$

and

$$B_k(\Delta) = \sum_{m=0}^{N-1} b_k(\Delta, m). \tag{2.15}$$

The random variables $B_k(\Delta)$ are *i.i.d.* Binomial random variables ([5], pg. 223) with mean $= N/2$ and variance $= N/4$. Now we can express r_{noise} as

$$\begin{aligned} r_{\text{noise}} &= \sum_{(\Delta,k)\neq(\bar{0},0)} \frac{1}{N} \sqrt{P(\bar{r}_k(\Delta))} \cos(\theta_k(\Delta)) \sum_{m=0}^{N-1} (2b_k(\Delta, m) - 1), \\ &= \sum_{(\Delta,k)\neq(\bar{0},0)} \frac{2}{N} \sqrt{P(\bar{r}_k(\Delta))} \cos(\theta_k(\Delta)) \left(B_k(\Delta) - \frac{N}{2} \right). \end{aligned} \tag{2.16}$$

The random variable r_{noise} is a sum of independent random variables each having mean zero similar to the corresponding random variable in the FH system given by equation (2.4). Thus,

$$\text{Mean}(r_{\text{noise}}) = 0, \tag{2.17}$$

$$\begin{aligned}
\text{Var}(r_{\text{noise}}) &= \text{E}\{r_{\text{noise}}^2\}, \\
&= \sum_{(\Delta,k)\neq(\bar{0},0)} \frac{4}{N^2} P(\bar{r}_k(\Delta)) \underbrace{\text{E}\left\{\cos^2(\theta_k(\Delta))\right\}}_{\frac{1}{2}} \underbrace{\text{E}\left\{\left(B_k(\Delta) - \frac{N}{2}\right)^2\right\}}_{\frac{N}{4}}, \\
&= \frac{1}{2N} \sum_{(\Delta,k)\neq(\bar{0},0)} P(\bar{r}_k(\Delta)), \\
&= \frac{1}{2N}\left[\sum_{k=1}^{N_s-1} P(\bar{r}_k(\bar{0})) + \sum_{\Delta\neq\bar{0}} \sum_{k=0}^{N_s-1} P(\bar{r}_k(\Delta))\right], \\
&= \frac{1}{2N}\left[(N_s-1) + N_s \sum_{\Delta\neq\bar{0}} \text{E}\{P(\bar{r}(\Delta))\}\right], \\
&\simeq \frac{1}{2}(a+1)p.
\end{aligned} \tag{2.18}$$

The interference parameter, a, is defined by equation (2.7). Note that the assumption of power control implies $P(\bar{r}_k(\bar{0})) = 1$ for each user in sector $\bar{0}$. We have also made use of the fact that since the users in each sector are uniformly distributed,

$$\sum_{k=0}^{N_s-1} P(\bar{r}_k(\Delta)) = N_s \text{E}\{P(\bar{r}(\Delta))\} \tag{2.19}$$

where $\bar{r}(\Delta)$ is a random position uniformly distributed over sector Δ. For the CDMA system, the additive noise, r_{noise}, is in fact well approximated using a Gaussian distribution. Thus, having computed the mean and variance of r_{noise}, we can write the marginal probability of bit error as

$$P_b[\text{No Fading}] = \frac{1}{2}\text{erfc}\left(\sqrt{\frac{1}{(a+1)p}}\right). \tag{2.20}$$

Remark. For the FH system, the additive noise given by equation (2.4) is due to at most one user in each sector. Thus, the total interference is due to a relatively small number of other users in the neighboring sectors. On the other hand, for the CDMA system the additive interference given by equation (2.13) is due to *all* other users in every sector. Thus, the additive interference in the CDMA system is effectively smoothed out over each cell in the system, making the distribution look

more like a Gaussian. Further justification for the Gaussian assumption in the CDMA system can be found in [6] and ([2], pg. 9).

2.4 Nonfading Channel Results

With respect to equations (2.3) and (2.12), both the FH and CDMA systems produce a receiver output, Y, of the form

$$Y = X + Z, \tag{2.21}$$

where

$$X = \pm 1 \text{ data bit transmitted,}$$

$$Z = \text{zero-mean additive noise.}$$

Equations (2.6) and (2.18) imply that the variance of the additive noise, Z, is

$$\text{Var}(Z) = \begin{cases} \frac{1}{2}ap & \text{for FH,} \\ \frac{1}{2}(a+1)p & \text{for CDMA.} \end{cases} \tag{2.22}$$

Figure 2.5 shows a plot of the average probability of bit error versus the normalized traffic for FH and CDMA systems. The FH performance curve was found by simulating the additive noise statistics of equation (2.4). The CDMA performance curve is given by equation (2.20). The performance curve for the FH system if the noise is Gaussian, given by equation (2.8), is also shown. We see that the simulated FH curve and the CDMA curve cross with CDMA performing better at lower levels of traffic and FH performing better at higher levels of traffic. At higher levels of traffic the FH simulation curve gets close to the FH Gaussian curve, which is always below the CDMA curve because of the fact that there is less interference power in the FH system. Since $a \simeq 1/2$, about 2/3 of the interference power seen by the CDMA system is from users in the same sector, while the orthogonal hopping patterns in the FH system ensure that no interference power is seen from the same sector. Thus, it seems that the better performance of FH at higher levels of traffic is due to the fact that there is less interference power in the FH system. On the other hand, the better performance of CDMA at lower levels of traffic must be related to the fact that the FH noise becomes significantly different from a Gaussian at low levels of traffic. Figure 2.5 does not, however, show

the main advantage of a CDMA system which is its ability to perform in a frequency selective fading environment. In chapter 3, the methods of analysis applied in this chapter are extended to treat a frequency selective fading channel.

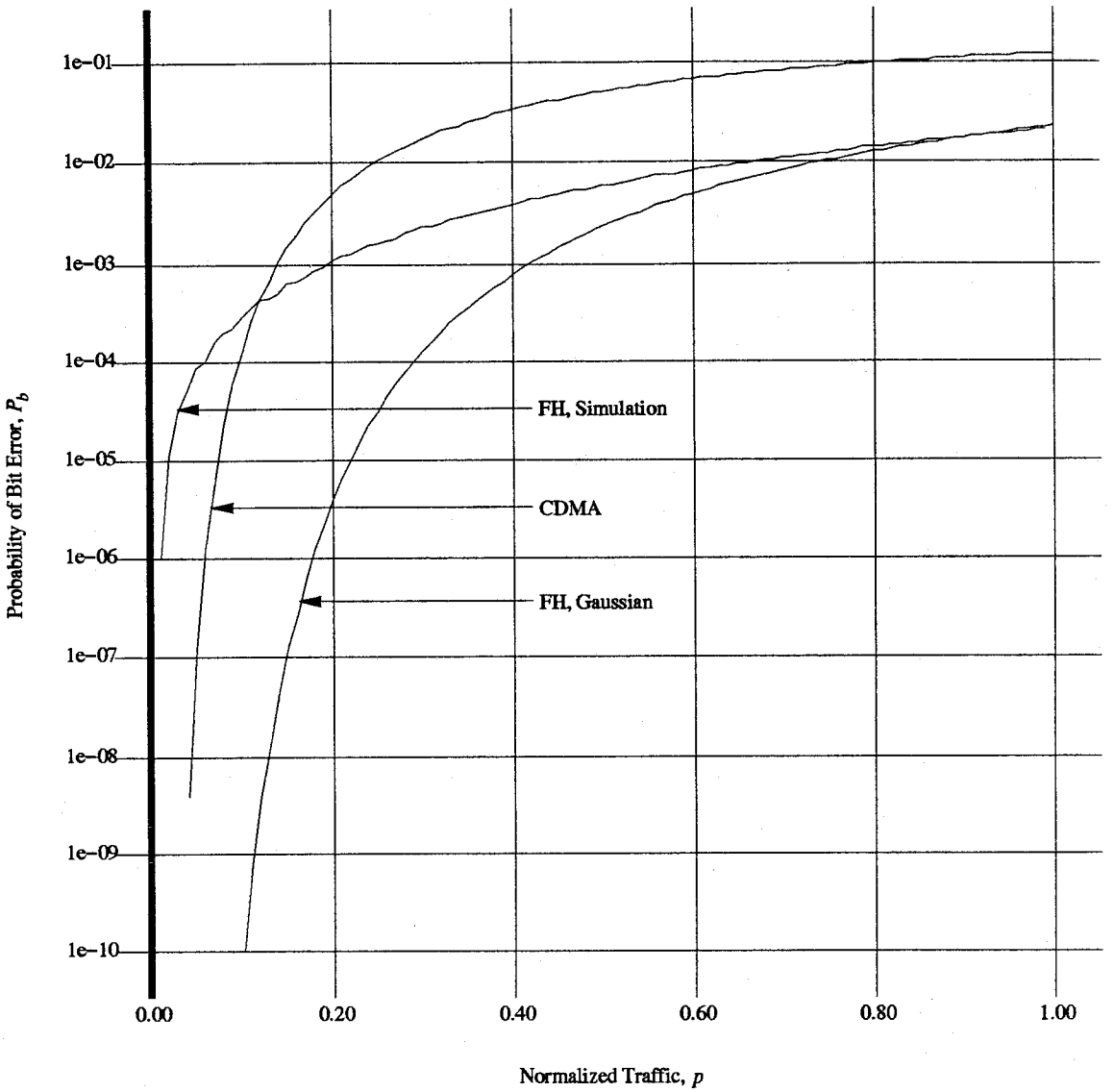

Figure 2.5: *Probability of bit error versus normalized traffic for FH and CDMA systems in a nonfading environment. For the FH system, curves are shown for the exact distribution of additive noise, determined by simulation, and for Gaussian additive noise.*

3. Fading Channel

3.1 Rayleigh Fading Channel Model

In this chapter, we compute the average probability of bit error for FH and CDMA using Binary Phase Shift Keying (BPSK) modulation over a frequency selective Rayleigh fading channel. We begin by developing a general channel model that can be used for both FH and CDMA systems. Figure 3.1 shows the transmission of a complex baseband signal, $u(t)$, over a fading channel.

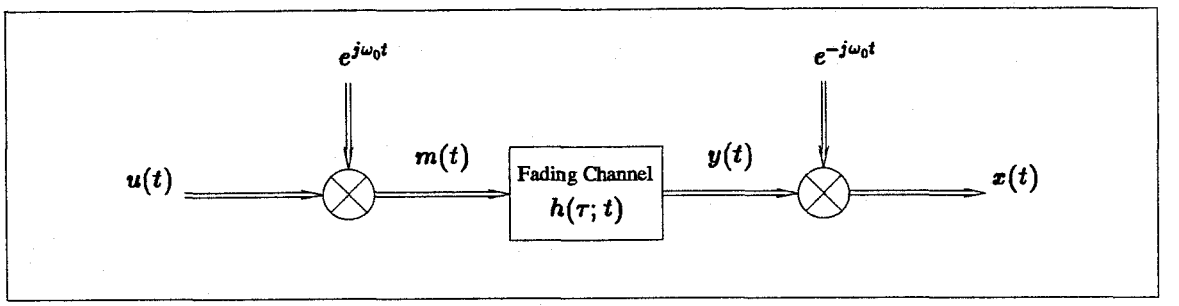

Figure 3.1: *Transmission of complex baseband signal, $u(t)$, over a fading channel.*

The channel is described by a time-variant impulse response, $h(\tau;t)$, which is the response of the channel at time t to an impulse at time $t-\tau$. The channel response, $h(\tau;t)$, is modelled as a zero-mean complex-valued Gaussian random process ([1], pg. 705). The following assumptions are made regarding the characteristics of the fading channel.

(1) Channel response is due to uncorrelated scattering.

(2) Multipath delay spread, T_m, satisfies $T_m \ll T_b$.

(3) Coherence time of the channel is sufficiently slow so that the channel parameters, $\mathcal{A}_W(n,\omega_0;t)$, remain constant over many bits and can be measured by the receiver.

If the midband signal, $m(t)$, has bandwidth W (Hz), the baseband signal, $u(t)$, must be bandlimited to $W/2$. Hence, the function $u(t-\tau)$ can be expressed as a sampling expansion ([7], pg. 522) in the variable τ, sampled at rate W (samples/sec). This gives

$$u(t-\tau) = \sum_{n=-\infty}^{\infty} u\left(t-\frac{n}{W}\right)\mathrm{sinc}(n-W\tau), \tag{3.1}$$

where the sinc function is defined as

$$\mathrm{sinc}(x) = \frac{\sin(\pi x)}{\pi x}. \tag{3.2}$$

The baseband received signal, $x(t)$, is then given by

$$\begin{aligned} x(t) &= e^{-j\omega_0 t}\left[h(\tau;t) * \left(u(t)e^{j\omega_0 t}\right)\right], \\ &= e^{-j\omega_0 t}\left[\int_{-\infty}^{\infty} h(\tau;t)u(t-\tau)e^{j\omega_0(t-\tau)}\,d\tau\right], \\ &= \int_{-\infty}^{\infty} h(\tau;t)u(t-\tau)e^{-j\omega_0\tau}\,d\tau, \\ &= \sum_{n=-\infty}^{\infty} u\left(t-\frac{n}{W}\right)\int_{-\infty}^{\infty} h(\tau;t)\,\mathrm{sinc}(n-W\tau)e^{-j\omega_0\tau}\,d\tau, \\ &= \sum_{n=-\infty}^{\infty} u\left(t-\frac{n}{W}\right)\mathcal{A}_W(n,\omega_0;t), \end{aligned} \tag{3.3}$$

where the channel parameters, $\mathcal{A}_W(n,\omega_0;t)$, are defined as

$$\mathcal{A}_W(n,\omega_0;t) = \int_{-\infty}^{\infty} h(\tau;t)\,\mathrm{sinc}(n-W\tau)e^{-j\omega_0\tau}\,d\tau. \tag{3.4}$$

Since the channel response, $h(\tau;t)$, is taken to be a complex Gaussian random process, the channel parameters, $\mathcal{A}_W(n,\omega_0;t)$, are also complex Gaussian random processes. Let the magnitude and phase of $\mathcal{A}_W(n,\omega_0;t)$ be given by

$$A_W(n,\omega_0;t) = |\mathcal{A}_W(n,\omega_0;t)|, \tag{3.5}$$

$$\phi_W(n,\omega_0;t) = \mathrm{Arg}\left(\mathcal{A}_W(n,\omega_0;t)\right). \tag{3.6}$$

Then, $A_W(n,\omega_0;t)$ and $\phi_W(n,\omega_0;t)$ are independent, $A_W(n,\omega_0;t)$ is Rayleigh distributed, and $\phi_W(n,\omega_0;t)$ is uniformly distributed on $(0,2\pi)$.

The fading process is assumed to undergo uncorrelated scattering. This means that, for $\tau_1 \neq \tau_2$, the responses of the channel at time t to impulses at times $t-\tau_1$ and $t-\tau_2$ respectively are uncorrelated ([1], pg. 706). Mathematically, this is expressed as

$$\mathrm{E}\left\{h^*(\tau_1;t_1)h(\tau_2;t_2)\right\} = \phi_c(\tau_1)g(t_2-t_1)\delta(\tau_2-\tau_1). \tag{3.7}$$

The function $\phi_c(\tau)$ is the multipath-intensity profile of the channel, and is assumed to be normalized such that

$$\int_{-\infty}^{\infty} \phi_c(\tau)\,d\tau = 1. \tag{3.8}$$

The multipath delay spread, T_m, is defined to be the range of values over which $\phi_c(\tau)$ is essentially nonzero ([1], pg. 707). The function $g(\Delta t)$ characterizes the manner in which the channel response, $h(\tau;t)$, is changing as a function of time, and thus depends on the vehicle speed and the frequency at which the mobile transmits. It is shown in ([8], pg. 26) that if the power received from the mobile is transmitted uniformly in all directions, then

$$g(\Delta t) = \mathrm{J}_0\left(\frac{v\,\omega_0}{c}\Delta t\right), \tag{3.9}$$

where J_0 is the Bessel function of order zero, v is the mobile's velocity, ω_0 is the transmitted frequency, and c is the speed of light.

The channel parameters $\mathcal{A}_W(n,\omega_0;t)$ and $\mathcal{A}_W(m,\omega_0;t)$ are, in general, not uncorrelated. Covariances among the channel parameters can be computed using (3.4). This gives

$$\begin{aligned}
\rho_{nm} &= \mathrm{E}\left\{\mathcal{A}_W^*(n,\omega_0;t)\mathcal{A}_W(m,\omega_0;t)\right\}, \\
&= \mathrm{E}\left\{\int_{-\infty}^{\infty}\int_{-\infty}^{\infty} h(\tau_1;t)h^*(\tau_2;t)\,\mathrm{sinc}(n-W\tau_1)\,\mathrm{sinc}(m-W\tau_2)\,d\tau_1\,d\tau_2\right\}, \\
&= \int_{-\infty}^{\infty}\int_{-\infty}^{\infty} \phi_c(\tau_1)g(0)\delta(\tau_2-\tau_1)\,\mathrm{sinc}(n-W\tau_1)\,\mathrm{sinc}(m-W\tau_2)\,d\tau_1\,d\tau_2, \\
&= \int_{-\infty}^{\infty} \phi_c(\tau)\,\mathrm{sinc}(n-W\tau)\,\mathrm{sinc}(m-W\tau)\,d\tau.
\end{aligned} \tag{3.10}$$

Note that the mean square values of the Rayleigh distributed random variables $A_W(n,\omega_0;t)$ are given by

$$\rho_{nn} = \int_{-\infty}^{\infty} \phi_c(\tau)\,\mathrm{sinc}^2(n-W\tau)\,d\tau. \tag{3.11}$$

We next show that the ρ_{nn}'s sum to unity. For fixed values of W and τ, consider the function $\mathrm{sinc}(t-W\tau)$. This is a bandlimited function of t and thus can be expressed in terms of a sampling expansion as

$$\mathrm{sinc}(t-W\tau) = \sum_{n=-\infty}^{\infty} \mathrm{sinc}(n-W\tau)\,\mathrm{sinc}(t-n). \tag{3.12}$$

Since this is true for all values of t, if we let $t = W\tau$ we have

$$\sum_{n=-\infty}^{\infty} \mathrm{sinc}^2(n-W\tau) = 1. \tag{3.13}$$

Using equations (3.11) and (3.13) and the fact the $\phi_c(\tau)$ satisfies equation (3.8), we conclude that

$$\sum_{n=-\infty}^{\infty} \rho_{nn} = 1. \tag{3.14}$$

3.2 Analysis of FH System

We proceed with an analysis of the FH system in the presence of a fading channel. Figure 3.2 shows a single user in sector $\bar{0}$ transmitting over a fading channel at frequency ω_0. Since this frequency channel has bandwidth R, the corresponding channel parameters are obtained by setting $W = R$ in equation (3.4). This gives

$$\mathcal{A}_R(n, \omega_0; t) = \int_{-\infty}^{\infty} h(\tau; t)\,\mathrm{sinc}\left(n - \frac{\tau}{T_b}\right) e^{-j\omega_0 \tau}\, d\tau. \tag{3.15}$$

Since $T_m \ll T_b$, the mean square magnitude of these parameters, given by ρ_{nn} in equation (3.11), are all essentially zero except for $n = 0$, for which $\rho_{00} = 1$. Furthermore, since the channel parameters are assumed to vary sufficiently slowly so that they remain constant over many bits, each bit transmitted through the FH system sees only a single sample of the random process $\mathcal{A}_R(0, \omega_0; t)$. Thus, fading in the FH system is produced by multiplication by a complex Gaussian random variable having a mean square magnitude of unity. Consider the transmission of a single bit through the system. For each sector Δ, let

$A(\Delta) =$ amplitude fade between interfering user in sector Δ and base station in sector $\bar{0}$.

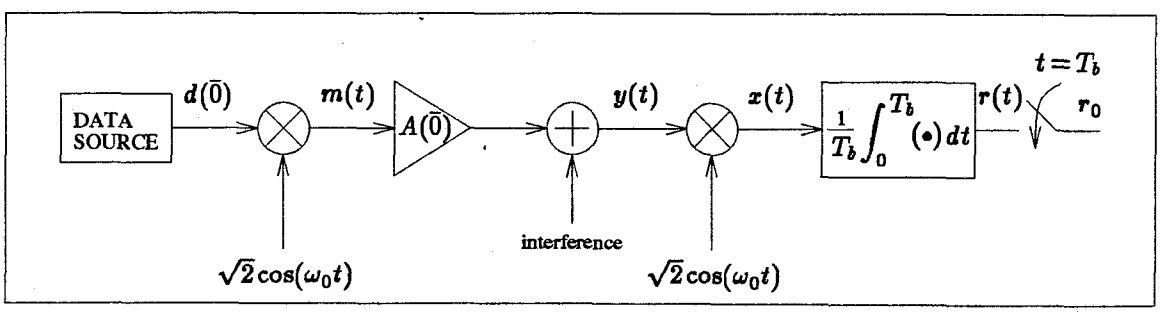

Figure 3.2: *Equivalent BPSK system using FH for communication from a single user in sector* $\bar{0}$ *transmitting over a fading channel at frequency* ω_0 *to the corresponding base-station receiver.*

The random variable $A(\Delta)$ is Rayleigh distributed with mean square value one, and thus has probability density function

$$p(A(\Delta)) = \begin{cases} 2A(\Delta)e^{-A(\Delta)^2} & A(\Delta) > 0, \\ 0 & \text{otherwise.} \end{cases} \tag{3.16}$$

For this distribution,

$$\mathrm{E}\{A(\Delta)^2\} = 1, \quad \text{and} \quad \mathrm{E}\{A(\Delta)\} = \sqrt{\pi}/2. \tag{3.17}$$

For $t \in (0, T_b)$,

$$y(t) = \sqrt{2}A(\bar{0})d(\bar{0})\cos(\omega_0 t) + \sum_{\Delta \neq \bar{0}} \chi(\Delta)\sqrt{2P(\bar{r}(\Delta))}A(\Delta)d(\Delta)\cos(\omega_0 t + \theta(\Delta)). \tag{3.18}$$

The sample at the output of the receiver, r_0, is thus given by

$$r_0 = \underbrace{A(\bar{0})d(\bar{0})}_{r_{\text{signal}}} + \underbrace{\sum_{\Delta \neq \bar{0}} \chi(\Delta)\sqrt{P(\bar{r}(\Delta))}A(\Delta)d(\Delta)\cos(\theta(\Delta))}_{r_{\text{noise}}}, \tag{3.19}$$

which, like the corresponding sample in the nonfading system given by equation (2.3), is composed of a signal part and a noise part. Note that the signal part is the product of the transmitted data bit and the fading parameter, $A(\bar{0})$, which is assumed to be known to the receiver. The noise part is due to other interfering users in the system and is given by

$$r_{\text{noise}} = \sum_{\Delta \neq \bar{0}} \chi(\Delta)\sqrt{P(\bar{r}(\Delta))}A(\Delta)d(\Delta)\cos(\theta(\Delta)). \tag{3.20}$$

The random variable r_{noise} is a sum of independent random variables each having mean zero. Thus,

$$\mathrm{Mean}(r_{\text{noise}}) = 0, \tag{3.21}$$

$$\begin{aligned} \mathrm{Var}(r_{\text{noise}}) &= \mathrm{E}\{r_{\text{noise}}^2\}, \\ &= \sum_{\Delta \neq \bar{0}} \underbrace{\mathrm{E}\{\chi^2(\Delta)\}}_{p} \mathrm{E}\{P(\bar{r}(\Delta))\} \underbrace{\mathrm{E}\{A(\Delta)^2\}}_{1} \underbrace{\mathrm{E}\{\cos^2(\theta(\Delta))\}}_{\frac{1}{2}}, \\ &= \frac{1}{2}ap. \end{aligned} \tag{3.22}$$

The interference parameter, a, is defined by equation (2.7). Note that the mean and variance of r_{noise} are identical with or without fading. Using geometrical properties of the hexagonal grid, under the conditions of power control and R^{-4} propagation loss in power, the probability distribution of

the random variable r_{noise} is computed in appendix A.3. With the results of appendix A.3, the probability of bit error can be determined as follows. Assuming that $d(\bar{0}) = +1$,

$$P_b(A(\bar{0}), r_{\text{noise}}) = \Pr\{A(\bar{0}) + r_{\text{noise}} < 0\}. \tag{3.23}$$

We express r_{noise} as in equation $(A.20)$ where W is a zero-mean, unity variance, Gaussian random variable, and V is the random variable defined by equation $(A.19)$. Note that the distribution of V has been computed numerically in appendix A.3, and also that $\mathrm{E}\{V^2\} = ap$. Thus, we have

$$P_b(A(\bar{0}), W, V) = \Pr\left\{A(\bar{0}) + \frac{WV}{\sqrt{2}} < 0\right\}. \tag{3.24}$$

Averaging over the Gaussian statistics of W gives

$$P_b(A(\bar{0}), V) = \frac{1}{2}\mathrm{erfc}\left(\sqrt{\frac{A(\bar{0})^2}{V^2}}\right). \tag{3.25}$$

Next, averaging over the Rayleigh statistics of $A(\bar{0})$ gives

$$\begin{aligned} P_b(V) &= \int_{-\infty}^{+\infty} p(A(\bar{0}))P_b(A(\bar{0}), V)\, dA(\bar{0}), \\ &= \int_0^{\infty} 2Ae^{-A^2}\frac{1}{2}\mathrm{erfc}\left(\sqrt{\frac{A^2}{V^2}}\right) dA. \end{aligned} \tag{3.26}$$

Integration by parts yields

$$P_b(V) = \frac{1}{2}\left[1 - \frac{1}{\sqrt{V^2+1}}\right]. \tag{3.27}$$

Finally, the probability of bit error can be computed numerically using the probability density function of V, $p_V(v)$, which has been computed numerically in appendix A.3. Thus,

$$P_b[\text{Fading, Exact}] = \int_v p_V(v)\frac{1}{2}\left[1 - \frac{1}{\sqrt{v^2+1}}\right] dv. \tag{3.28}$$

For the purpose of comparison, we compute the probability of bit error where the additive noise term, r_{noise}, is approximated with a zero-mean Gaussian distribution with variance given by equation (3.22). In this case, we take $V = \sqrt{ap}$ in equation (3.24), and average over $A(\bar{0})$ and W. This gives

$$P_b[\text{Fading, Gaussian}] = \frac{1}{2}\left[1 - \frac{1}{\sqrt{ap+1}}\right]. \tag{3.29}$$

Note that since $T_m \ll T_b$, each frequency channel has a bandwidth that is $\ll 1/T_m$, and equation (3.29) is identical to BPSK signaling over a slowly-varying frequency non-selective fading channel ([1], pg. 717).

Finally, we show that P_b[Fading, Exact] $\leq P_b$[Fading, Gaussian]. Equation (3.28) expresses the exact probability of bit error as the expected value of a function of V^2. Let $X = V^2$, and consider the function

$$f(x) = \frac{1}{2}\left[1 - \frac{1}{\sqrt{x+1}}\right]. \tag{3.30}$$

The function $f(x)$ is a convex $\cap$ function of x because

$$f''(x) = -\frac{3}{8}(x+1)^{-\frac{5}{2}} \leq 0. \tag{3.31}$$

Thus, by Jensen's Inequality ([9], pg. 153)

$$\mathrm{E}\{f(x)\} \leq f(\mathrm{E}\{x\}). \tag{3.32}$$

This gives

$$\begin{aligned} P_b[\text{Fading, Exact}] &\leq \frac{1}{2}\left[1 - \frac{1}{\sqrt{\mathrm{E}\{V^2\}+1}}\right], \\ &= \frac{1}{2}\left[1 - \frac{1}{\sqrt{ap+1}}\right], \\ &= P_b[\text{Fading, Gaussian}], \end{aligned} \tag{3.33}$$

as desired.

3.3 Analysis of CDMA System

Next, we consider the performance of a direct sequence CDMA system and a fading channel using an ideal RAKE receiver ([2], pg. 48; [1], pg. 732). For the purpose of theoretical analysis, the number of tap coefficients in the RAKE receiver, L, is taken to be arbitrarily large. This is approximated in practice by a finite number of taps satisfying $L > T_m/T_c$ ([2], pg. 45). Figure 3.3 shows a CDMA system for user 0 in sector $\bar{0}$. Since the CDMA signal is spread over the entire system bandwidth, B, the corresponding channel parameters are obtained by setting $W = B$ in equation (3.4). This gives

$$\mathcal{A}_B(n, \omega_0; t) = \int_{-\infty}^{\infty} h(\tau; t)\,\mathrm{sinc}\left(n - \frac{\tau}{T_c}\right) e^{-j\omega_0\tau}\, d\tau. \tag{3.34}$$

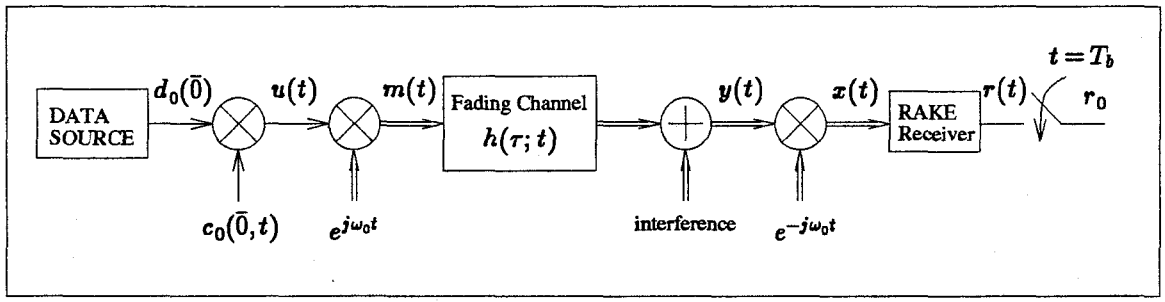

Figure 3.3: *Equivalent BPSK system using CDMA for communication from user 0 in sector* $\bar{0}$ *over a fading channel to the corresponding base-station receiver.*

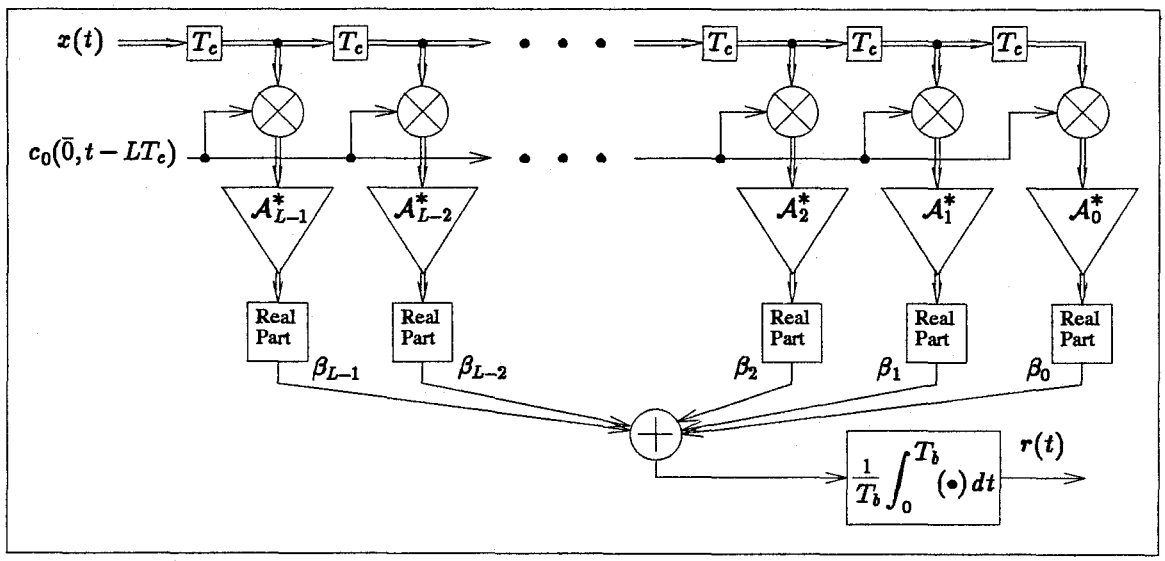

Figure 3.4: *Ideal CDMA RAKE receiver with L taps.*

Since the channel parameters are assumed to vary sufficiently slowly so that they remain constant over many bits, each bit transmitted through the system sees a single sample of these random processes. Consider the transmission of a single bit through the system. Figure 3.4 shows a CDMA RAKE receiver with L taps. Let

$x(t;\Delta,k) =$ component of $x(t)$ due to user k in sector Δ,

$\beta_q(\Delta,k) =$ component of β_q due to user k in sector Δ,

$r(\Delta,k) =$ component of r_0 due to user k in sector Δ.

First, consider the response of the receiver to user 0 in sector $\bar{0}$. Let

$$\mathcal{A}_n = \mathcal{A}_B(n, \omega_0; t = 0) \tag{3.35}$$

denote the complex channel parameters between this user and the receiver in sector $\bar{0}$. These parameters are assumed to be known by the receiver. Let

$$A_n = |\mathcal{A}_n| \tag{3.36}$$

which is a Rayleigh distributed random variable. For $t \in (0, T_b)$, the baseband CDMA signal at the transmitter is

$$u(t) = d_0(\bar{0})c_0(\bar{0}, t). \tag{3.37}$$

Inserting this into equation (3.3), the portion of the input to the RAKE receiver due to user 0 of sector $\bar{0}$ is

$$x(t; \bar{0}, 0) = \sum_n d_0(\bar{0})c_0(\bar{0}, t - nT_c)\mathcal{A}_n. \tag{3.38}$$

Using this to compute $\beta_q(\bar{0}, 0)$, we find

$$\begin{aligned}
\beta_q(\bar{0}, 0) &= \mathcal{A}_q^* c_0(\bar{0}, t - LT_c)x(t - (L - q)T_c; \bar{0}, 0), \\
&= \mathcal{A}_q^* \sum_n d_0(\bar{0})c_0(\bar{0}, t - LT_c)c_0(\bar{0}, t - (L - q + n)T_c)\mathcal{A}_n, \\
&= d_0(\bar{0})A_q^2 + \underbrace{\sum_{n \neq q} d_0(\bar{0})c_0(\bar{0}, t - LT_c)c_0(\bar{0}, t - (L - q + n)T_c)\mathcal{A}_q^*\mathcal{A}_n}_{\text{self-noise}}.
\end{aligned} \tag{3.39}$$

Since we are primarily interested in performance where there is a large number of interfering users and thus a low SIR, we neglect the terms due to self-noise ([1], pg. 733). Thus, we have

$$\beta_q(0, \bar{0}) = d_0(\bar{0})A_q^2. \tag{3.40}$$

Summing over all the taps in the RAKE receiver and performing the integration over the bit interval gives

$$r(\bar{0}, 0) = d_0(\bar{0}) \sum_q A_q^2. \tag{3.41}$$

Next, consider the response of the receiver to the interfering user k in sector Δ. Let

$\mathcal{A}_k(\Delta, q) =$ sample at time $(t = 0)$ of complex channel parameters between user k in sector Δ and receiver for user 0 in sector $\bar{0}$.

Using equation (3.3), the portion of the input to the RAKE receiver due to user k of sector Δ is

$$x(t; \Delta, k) = \sqrt{P(r_k(\Delta))} d_k(\Delta) \sum_n c_k(\Delta, t - nT_c) \mathcal{A}_k(\Delta, n). \tag{3.42}$$

Using this to compute $\beta_q(\Delta, k)$, we find

$$\beta_q(\Delta, k) = \sqrt{P(r_k(\Delta))} d_k(\Delta) \left[\sum_n c_k(\Delta, t - (L - q + n)T_c) \mathcal{A}_k(\Delta, n) \right] \mathcal{A}_q^* c_0(\bar{0}, t - LT_c). \tag{3.43}$$

Summing over all the taps in the RAKE receiver and performing the integration over the bit interval gives

$$r(\Delta, k) = \frac{1}{N} \sqrt{P(r_k(\Delta))} \sum_q \sum_n \sum_{m=0}^{N-1} b_k(\Delta, q, n, m) A_k(\Delta, n) A_q \cos\left(\phi_k(\Delta, n, q)\right), \tag{3.44}$$

where

$$b_k(\Delta, q, n, m) = d_k(\Delta) c_k(\Delta, m - L + q - n) c_0(\bar{0}, m - L) \tag{3.45}$$

is (± 1) equally likely, and

$$\phi_k(\Delta, n, q) = \arg(\mathcal{A}_k(\Delta, n) \mathcal{A}_q^*) \tag{3.46}$$

is uniformly distributed over the interval 0 to 2π. Since the RAKE receiver has measurements of the random variables A_q, we wish to compute the probability of error conditioned on these measurements, then average over the statistics of the A_q's. Treating the A_q's as constants, we can compute the conditional mean and variance of $r(\Delta, k)$, which is a weighted sum of independent zero-mean random variables, as

$$\text{Mean}(r(\Delta, k)) = 0, \tag{3.47}$$

$$\begin{aligned} \text{Var}(r(\Delta, k)) &= \text{E}\{r^2(\Delta, k)\}, \\ &= \frac{1}{N^2} \text{E}\{P(r_k(\Delta))\} \sum_q \sum_n \sum_{m=0}^{N-1} \underbrace{\text{E}\{A_k^2(\Delta, n)\}}_{\rho_{nn}} A_q^2 \underbrace{\text{E}\{\cos^2\left(\phi_k(\Delta, n)\right)\}}_{\frac{1}{2}}, \\ &= \frac{1}{2N^2} \text{E}\{P(r_k(\Delta))\} \sum_q \underbrace{\sum_n \rho_{nn}}_{1} N A_q^2, \\ &= \frac{1}{2N} \text{E}\{P(r_k(\Delta))\} \sum_q A_q^2. \end{aligned} \tag{3.48}$$

The total noise, r_{noise}, is the sum of the contributions of all users except user 0 in sector $\bar{0}$. Since each user is independent, r_{noise} is a sum of independent random variables. Thus, its mean and variance are given by the sum of the means and variances for each user. Therefore,

$$r_{\text{noise}} = \sum_{(\Delta,k)\neq(\bar{0},0)} r(\Delta,k), \tag{3.49}$$

$$\text{Mean}(r_{\text{noise}}) = \sum_{(\Delta,k)\neq(\bar{0},0)} \text{Mean}(r(\Delta,k)) = 0, \tag{3.50}$$

$$\begin{aligned}\text{Var}(r_{\text{noise}}) &= \sum_{(\Delta,k)\neq(\bar{0},0)} \text{Var}(r(\Delta,k)), \\ &= \sum_{(\Delta,k)\neq(\bar{0},0)} \frac{1}{2N}\text{E}\{P(r_k(\Delta))\}\sum_q A_q^2.\end{aligned} \tag{3.51}$$

Using equation (2.18), we find

$$\text{Var}(r_{\text{noise}}) = \frac{1}{2}(a+1)p\left(\sum_q A_q^2\right). \tag{3.52}$$

Thus, the receiver output, r_0, is given by

$$r_0 = d_0(\bar{0})\sum_q A_q^2 + r_{\text{noise}}, \tag{3.53}$$

where r_{noise} has variance given by equation (3.52). Since the A_q's are known to the receiver, r_0 can be divided by $\sqrt{\sum A_q^2}$ to form a receiver output of the form

$$Y = d_0(\bar{0})\sqrt{\sum_q A_q^2} + Z, \tag{3.54}$$

where

$$\text{Var}(Z) = \frac{1}{2}(a+1)p. \tag{3.55}$$

Note that the complex channel parameters, $\mathcal{A}_q$, are not independent and have a covariance matrix given by equation (3.10) with $W = B$

$$\rho_{nm} = \int_{-\infty}^{\infty} \phi_c(\tau)\,\text{sinc}\left(n - \frac{\tau}{T_c}\right)\text{sinc}\left(m - \frac{\tau}{T_c}\right)d\tau. \tag{3.56}$$

The receiver output given by equation (3.54) is dependent on the random variable

$$A = \sqrt{\sum_q A_q^2}. \tag{3.57}$$

In appendix A.5, it is shown that for $A_q = |\mathcal{A}_q|$, where the $\mathcal{A}_q$'s are complex joint Gaussian random variables with covariance matrix $[\rho_{nm}]$, the random variable A can equivalently be written as

$$A = \sqrt{\sum_q B_q^2}, \tag{3.58}$$

where the B_q's are *independent* Rayleigh distributed random variables with mean square values b_q given by the eigenvalues of the covariance matrix $[\rho_{nm}]$. The probablility density function of A is then given by ([1] pg. 734)

$$p(A) = \begin{cases} 2\sum_k \frac{\pi_k}{b_k} A e^{-\frac{A^2}{b_k}} & A > 0, \\ 0 & \text{otherwise}, \end{cases} \tag{3.59}$$

where

$$\pi_k = \prod_{i \neq k} \frac{b_k}{b_k - b_i}. \tag{3.60}$$

Since the trace of any matrix is equal to the sum of its eigenvalues, it follows that $\sum \rho_{nn} = \sum b_n$. Combining this with equation (3.14) gives

$$\sum_{n=-\infty}^{\infty} b_n = 1. \tag{3.61}$$

Thus,

$$\mathrm{E}\{A^2\} = \mathrm{E}\left\{\sum_n B_n^2\right\} = \sum_n b_n = 1. \tag{3.62}$$

Assuming Z has a Gaussian distribution, equations (3.54), (3.55), and (3.57) can be used to compute the probability of bit error conditioned on the random variable A. This gives

$$P_b(A) = \frac{1}{2}\operatorname{erfc}\left(\sqrt{\frac{A^2}{(a+1)p}}\right). \tag{3.63}$$

Averaging (3.63) over the random variable A, using the probability density function given by equation (3.59), gives ([1] pg. 735)

$$P_b[\text{Fading}] = \frac{1}{2}\sum_k \pi_k \left(1 - \sqrt{\frac{b_k}{b_k + (a+1)p}}\right). \tag{3.64}$$

Remark. If the random variables $\mathcal{A}_q$ are in fact independent, the covariance matrix is diagonal and thus has eigenvalues $b_k = \rho_{kk} = \mathrm{E}\{A_k^2\}$. In this case, equation (3.64) reduces to the result shown in ([1], pg. 735) and ([2], pg. 46) where the channel parameters are taken to be independent.

3.4 Fading Channel Results

With respect to equations (3.19) and (3.54), both the FH and CDMA systems produce a receiver output of the form

$$Y = AX + Z, \tag{3.65}$$

where

$X = \pm 1$ data bit transmitted,

A = multiplicative channel fade,

Z = zero-mean additive noise.

Equations (3.22) and (3.55) imply that the variance of the zero-mean additive noise, Z, is

$$\mathrm{Var}(Z) = \begin{cases} \frac{1}{2}ap & \text{for FH,} \\ \frac{1}{2}(a+1)p & \text{for CDMA.} \end{cases} \tag{3.66}$$

Equations (3.19) and (3.54) imply that the multiplicative fade, A, has the form

$$A = \begin{cases} \text{Rayleigh} & \text{for FH,} \\ \text{Square root of sum of Rayleigh-squared} & \text{for CDMA.} \end{cases} \tag{3.67}$$

Note that for both systems we have shown that the mean square value of A is one.

We wish to compare the performances of FH and CDMA with a specific fading channel model. The channel is assumed to have an exponential multipath-intensity profile, which is typical for cellular mobile communications ([8], pg. 50), and is given by

$$\phi_c(\tau) = \begin{cases} \frac{1}{\tau_{\mathrm{RMS}}} e^{-\frac{\tau}{\tau_{\mathrm{RMS}}}} & \tau > 0, \\ 0 & \text{otherwise,} \end{cases} \tag{3.68}$$

where τ_{RMS} is the RMS delay spread of the channel. We will take $\tau_{RMS} = 3T_c$, and for the CDMA RAKE receiver use $L = 12$ taps. The covariances among the tap coefficients of the CDMA RAKE receiver can be computed using equation (3.56). This gives

$$\begin{aligned} \rho_{nm} &= \int_{-\infty}^{\infty} \frac{1}{3T_c} e^{-\frac{\tau}{3T_c}} \operatorname{sinc}\left(n - \frac{\tau}{T_c}\right) \operatorname{sinc}\left(m - \frac{\tau}{T_c}\right) d\tau, \\ &= \frac{1}{3} \int_{-\infty}^{\infty} e^{-\frac{x}{3}} \operatorname{sinc}(n-x) \operatorname{sinc}(m-x)\, dx. \end{aligned} \tag{3.69}$$

Table 3.1 shows the covariance matrix, $[\rho_{nm}]$, and its eigenvalues. The eigenvalues sum to 0.947 which is less than 1 as a consequence of using a finite number of taps in the RAKE receiver.

Figure 3.5 shows a plot of the average probability of bit error versus the normalized traffic for FH and CDMA systems. The FH performance curve was found using the exact distribution of additive noise found in appendix A.3. The CDMA performance curve is given by equation (3.64). The performance curve for the FH system if the noise is Gaussian, given by equation (3.29), is also shown. We observe that this is in fact an upper bound on the performance curve determined using the exact distribution as predicted by equation (3.33). Again, we see that the FH and CDMA curves cross with CDMA performing better at lower levels of traffic and FH performing better at higher levels of traffic. We also see that in a fading environment the FH system performs almost exactly as if the additive noise were Gaussian. Also, note that the degradation in performance due to fading, compared to the nonfading channel, is much more severe to the FH system than to the CDMA system.

Covariance Matrix: $[\rho_{nm}]$

0.1445	0.0479	-0.0290	0.0204	-0.0155	0.0123	-0.0101	0.0085	-0.0073	0.0064	-0.0057	0.0051
0.0479	0.2219	0.0100	-0.0067	0.0047	-0.0034	0.0025	-0.0019	0.0015	-0.0012	0.0010	-0.0008
-0.0290	0.0100	0.1655	0.0033	-0.0020	0.0012	-0.0007	0.0003	-0.0001	-0.0000	0.0001	-0.0001
0.0204	-0.0067	0.0033	0.1209	0.0007	-0.0001	-0.0001	0.0003	-0.0005	0.0005	-0.0006	0.0006
-0.0155	0.0047	-0.0020	0.0007	0.0878	-0.0003	0.0006	-0.0007	0.0008	-0.0008	0.0008	-0.0008
0.0123	-0.0034	0.0012	-0.0001	-0.0003	0.0636	-0.0008	0.0009	-0.0009	0.0009	-0.0009	0.0009
-0.0101	0.0025	-0.0007	-0.0001	0.0006	-0.0008	0.0460	-0.0010	0.0010	-0.0009	0.0009	-0.0009
0.0085	-0.0019	0.0003	0.0003	-0.0007	0.0009	-0.0010	0.0333	-0.0010	0.0009	-0.0009	0.0009
-0.0073	0.0015	-0.0001	-0.0005	0.0008	-0.0009	0.0010	-0.0010	0.0241	-0.0009	0.0009	-0.0008
0.0064	-0.0012	-0.0000	0.0005	-0.0008	0.0009	-0.0009	0.0009	-0.0009	0.0175	-0.0008	0.0008
-0.0057	0.0010	0.0001	-0.0006	0.0008	-0.0009	0.0009	-0.0009	0.0009	-0.0008	0.0127	-0.0007
0.0051	-0.0008	-0.0001	0.0006	-0.0008	0.0009	-0.0009	0.0009	-0.0008	0.0008	-0.0007	0.0092

Eigenvalues:	Products:
$b_0 = 0.04410$	$\pi_0 = 1.96328\times10^{0}$
$b_1 = 0.03234$	$\pi_1 = -1.76491\times10^{1}$
$b_2 = 0.02356$	$\pi_2 = 9.91937\times10^{3}$
$b_3 = 0.01709$	$\pi_3 = -3.33122\times10^{4}$
$b_4 = 0.01234$	$\pi_4 = 5.99353\times10^{6}$
$b_5 = 0.00887$	$\pi_5 = -4.30838\times10^{8}$
$b_6 = 0.05955$	$\pi_6 = -1.37094\times10^{1}$
$b_7 = 0.07933$	$\pi_7 = 5.81716\times10^{1}$
$b_8 = 1.04437$	$\pi_8 = -1.44665\times10^{2}$
$b_9 = 1.37538$	$\pi_9 = 2.08682\times10^{2}$
$b_{10} = 0.18294$	$\pi_{10} = -1.64914\times10^{2}$
$b_{11} = 0.24522$	$\pi_{11} = 5.56387\times10^{1}$

Table 3.1: *Covariance matrix among complex tap coefficients in a CDMA RAKE receiver. The eigenvalues of the covariance matrix and the product terms, π_k, are also shown.*

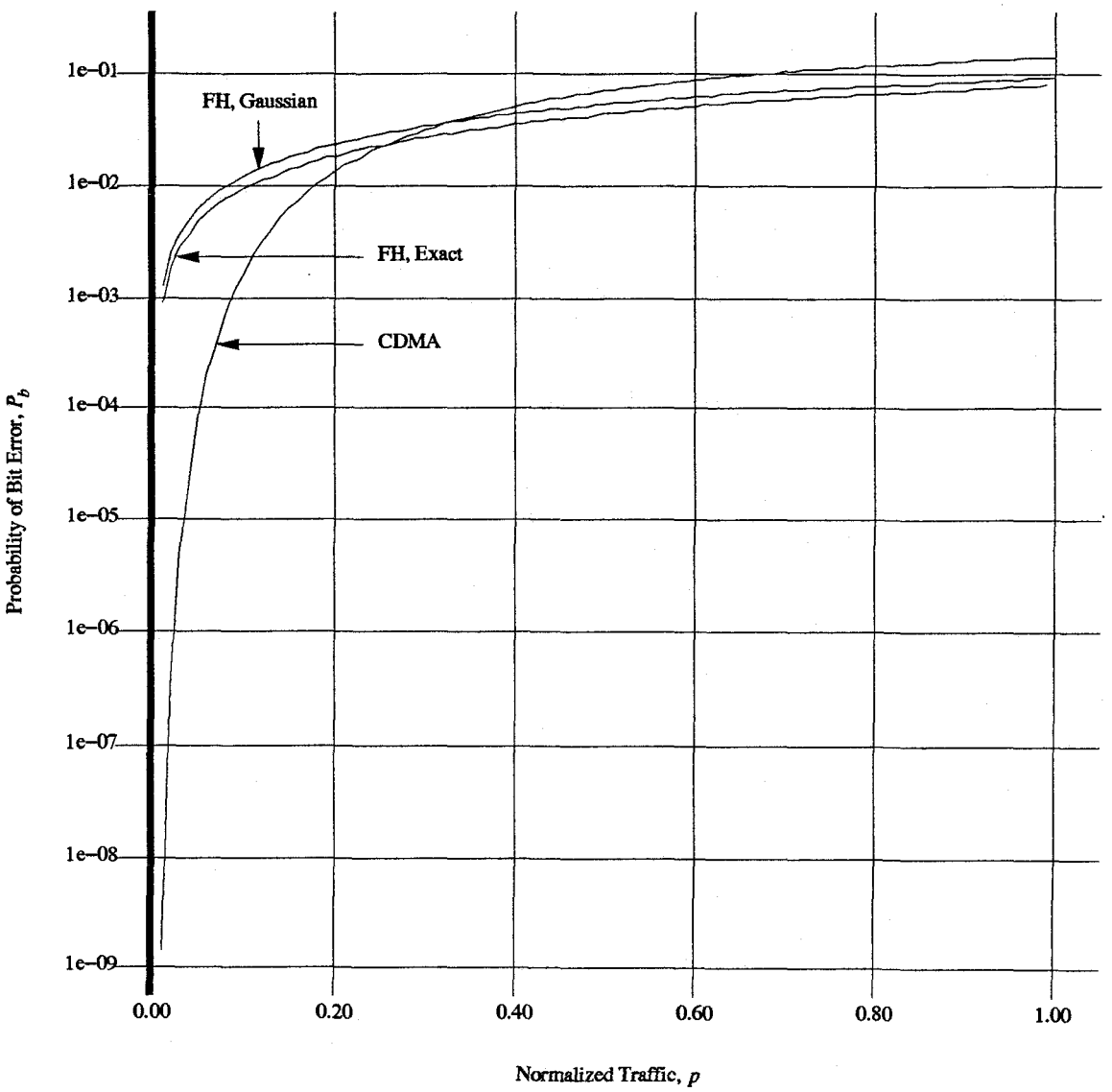

Figure 3.5: *Probability of bit error versus normalized traffic for FH and CDMA systems in a fading environment. For the FH system, curves are shown for the exact distribution of additive noise, and also for Gaussian additive noise.*

4. Information Theory

4.1 Introduction

In this chapter, we apply information theory to the channel models developed in the previous chapter. It is important to note that we are dealing with an extremely complicated multiuser channel. Unfortunately, very little is known about multiuser information theory. For many simple channel models, determination of the multiuser capacity region is an unsolved problem ([10], pg. 384). Chapter 6 investigates some properties of interference channels for which the determination of the capacity region is unknown. Because of this, we will make some assumptions about how the channel is used so that the problem is reduced to a single-user channel. Rather than attempting to compute the ultimate capacity, we will compute the capacities when the system is constrained to use a specific modulation for FH and CDMA.

The capacity, **C**, is defined to be the largest value of normalized traffic, p, such that it is possible for each user in the system to communicate at the data rate, R, with an arbitrarily small probability of bit error. We begin with some assumptions about how the channel is used.

(1) There is no cooperation among users on the level of coding. Interfering users use binary codes that appear to be ± 1 equally likely. Note that cooperation on the level of modulation is implicitly assumed in the FH system because of the fact that users in a sector have orthogonal hopping patterns.

(2) The receiver has complete knowledge of the fade in the FH system, and of the optimal tap coefficient values in the CDMA system.

(3) Each transmitted codeword symbol sees an independent channel. This can be approximated in the FH system by using sufficient interleaving and hopping rate, and in a CDMA system using sufficient interleaving.

4.2 Coded Channel Model

We begin by developing a channel model when coding is used. Let

$r_{\text{code}} =$ code rate.

Consider, first, the transmission of a single ± 1 codeword symbol through the FH system. If, for

example, a rate 1/2 code is used, we note that the information bits generated at rate R produce codeword symbols at rate $2R$. We assume that the bandwidth of each FH channel remains R, but that at a given time each user transmits simultaneously over 2 such channels to achieve the symbol rate of $2R$. Since the N_s users in each sector remain orthogonal, the total number of FH channels in use at a given time in a sector is $2N_s$. Thus, we must have $2N_s \leq N$, or equivalently, the normalized traffic must satisfy $2p \leq 1$. Furthermore, the probability that there is an interfering user in an arbitrary sector $\Delta \neq \bar{0}$ is $2N_s/N = 2p$. Thus, for the FH system, the additive noise at the receiver output, r_{noise}, is the same as that given by equation (3.20) with p replaced by $2p$ in the definition of $\chi(\Delta)$. Similarly, for the CDMA system, each ± 1 codeword symbol is now spread by a factor of $N/2$. Thus, analysis of the CDMA system simply requires replacing N by $N/2$ in equations (3.54) and (3.55). Note that N appears only through the normalized traffic $p = N_s/N$, so we can equivalently replace p by $2p$.

In general, for a code of rate r_{code}, each user transmits, on average, over $1/r_{\text{code}}$ channels at a time in the FH system. The assumption of orthogonality within a sector implies that $N_s/r_{\text{code}} \leq N$. This can be expressed in terms of the effective coded normalized traffic, $\bar{p}$, as

$$\bar{p} \leq 1, \tag{4.1}$$

where the effective coded normalized traffic is defined as

$$\bar{p} = \frac{p}{r_{\text{code}}}. \tag{4.2}$$

The probability that there is an interfering user in an arbitrary sector $\Delta \neq \bar{0}$ is then given by $(N_s/r_{\text{code}})/N = \bar{p}$. Thus, for the FH system the additive noise at the receiver output is obtained by replacing p by $\bar{p}$ in the uncoded system. Furthermore, for the CDMA system each ± 1 codeword symbol is now spread by a factor of Nr_{code}. With respect to equations (3.54) and (3.55), replacing N by Nr_{code} is equivalent to replacing p by $\bar{p}$. Thus, for both FH and CDMA, analysis of the coded system is obtained by replacing p by $\bar{p}$ in the uncoded system.

Hence, with respect to equations (3.65), (3.66), and (3.67), for the transmission of a single ± 1 codeword symbol using a code of rate r_{code}, both the FH and CDMA systems produce a receiver

output of the form

$$Y = AX + Z, \tag{4.3}$$

where

$X = \pm 1$ codeword symbol transmitted,

$A =$ multiplicative channel fade,

$Z =$ zero-mean additive noise.

The variance of the additive noise, Z, is

$$\mathrm{Var}(Z) = \begin{cases} \frac{1}{2}a\bar{p} & \text{for FH,} \\ \frac{1}{2}(a+1)\bar{p} & \text{for CDMA.} \end{cases} \tag{4.4}$$

The multiplicative fade, however, remains the same as in the uncoded system, and is thus given by

$$A = \begin{cases} \text{Rayleigh} & \text{for FH,} \\ \text{Square root of sum of Rayleigh-squared} & \text{for CDMA.} \end{cases} \tag{4.5}$$

4.3 Information-Theoretic Capacity

Note that the distribution of the additive noise, Z, in equation (4.3) is a function of $\bar{p}$. Under the assumption that A is known, for a specific distribution on the random variable X, and a specific value of $\bar{p}$, we can compute (numerically) the conditional mutual information $I(X;Y \mid A)$. For a given value of $\bar{p}$ we pick the distribution on X that maximizes $I(X;Y \mid A)$. The resulting maximum is a function only of $\bar{p}$ and is denoted by

$$I(\bar{p}) = \max I(X;Y \mid A). \tag{4.6}$$

This value corresponds to the information transfer of a single codeword symbol. If, for example, a code of rate 1/2 were used, in an arbitrary time interval there would be twice as many codeword symbols as information bits. Thus, for reliable communication each codeword symbol must carry, on average, at least 1/2 bit of mutual information. In general, for a code of rate r_{code}, each codeword symbol must carry, on average, at least r_{code} bits of mutual information. Thus, for reliable communication at the data rate R, we require that

$$I(\bar{p}) \geq r_{\text{code}}. \tag{4.7}$$

Multiplying both sides of equation (4.7) by $\bar{p}$ and noting that $\bar{p}r_{\text{code}} = p$, we see that reliable communication is possible for values of normalized traffic that satisfy

$$p \leq \bar{p}I(\bar{p}). \tag{4.8}$$

The capacity of the system, **C**, is defined to be the largest possible value of normalized traffic, p, for which communication at the data rate, R, can be achieved with an arbitrarily small probability of error. Therefore, the capacity of the system is given by

$$\mathbf{C} = \max_{\bar{p} \in S} \{\bar{p}I(\bar{p})\}, \tag{4.9}$$

where

$$S = \begin{cases} [0,1] & \text{for FH,} \\ [0,\infty) & \text{for CDMA.} \end{cases}$$

Remark: Note the analogy between this information-theoretic analysis and that of the classical single-user channel. In the classical problem, a single user wishes to communicate over a channel with a fixed amount of noise. Information theory then predicts the maximum possible data rate at which the user can communicate. For the multiuser channel model considered here, the data rate for each user is fixed, and information theory is used to predict the maximum amount of interference the system can tolerate while maintaining that data rate for each user. This maximum tolerable interference corresponds directly to a maximum tolerable number of interfering users and thus to a maximum traffic. In this respect, the multiuser channel analysis presented here is somewhat similar to solving the classical single-user problem backwards.

4.4 BPSK Capacity

We now set up an expression for numerical computation of $I(\bar{p})$ when BPSK modulation is used. With respect to equation (4.3), let

$p_A(\alpha) =$ probability density function of multiplicative fade, A,

$p_Z(z) =$ probability density function of additive noise, Z,

$p_X(x) =$ probability density function of transmitted codeword symbol, X,

$p_Y(y) =$ probability density function of receiver output, Y.

By the symmetry of the problem, the optimal distribution for X is ± 1 equally likely. The corresponding probability density function of X can be written in terms of delta functions as

$$p_X(x) = \frac{1}{2}\delta(x+1) + \frac{1}{2}\delta(x-1). \tag{4.10}$$

The joint probability density function among all four random variables can be written as

$$p_{X,A,Z,Y}(x,\alpha,z,y) = p_X(x)p_A(\alpha)p_Z(z)\delta(y-\alpha x-z). \tag{4.11}$$

Recall that $I(\bar{p})$ is the mutual information $I(X;Y \mid A)$, and thus is given by ([11], pg. 244)

$$I(\bar{p}) = \mathrm{E}\left\{\log_2\left(\frac{p_{Y|A,X}(Y \mid A,X)}{p_{Y|A}(Y \mid A)}\right)\right\}. \tag{4.12}$$

The functions $p_{Y|A,X}(y \mid \alpha, x)$ and $p_{Y|A}(y \mid \alpha)$ are given by

$$p_{Y|A,X}(y \mid \alpha, x) = p_Z(y-\alpha x), \tag{4.13}$$

and

$$p_{Y|A}(y \mid \alpha) = \frac{1}{2}p_Z(y+\alpha) + \frac{1}{2}p_Z(y-\alpha). \tag{4.14}$$

Inserting these expressions into equation (4.12) gives

$$I(\bar{p}) = \iiint\limits_{(x,\alpha,z,y)} p_X(x)p_A(\alpha)p_Z(z)\delta(y-\alpha x-z)\log_2\left[\frac{p_Z(y-\alpha x)}{\frac{1}{2}p_Z(y+\alpha)+\frac{1}{2}p_Z(y-\alpha)}\right] dy\,dz\,d\alpha\,dx. \tag{4.15}$$

Performing the integration over y and x gives

$$I(\bar{p}) = \int_{\alpha=0}^{\infty}\int_{z=-\infty}^{\infty} p_A(\alpha)p_Z(z)\frac{1}{2}\log_2\left[\frac{p_Z(z)}{\frac{1}{2}p_Z(z)+\frac{1}{2}p_Z(z-2\alpha)}\cdot\frac{p_Z(z)}{\frac{1}{2}p_Z(z)+\frac{1}{2}p_Z(z+2\alpha)}\right] dz\,d\alpha. \tag{4.16}$$

Finally, using the fact that the additive noise distribution, $p_Z(z)$, is an even function of z, $I(\bar{p})$ can be expressed as

$$I(\bar{p}) = \int_{\alpha=0}^{\infty}\int_{z=0}^{\infty} p_A(\alpha)p_Z(z)\log_2\left[\frac{4}{\left(1+\frac{p_Z(z-2\alpha)}{p_Z(z)}\right)\left(1+\frac{p_Z(z+2\alpha)}{p_Z(z)}\right)}\right] dz\,d\alpha. \tag{4.17}$$

Figure 4.1 show plots of $I(\bar{p})$ versus $\bar{p}$ and of $\bar{p}I(\bar{p})$ versus $\bar{p}$ for the FH and CDMA systems. These were computed numerically by using the Rayleigh distribution given by equation (3.16) for $p_A(\alpha)$ in the FH system, and using the square root of a sum of Rayleigh-squared distribution given

by equation (3.59) for $p_A(\alpha)$ in the CDMA system. The additive noise was taken to be Gaussian in the CDMA system and for the FH system the distribution derived in appendix A.3 was used. Note that for both systems, $\bar{p}I(\bar{p})$ is a monotonically increasing functions of $\bar{p}$. For the FH system, the maximum occurs at $\bar{p} = 1$ and gives a capacity

$$\mathbf{C}_{\mathrm{FH}}[\text{BPSK, Soft Decision, Fading}] = 0.729. \tag{4.18}$$

For the CDMA system, it is shown in appendix A.7 that as $\bar{p} \rightarrow \infty$ the capacity is given by

$$\mathbf{C}_{\mathrm{CDMA}}[\text{BPSK, Soft Decision, Fading}] = \frac{\log_2(e)}{a+1} = 0.988. \tag{4.19}$$

For the purpose of comparison, capacity results for a nonfading channel can be obtained by setting $p_A(\alpha) = \delta(A-1)$ in equation (4.17) and inserting the appropriate additive noise distributions. For the FH system this gives a capacity of

$$\mathbf{C}_{\mathrm{FH}}[\text{BPSK, Soft Decision, No Fading}] = 0.896. \tag{4.20}$$

It is also shown in appendix A.7 that the capacity of the CDMA system for a nonfading channel remains the same as that of the fading channel. Thus,

$$\mathbf{C}_{\mathrm{CDMA}}[\text{BPSK, Soft Decision, No Fading}] = \frac{\log_2(e)}{a+1} = 0.988. \tag{4.21}$$

At this point we wish to extend these information-theoretic results a step further and consider hard decision decoders. If the receiver makes a hard decision on each binary codeword symbol, the probability that a codeword symbol is in error is given by replacing p by $\bar{p}$ in the expressions for uncoded bit error probability in chapter 3. Thus, each codeword symbol sees a binary symmetric channel ([11], pg. 161) with crossover probability, $P_b(\bar{p})$. The mutual information, $I(\bar{p})$, is thus given by

$$I(\bar{p}) = 1 - \mathcal{H}[P_b(\bar{p})]. \tag{4.22}$$

For the FH system, $\bar{p}I(\bar{p})$ achieves its maximum value at $\bar{p} = 1$ and gives

$$\mathbf{C}_{\mathrm{FH}}[\text{BPSK, Hard Decision, Fading}] = 0.599. \tag{4.23}$$

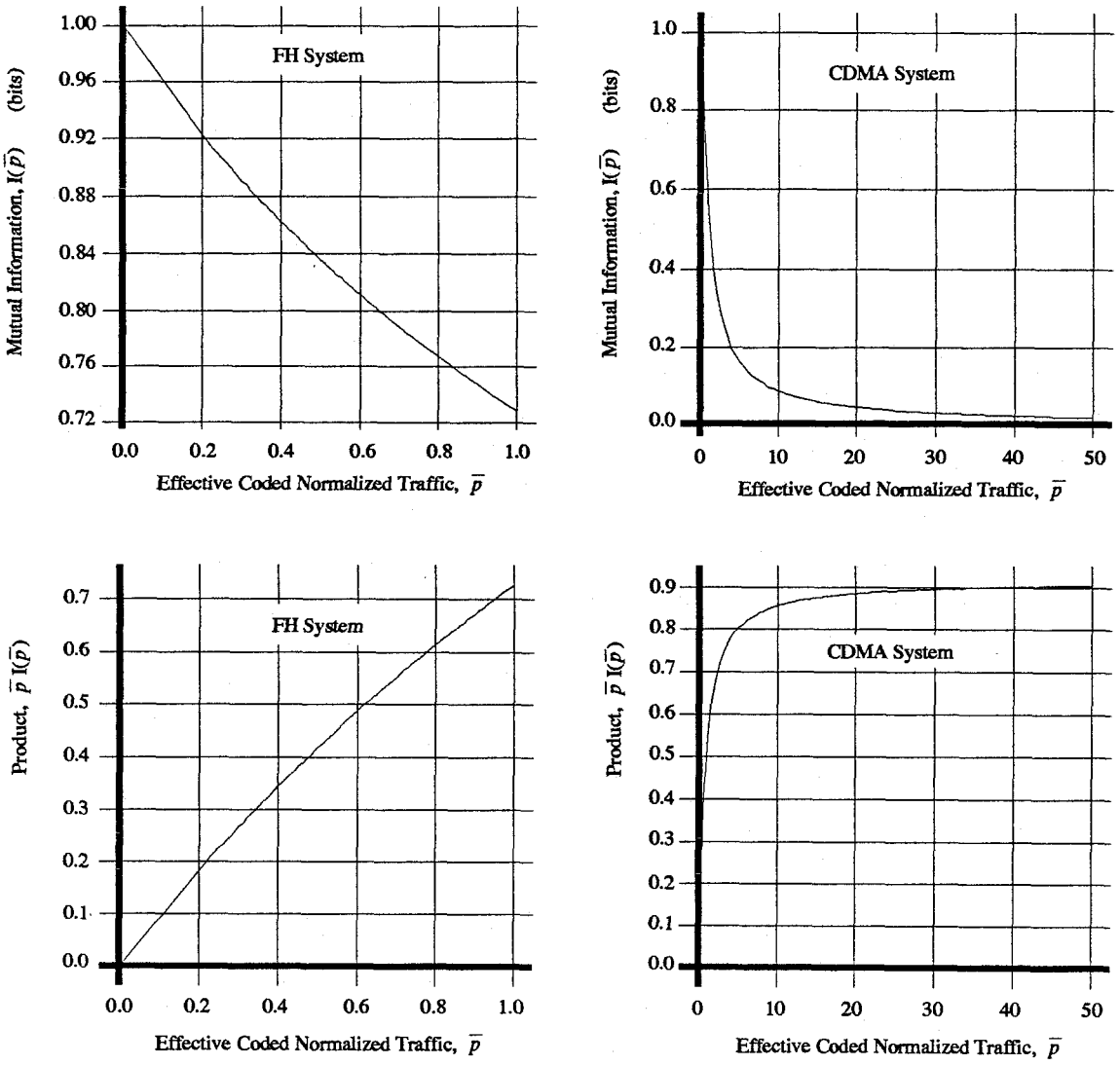

Figure 4.1: *Plots of the mutual information, $I(\bar{p})$, and the product, $\bar{p}I(\bar{p})$, versus the effective coded normalized traffic, $\bar{p}$, for the FH and CDMA systems.*

For the CDMA system, $\bar{p}I(\bar{p})$ achieves its maximum value as $\bar{p} \rightarrow \infty$. This limit is computed analytically in appendix A.8, and gives the result

$$\mathbf{C}_{\text{CDMA}}[\text{BPSK, Hard Decision, Fading}] = \frac{\log_2(e)}{2(a+1)} \left(\sum_k \pi_k \sqrt{b_k} \right)^2 . \tag{4.24}$$

For the channel model used in section 3.4 with an RMS delay spread of $3T_c$, this gives a capacity of 0.575.

For the purpose of comparison, capacity results for a nonfading channel can be obtained for FH and CDMA systems by using the corresponding expression for P_b given in chapter 2. For the FH

system, numerical computation gives

$$C_{FH}[\text{BPSK, Hard Decision, No Fading}] = 0.836. \tag{4.25}$$

For the CDMA system, capacity is achieved as $\bar{p} \rightarrow \infty$. This limit is computed analytically in appendix A.9, and gives the result

$$C_{CDMA}[\text{BPSK, Hard Decision, No Fading}] = \frac{\log_2(e)}{a+1} \cdot \frac{2}{\pi} = 0.630. \tag{4.26}$$

4.5 MASK Capacity

In this section, we attempt to extend these information-theoretic results to treat multilevel modulation schemes. In the BPSK system considered up to this point, a ± 1 symbol is used to modulate a sinusoidal carrier. We will now consider an MASK system where a multilevel signal is used to modulate a sinusoidal carrier. In particular, we will consider the limit as the number of levels approaches infinity and the sinusoidal carrier is modulated by a continuously varying signal level. The multipath fading characteristics of the channel remain the same and thus the statistical properties of the multiplicative fade are identical to that of the corresponding BPSK system. Under the assumption that power control is maintained, the mean and variance of the additive noise remain the same as in the corresponding BPSK system. However, the actual distribution of the additive noise is somewhat different because now each user can contribute a continuum of interference levels. In fact, the actual distribution becomes extremely complicated because it depends on the continuous probability density function with which each interfering user transmits. We will thus make the simplifying assumption that the additive interference has a Gaussian distribution for both the FH and CDMA systems and look for analytic solutions. Thus, equations (4.3), (4.4), and (4.5) for BPSK can be modified, in accordance with the previous comments, for MASK. This resulting MASK system model produces a receiver output of the form

$$Y = AX + Z, \tag{4.27}$$

where

X = continuous level codeword symbol transmitted,

A = multiplicative channel fade,

Z = zero-mean additive noise.

The additive noise, Z, is Gaussian with variance given by

$$\mathrm{Var}(Z) = \begin{cases} \frac{1}{2}a\bar{p} & \text{for FH,} \\ \frac{1}{2}(a+1)\bar{p} & \text{for CDMA,} \end{cases} \tag{4.28}$$

and the multiplicative fade is given by

$$A = \begin{cases} \text{Rayleigh} & \text{for FH,} \\ \text{Square root of sum of Rayleigh-squared} & \text{for CDMA.} \end{cases} \tag{4.29}$$

It is assumed, without loss of generality, that under power control all users are received at power level one. Thus,

$$\mathrm{E}\{X^2\} = 1. \tag{4.30}$$

We will first find the probability density function of X, $p_X(x)$, that maximizes the mutual information $I(X;Y \mid A)$. This mutual information can be written as

$$\begin{aligned} I(X;Y \mid A) &= \int_\alpha \int_x \int_y p_{A,X,Y}(\alpha,x,y) \log_2 \left(\frac{p_{Y|A,X}(y \mid \alpha, x)}{p_{Y|A}(y \mid \alpha)} \right) dy\, dx\, d\alpha, \\ &= \int_\alpha p_A(\alpha) \left[\int_x \int_y p_{X,Y|A}(x,y \mid \alpha) \log_2 \left(\frac{p_{Y|A,X}(y \mid \alpha, x)}{p_{Y|A}(y \mid \alpha)} \right) dy\, dx \right] d\alpha, \\ &= \int_\alpha p_A(\alpha) I(X;Y \mid A = \alpha) d\alpha. \end{aligned} \tag{4.31}$$

If the exact value of A is known, say $A = \alpha$, where α is a constant, then equation (4.27) is equivalent to the classical additive Gaussian noise channel ([11], pg. 247). In this case, it is known that the optimal choice for $p_X(x)$ is a Gaussian distribution, for which

$$I(X;Y \mid A = \alpha) = \frac{1}{2} \log_2 \left[1 + \frac{\alpha^2}{\sigma^2} \right], \tag{4.32}$$

where

$$\sigma^2 = \mathrm{Var}(Z). \tag{4.33}$$

Note that this choice of $p_X(x)$ is independent of the value of α, and thus maximizes $I(X;Y \mid A = \alpha)$ for *all* values of α, and hence is the maximizing distribution for $I(X;Y \mid A)$. Thus, we will take

$$p_X(x) = \frac{1}{\sqrt{2\pi}} e^{-\frac{x^2}{2}}. \tag{4.34}$$

The resulting mutual information is a function only of $\bar{p}$ and can thus be written as

$$I(\bar{p}) = I(X;Y \mid A) = \frac{1}{2}\int_{\alpha} p_A(\alpha)\log_2\left[1+\frac{\alpha^2}{\sigma^2}\right]d\alpha. \tag{4.35}$$

For the FH system, A has the Rayleigh probability density function given by equation (3.16). This gives

$$I(\bar{p}) = \frac{1}{2}\int_0^{\infty} 2\alpha e^{-\alpha^2}\log_2\left[1+\frac{\alpha^2}{\sigma^2}\right]d\alpha. \tag{4.36}$$

Making a change of variables and integrating by parts gives

$$I(\bar{p}) = \frac{\log_2(e)}{2}\left[-e^{\sigma^2}\mathrm{Ei}(-\sigma^2)\right], \tag{4.37}$$

where $\mathrm{Ei}(x)$ is the Exponential integrating function defined by

$$\mathrm{Ei}(x) = \int_{-\infty}^{x}\frac{e^t}{t}dt. \tag{4.38}$$

Finally, inserting the expression for σ^2, from equation (4.28) for FH, gives

$$I(\bar{p}) = \frac{\log_2(e)}{2}\left[-e^{\frac{1}{2}a\bar{p}}\mathrm{Ei}(-\frac{1}{2}a\bar{p})\right]. \tag{4.39}$$

Again, it turns out that the function $\bar{p}I(\bar{p})$ is a monotonically increasing function of $\bar{p}$. Thus, on the interval $[0,1]$, $\bar{p}I(\bar{p})$ achieves its maximum value at $\bar{p}=1$ giving a capacity of

$$C_{\mathrm{FH}}[\mathrm{MASK,\ Fading}] = \frac{\log_2(e)}{2}e^{\frac{a}{2}}[-\mathrm{Ei}(-\frac{a}{2})] = 1.010. \tag{4.40}$$

For the CDMA system, A has the probability distribution of the square root of a sum of Rayleigh-squared random variables, given by equation (3.59). This gives

$$\begin{aligned} I(\bar{p}) &= \int_0^{\infty}\sum_k \frac{\pi_k}{b_k}\alpha e^{-\frac{\alpha^2}{b_k}}\log_2\left[1+\frac{\alpha^2}{\sigma^2}\right]d\alpha, \\ &= \sum_k \frac{\pi_k}{b_k}\left(\int_0^{\infty}\alpha e^{-\frac{\alpha^2}{b_k}}\log_2\left[1+\frac{\alpha^2}{\sigma^2}\right]d\alpha\right). \end{aligned} \tag{4.41}$$

Making a change of variables and integrating by parts gives

$$I(\bar{p}) = -\frac{\log_2(e)}{2}\left[\sum_k \pi_k e^{\frac{\sigma^2}{b_k}}\mathrm{Ei}\left(-\frac{\sigma^2}{b_k}\right)\right]. \tag{4.42}$$

The definition of the Exponential integrating function, $\mathrm{Ei}(x)$, is given by equation (4.38). Finally, inserting the expression for σ^2, given in equation (4.28) for CDMA, gives

$$I(\bar{p}) = -\frac{\log_2(e)}{2}\left[\sum_k \pi_k e^{\frac{(a+1)\bar{p}}{2b_k}}\,\mathrm{Ei}\left(-\frac{(a+1)\bar{p}}{2b_k}\right)\right]. \tag{4.43}$$

Again, $\bar{p}(\bar{p})$ is a monotonically increasing function of $\bar{p}$ and thus achieves its maximum value as $\bar{p} \to \infty$. It is shown in appendix A.10 that as $\bar{p} \to \infty$ the capacity is given by

$$\mathbf{C}_{\mathrm{CDMA}}[\mathrm{MASK,\ Fading}] = \frac{\log_2(e)}{a+1} = 0.988. \tag{4.44}$$

For the purpose of comparison, capacity results for a nonfading channel can be obtained by setting $A = 1$ in equation (4.27) and noting that this reduces to the classical additive Gaussian noise channel. Thus, $I(\bar{p})$ is given by ([11], pg. 247)

$$I(\bar{p}) = \frac{1}{2}\log_2\left[1 + \frac{1}{\sigma^2}\right]. \tag{4.45}$$

For the FH system, we have

$$\bar{p}I(\bar{p}) = \frac{\bar{p}}{2}\log_2\left[1 + \frac{2}{a\bar{p}}\right], \tag{4.46}$$

which is a monotonically increasing function of $\bar{p}$. Thus, it achieves its maximum value at $\bar{p} = 1$ giving a capacity

$$\mathbf{C}_{\mathrm{FH}}[\mathrm{MASK,\ No\ Fading}] = \frac{1}{2}\log_2\left[1 + \frac{2}{a}\right] = 1.212. \tag{4.47}$$

Similarly, for the CDMA system, we have

$$\bar{p}I(\bar{p}) = \frac{\bar{p}}{2}\log_2\left[1 + \frac{2}{(a+1)\bar{p}}\right], \tag{4.48}$$

which is also a monotonically increasing function of $\bar{p}$. Taking the limit as $\bar{p} \to \infty$ gives

$$\mathbf{C}_{\mathrm{CDMA}}[\mathrm{MASK,\ No\ Fading}] = \frac{\log_2(e)}{a+1} = 0.988. \tag{4.49}$$

4.6 Capacity Results

Table 4.1 summarizes the information-theoretic results of this chapter. We see that using BPSK over a fading channel the CDMA system performs a little better than the FH system. The reason

	FH	CDMA
BPSK Soft Decision No Fading	0.896	$\frac{\log_2(e)}{a+1} = 0.988$
BPSK Soft Decision Fading	0.729	$\frac{\log_2(e)}{a+1} = 0.988$
BPSK Hard Decision No Fading	0.836	$\frac{2\log_2(e)}{\pi(a+1)} = 0.630$
BPSK Hard Decision Fading	0.599	$\frac{\log_2(e)}{2(a+1)}\left(\sum_k \pi_k\sqrt{b_k}\right)^2 = 0.575$
MASK No Fading	$\frac{1}{2}\log_2\left[1+\frac{2}{a}\right] = 1.21$	$\frac{\log_2(e)}{a+1} = 0.988$
MASK Fading	$\frac{\log_2(e)}{2}e^{\frac{a}{2}}[-\mathrm{Ei}(-\frac{a}{2})] = 1.01$	$\frac{\log_2(e)}{a+1} = 0.988$

Table 4.1: *Summary of information-theoretic results.*

for this is as follows. It is necessary to require that $\bar{p} \leq 1$ in order to maintain orthogonality in the FH system. Subsequently, if a low rate code were used, a relatively small number of users would use up all the system bandwidth. However, the CDMA system does not have this restriction and allows the use of codes with rates as low as $1/N$. This is demonstrated by the fact that for each FH entry in table 4.1, the capacity is approached as $\bar{p} \to 1$; for each CDMA entry, the capacity is approached as $\bar{p} \to \infty$. The fact that CDMA capacity is approached for $\bar{p} \to \infty$ agrees with the result in [12] which says that in a multiuser Direct Sequence CDMA system, the performance improves as the code rate decreases. Furthermore, we see that the capacity of CDMA is the same for fading and nonfading channels using BPSK and MASK. This is due to the fact that the information-theoretic analysis allows for arbitrarily complex codes at very low rates. Such codes allow the fading statistics to be averaged over an arbitrarily large number of samples offering an infinite diversity to the fading environment.

5. Channel Simulation.

5.1 Introduction.

The information-theoretic results of the previous chapter give the best possible system performance that can be achieved using arbitrarily complicated coding schemes. Unfortunately, arbitrarily complex codes include arbitrarily long block lengths, and thus arbitrarily long delays. In this chapter, we investigate the performance of specific coding schemes and the effects of a finite, controlled, delay using interleaving. These results are obtained primarily through simulation. We begin by looking at repetition codes and then consider an $(8,4)$ biorthogonal block code. For a specific code, it is possible to measure the performance for infinite interleaving and zero interleaving. To evaluate the performance using infinite interleaving, it is assumed that each codeword symbol sees independent channel statistics. On the other hand, the performance using zero interleaving is evaluated by assuming that each codeword symbol sees an identical, 100% correlated, channel. Finally, making some assumptions about the vehicle speed and transmitter frequency, we evaluate performance using a finite amount of interleaving delay by taking into account the actual amount of correlation among channel samples as seen from one codeword symbol to the next.

5.2 Repetition Codes.

In this section, we compute the average probability of bit error for FH and CDMA over a frequency selective Rayleigh fading channel using D-fold repetition codes. Each data bit is transmitted D times. Note that the code rate, r_{code}, is equal to $1/D$. Thus, the effective coded normalized traffic, $\bar{p}$, is given by

$$\bar{p} = Dp. \tag{5.1}$$

We begin by considering the infinite interleaving performance where each of these D transmissions experiences independent channel statistics. Consider the transmission of a single codeword of D symbols. A maximum likelihood receiver for this system consists of D simple BPSK receivers ([1], pg. 721). With respect to equations (4.3), (4.4), and (4.5), each receiver output is of the form

$$Y_m = A_m X + Z_m, \qquad (m = 1, 2, \ldots, D) \tag{5.2}$$

where

$$X = \pm 1 \text{ data bit},$$

$$A_m = \text{multiplicative channel fade},$$

$$Z_m = \text{zero-mean additive noise}.$$

The additive noise samples, Z_m, are taken to be *i.i.d.* each having variance

$$\sigma^2 = \begin{cases} \frac{1}{2}aDp & \text{for FH}, \\ \frac{1}{2}(a+1)Dp & \text{for CDMA}. \end{cases} \tag{5.3}$$

The multiplicative fades, A_m, are also taken to be *i.i.d.* and of the form

$$A_m = \begin{cases} \text{Rayleigh} & \text{for FH}, \\ \text{Square root of sum of Rayleigh-squared} & \text{for CDMA}. \end{cases} \tag{5.4}$$

The maximum likelihood receiver forms the decision variable Y as a weighted sum of the Y_m's given by

$$Y = \sum_{m=1}^{D} A_m Y_m = \sum_{m=1}^{D} A_m^2 X + \sum_{m=1}^{D} A_m z_m. \tag{5.5}$$

Thus, the maximum likelihood receiver for a D-fold repetition code produces an output of the form

$$Y = AX + Z, \tag{5.6}$$

where

$$A = \sum_{m=1}^{D} A_m^2, \tag{5.7}$$

and

$$Z = \sum_{m=1}^{D} A_m z_m. \tag{5.8}$$

The random variable Z thus has a variance, conditioned of the values of the A_m's, given by

$$\text{Var}(Z \mid A_1, A_2, \ldots, A_D) = \left(\sum_{m=1}^{D} A_m^2 \right) \sigma^2 = A\sigma^2. \tag{5.9}$$

For the FH system, the A_m's are *i.i.d.* Rayleigh random variables. Each of the terms A_m^2 can then equivalently be expressed as the sum of two *i.i.d.* Gaussian random variables having mean

zero and variance 1/2. Thus, A is has a chi-square distribution with $2D$ degrees of freedom. The probability density function of A is then given by ([1], pg. 26)

$$p(A) = \frac{1}{(D-1)!} A^{D-1} e^{-A}, \qquad (A > 0). \tag{5.10}$$

At this point, the probability of bit error performance can be computed numerically using the FH additive noise distribution found in appendix A.3. For the purpose of comparison, if the additive noise term, Z, is approximated with a zero-mean Gaussian distribution with conditional variance given by equation (5.9), the probability of bit error can be determined analytically as follows. This approximation is justified by the fact that, for a fading channel, the performance curves using the exact distribution and the Gaussian distribution are very similar as shown in figure 3.5. The probability of bit error conditioned on the random variable A is given by

$$P_b(A) = \frac{1}{2}\text{erfc}\left(\sqrt{\frac{A}{aDp}}\right). \tag{5.11}$$

Averaging equation (5.11) over the probability distribution of A gives

$$P_b = \int_0^\infty \frac{1}{(D-1)!} A^{D-1} e^{-A} \frac{1}{2}\text{erfc}\left(\sqrt{\frac{A}{aDp}}\right) dA. \tag{5.12}$$

Making use of the integration formula of appendix A.11, the probability of bit error, P_b, can be expressed as

$$P_b = \left(\frac{1-\mu}{2}\right)^D \sum_{k=0}^{D-1} \binom{D+k-1}{k} \left(\frac{1+\mu}{2}\right)^k, \tag{5.13}$$

where

$$\mu = \sqrt{\frac{1}{1+aDp}}. \tag{5.14}$$

Note that equation (5.13) is identical to BPSK signaling over a slowly-varying frequency non-selective fading channel with diversity D ([1], pg. 723).

For the CDMA system, the A_m's are *i.i.d.* random variables with the probability distribution given by equation (3.59). Assuming the additive noise term, Z, has a Gaussian distribution with conditional variance given by equation (5.9), the probability of bit error conditioned on the random variable A is given by

$$P_b(A) = \frac{1}{2}\text{erfc}\left(\sqrt{\frac{A}{(a+1)Dp}}\right). \tag{5.15}$$

In appendix A.12, it is shown that for a RAKE receiver with L taps, averaging equation (5.15) over the probability distribution of A gives

$$P_b = \sum_{q=0}^{L-1} \pi_q^D \sum_{k=0}^{D-1} F(q,k) \left(\frac{1-\mu_q}{2}\right)^{(D-k)} \sum_{l=0}^{(D-k-1)} \binom{D-k-1+l}{l} \left(\frac{1+\mu_q}{2}\right)^l, \tag{5.16}$$

where

$$\mu_q = \sqrt{\frac{b_q}{(a+1)Dp + b_q}}, \tag{5.17}$$

$$F(q,k) = (-1)^k \sum_{S(q,k)} \left[\prod_{j=0}^{L-1} \binom{m_j + D - 1}{D-1} \left(\frac{b_j}{b_q - b_j}\right)^{m_j} \right], \tag{5.18}$$

$$S(q,k) = \left\{ (m_0, m_1, \ldots, m_{L-1}) : m_j = \text{nonnegative integer} \; ; \quad \sum_{j=0}^{L-1} m_j = k; \quad m_q = 0 \right\}. \tag{5.19}$$

The definition of π_q appears in equation (3.60).

The zero interleaving performance of repetition codes turns out to be equivalent to that of not using any coding. Each of the D codeword symbols is assumed to see exactly the same fade A_m. For the FH system, each user transmits simultaneously over D frequency channels. Assuming that each channel sees the same fade is equivalent to assuming that the spacing among these D channels is sufficiently small compared to the coherence bandwidth of the channel. Furthermore, it is assumed that the interference seen in each of these D channels is due to independent users and thus the additive noise terms are taken to be independent. For the CDMA system, assuming that each codeword symbol sees the same fade is equivalent to assuming that the fading process is slow compared to the bit time, T_b. Also, since users in the CDMA system are assumed to have random, mutually independent, PN sequences, the additive noise terms are taken to be independent in the CDMA system as well. Thus, for each codeword symbol, both the FH and CDMA systems produce an output of the form

$$Y_m = AX + Z_m, \qquad (m = 1, 1, \ldots, D) \tag{5.20}$$

where the Z_m's are independent and each have variance given by equation (5.3), and the multiplicative fade A has a distribution given by equation (5.4). A maximum likelihood receiver then forms

the decision variable Y as the average of the Y_m's given by

$$\begin{aligned} Y &= \frac{1}{D}\sum_{m=1}^{D} Y_m, \\ &= AX + \frac{1}{D}\sum_{m=1}^{D} Z_m, \\ &= AX + Z, \end{aligned} \tag{5.21}$$

where

$$Z = \frac{1}{D}\sum_{m=1}^{D} Z_m. \tag{5.22}$$

Note that since the Z_m's are *i.i.d.*, the variance of Z is given by

$$\mathrm{Var}(Z) = \frac{1}{D}\mathrm{Var}(Z_m), \tag{5.23}$$

where $\mathrm{Var}(Z_m)$ is given by equation (5.3). This gives

$$\mathrm{Var}(Z) = \begin{cases} \frac{1}{2}ap & \text{for FH,} \\ \frac{1}{2}(a+1)p & \text{for CDMA,} \end{cases} \tag{5.24}$$

which is exactly the same as equation (3.66) for no coding. If the additive noise terms, Z_m, are taken to be Gaussian, then Z is also Gaussian. Thus, CDMA system performance is exactly the same as that of no coding. Even if the additive noise terms, Z_m, are not taken to be Gaussian, by the central limit theorem the random variable Z approaches a Gaussian for large D. Thus, FH system performance will lie between the no coding performance using the exact distribution of the additive noise derived in appendix A.3 and the performance using a Gaussian approximation for the additive noise. Note, however, that the FH system is now restricted to values of normalized traffic that satisfy $p \leq 1/D$.

Remark: The fact that for CDMA, the zero interleaving performance of repetition codes is exactly the same as that of no coding is a tautology. Consider the uncoded CDMA transmitter shown in figure 3.3. In each bit interval, the signal $u(t)$ is the product of the data bit and the PN sequence. If a repetition encoder were inserted into the system, each data bit would be repeated D times, and the duration of each of these codeword symbols would be T_b/D. Nevertheless, over a full bit interval, the signal $u(t)$ would still be the same product of the data bit and the PN sequence.

5.3 Binary Block Codes

In this section, we will compare the performances of FH and CDMA systems over the frequency selective Rayleigh fading channel using binary (n, k) block codes ([10], pg. 47). The performance will be evaluated through simulation of an ideal soft decision decoder ([1], pg. 400). Binary, $\{0, 1\}$, codewords are changed to ± 1 codewords by changing 0 to -1. We begin by defining the parameters of the code. Let

$n =$ number of ± 1 symbols per codeword,

$k =$ number of information bits per codeword,

$M = 2^k =$ number of codewords in the code,

$C_i(m) =$ symbol m (± 1) of codeword i, $\quad (m \in [0, n-1], i \in [0, M-1])$

$C_{Tr}(m) =$ symbol m (± 1) of the *transmitted* codeword.

Note that the code rate, r_{code}, is equal to k/n. Thus, the effective coded normalized traffic, $\bar{p}$, is given by

$$\bar{p} = \frac{n}{k} p. \tag{5.25}$$

We begin by considering the infinite interleaving performance where each of the n symbols of a codeword experience independent channel statistics. Consider the transmission of a single codeword. With respect to equations (4.3), (4.4), and (4.5), each of these n codeword symbols is received as

$$Y_m = A_m C_{Tr}(m) + Z_m, \qquad (m = 0, 1, \ldots, n-1) \tag{5.26}$$

where

$A_m =$ multiplicative channel fade,

$Z_m =$ zero-mean additive noise.

The additive noise samples, Z_m, are taken to be *i.i.d.*, each having variance

$$\sigma^2 = \begin{cases} \frac{n}{2k} ap & \text{for FH,} \\ \frac{n}{2k}(a+1)p & \text{for CDMA.} \end{cases} \tag{5.27}$$

The multiplicative fades, A_m, are also taken to be *i.i.d.* and of the same form as with the use of repetition codes given by equation (5.4). Soft decision decoding is performed by computing the M

decision variables

$$D_i = \sum_{m=0}^{n-1} A_m Y_m C_i(m), \qquad (i = 0, 1, \ldots, M-1) \tag{5.28}$$

and choosing the codeword corresponding to the largest D_i. For the zero interleaving performance, each codeword symbol is received as

$$Y_m = AC_{Tr}(m) + Z_m, \qquad (m = 0, 1, \ldots, n-1) \tag{5.29}$$

where A is the channel fade having distribution given by equation (5.4), and the Z_m remain *i.i.d.* zero-mean with variance given by equation (5.3). The decision variables are now

$$D_i = \sum_{m=0}^{n-1} Y_m C_i(m), \qquad (i = 0, 1, \ldots, M-1). \tag{5.30}$$

At this point, the infinite interleaving and zero interleaving performance of a specific block code can be evaluated for both FH and CDMA systems by simulating the transmission of a large number of codewords using the appropriate channel statistics.

5.4 Channel Simulation Results

We wish to compare the performances of FH and CDMA using repetition codes and also using an (8,4) biorthogonal block code with generator matrix

$$G = \begin{pmatrix} 1 & 0 & 0 & 0 & 1 & 1 & 0 & 1 \\ 0 & 1 & 0 & 0 & 0 & 1 & 1 & 1 \\ 0 & 0 & 1 & 0 & 1 & 1 & 1 & 0 \\ 0 & 0 & 0 & 1 & 1 & 0 & 1 & 1 \end{pmatrix}. \tag{5.31}$$

The performances of these systems were obtained by simulating the transmission of a large number of random codewords and counting the number of bits in error. This simulation was iterated over many values of the normalized traffic, p, to generate plots of bit error probability versus normalized traffic. Figure 5.1 shows the performances of FH and CDMA for the cases of no coding, repeat coding with diversity two, and the (8,4) code with infinite interleaving. The information-theoretic capacity results from the previous chapter are also shown. We see that there is an increase in performance when going from no coding to two-fold repetition coding and then to the (8,4) biorthogonal code. Nevertheless, we also see that these performances are all far below the information-theoretic limits. Figure 5.2 shows the performances of FH and CDMA with the (8,4) code for infinite interleaving,

zero interleaving, and 20ms of interleaving. The simulation for 20ms of interleaving assumes a transmit frequency of 880MHz, a vehicle speed of 30mph, a data rate, R, of 9600bps, and total system bandwidth, B, of 1.23MHz. The value of N is thus, $N = B/R = 128$. The correlation among channel parameters from one codeword symbol to the next was simulated according to the Bessel function correlation of equation (3.9). For the FH system, a hopping rate of 100Hz (1 hop every 10ms) was simulated. The simulation used random hopping over the 128 FH channels and incorporated the effects of nonzero correlation among channels due to finite frequency separation. The power delay profile of the channel was assumed to be exponential with RMS delay spread equal to $3T_c$. We see that 20ms of interleaving offers significant improvement over zero interleaving. We also see that the effect of zero interleaving versus infinite interleaving is more drastic to the FH system than to the CDMA system. As in the previous sections, the performance curves of both systems cross, with the FH system better at larger levels of traffic, and the CDMA system better at smaller levels of traffic.

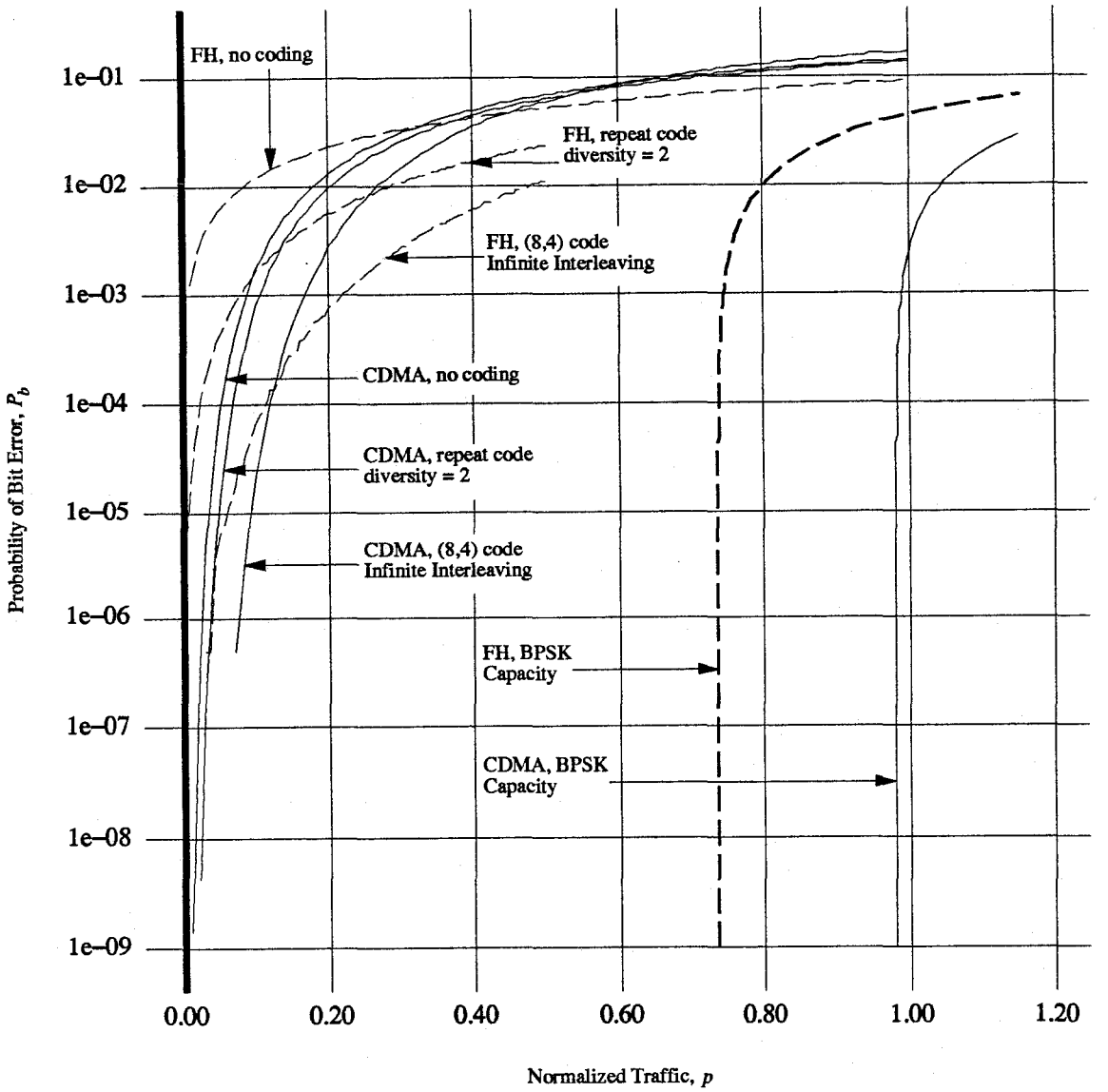

Figure 5.1: *Probability of bit error versus normalized traffic, p, for FH and CDMA systems over a fading channel using no code, repetition code with diversity two, and (8,4) block code with infinite interleaving. The information-theoretic capacity curves are also shown.*

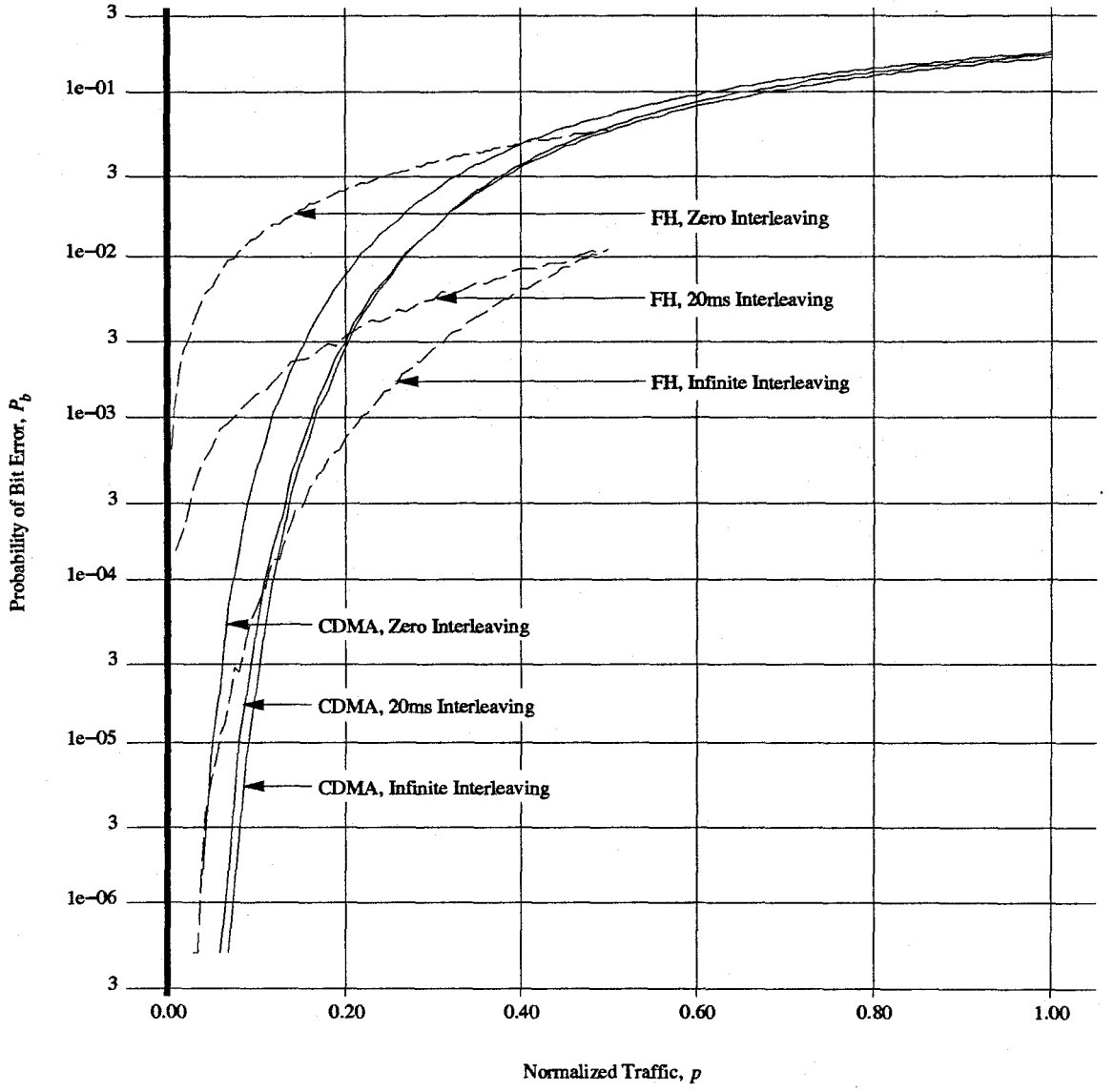

Figure 5.2: *Probability of bit error versus normalized traffic,p, for FH and CDMA systems using (8,4) block code. The performance for infinite interleaving, zero interleaving, and 20ms interleaving are shown.*

6. Some Properties of Memoryless Multiterminal Interference Channels

6.1 Introduction

This chapter is not closely related to the rest of this paper. Here we look at the information-theoretic problem of interference channels when there is no assumption that users do not cooperate on the level of coding. Very few results in the area of multiuser information theory are known. A general formula for the capacity of such channels is presented, however, this formula does not easily lend itself to computation. Alternatively, if the channel inputs are taken to be vectors of length N, examining the mutual informations among the input and output N-vectors gives achievable points in the capacity region. We examine the nature of these regions for small values of N. Two specific two-user interference channels are considered: a Gaussian interference channel and a binary interference channel. The Gaussian interference channel turns out to be a special case where the capacity region is actually known. It is shown that certain probability distributions on the input achieve points on the boundary of the capacity region for $N = 2$. For the binary interference channel, the capacity is in general not known. Our numerical results suggest that the capacity region can be determined by knowledge of the achievable region for $N = 1$. However, we have not been able to prove this result and it thus remains a conjecture.

6.2 Information Theory

We begin by considering the two-user interference channel shown in figure 6.1. It is desired that two independent users each communicate simultaneously with a single receiver. That is, source one communicates with receiver one at rate R_1, and source two communicates with receiver two at rate R_2. The multiterminal channel takes inputs, x_1 and x_2, from the channel input alphabet and produces outputs, y_1 and y_2, from the channel output alphabet according to the conditional probability distribution $p(y_1, y_2 \mid x_1, x_2)$. We assume that the channel outputs are independent conditioned on the inputs. That is,

$$p(y_1, y_2 \mid x_1, x_2) = p(y_1 \mid x_1, x_2)p(y_2 \mid x_1, x_2). \tag{6.1}$$

We are interested in the capacity region, i.e., the set of all rates (R_1, R_2) for which it is possible to communicate with an arbitrarily small probability of error.

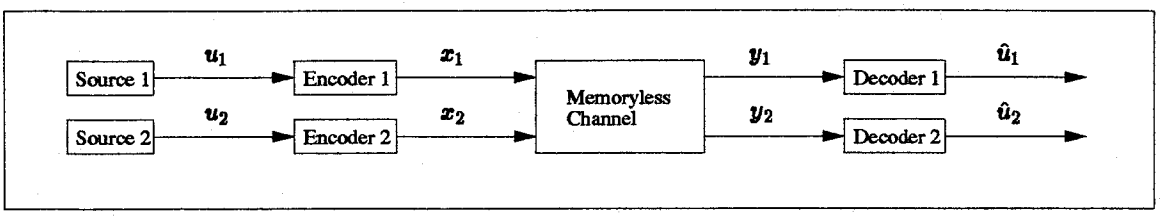

Figure 6.1: *Two-user interference channel. Each user independently communicates with a single receiver.*

Theorem: The capacity region of the two-user interference channel is given by

$$\mathbf{C} = \text{Closure}\left\{\bigcup_{N=1}^{\infty}\bigcup_{\mathbf{P}} R\left[\frac{1}{N}I(\mathbf{X}_1;\mathbf{Y}_1), \frac{1}{N}I(\mathbf{X}_2;\mathbf{Y}_2)\right]\right\}, \tag{6.2}$$

where $\mathbf{X}_1$, $\mathbf{X}_2$, $\mathbf{Y}_1$, $\mathbf{Y}_2$ are N-vectors, $\mathbf{P}$ is the set of all independent probability distributions on $\mathbf{X}_1$ and $\mathbf{X}_2$, and

$$R[x,y] = \{(R_1,R_2) : 0 \le R_1 \le x, \quad \text{and} \quad 0 \le R_2 \le y\}. \tag{6.3}$$

Unfortunately, this capacity formula does not lend itself to computation because the union is over all possible values of the vector size, N, from one to infinity. In general, given an arbitrary two-user interference channel, it is currently not known how to compute the capacity region. An interesting approach to this problem is to investigate the behavior of the mutual information functions for specific values of the vector size, N. Consider the following *achievable* region

$$\mathbf{A}_N = \left\{\bigcup_{\mathbf{P}} R\left[\frac{1}{N}I(\mathbf{X}_1;\mathbf{Y}_1), \frac{1}{N}I(\mathbf{X}_2;\mathbf{Y}_2)\right]\right\} \subseteq \mathbf{C}, \tag{6.4}$$

where P is the set of all independent probability distributions on the N-vectors $\mathbf{X}_1$ and $\mathbf{X}_2$. The full capacity region is given by the union of the A_N's as N varies from one to infinity. We are interested in the behavior of the A_N's for small values of N. This interest is motivated by the fact that for a single-user memoryless channel, $(1/N)\sup[I(\mathbf{X};\mathbf{Y})]$ is independent of N (where $\mathbf{X}$ and $\mathbf{Y}$ are N-vectors and the suprema is taken over all probability distributions on $\mathbf{X}$). In other words, for the single-user channel, the capacity can be determined by considering only $N = 1$ rather than having to let N tend to infinity. Perhaps there is an analogous simplification for the multiuser channel.

6.3 Additive Gaussian Interference Channel

For the additive Gaussian interference channel, the channel outputs, y_1 and y_2, are given by

$$y_1 = x_1 + x_2 + z_1, \tag{6.5}$$

$$y_2 = x_1 + x_2 + z_2, \tag{6.6}$$

where z_1 and z_2 are *i.i.d.* Gaussian random variables with mean zero and variance one. The independent channel inputs, x_1 and x_2, are required to satisfy $\mathrm{E}\{x_1^2\} \leq 1$, and $\mathrm{E}\{x_2^2\} \leq 1$. Since y_1 and y_2 are statistically equivalent, this multiterminal channel is a special case where the capacity region is actually known [13]. The capacity region is

$$\mathbf{C} = \left\{(R_1, R_2) : \ 0 \leq R_1 \leq \frac{1}{2}, \ 0 \leq R_2 \leq \frac{1}{2}, \text{ and } R_1 + R_2 \leq \log_2(3)\right\} \qquad \text{(bits)}. \tag{6.7}$$

We consider only a subset of the A_N's where the channel inputs have zero-mean Gaussian distributions. For $N = 1$, x_1 and x_2 are independent Gaussian random variables with variances σ_1^2 and σ_2^2 respectively. Letting σ_1^2 and σ_2^2 vary independently between zero and one, we obtain the shaded region shown in figure 6.2. The boundary of the capacity region, given by equation (6.7), is also shown in figure 6.2. We observe that the shaded region is in fact a subset of the capacity region and also that it does not contain any points on the boundary of the capacity region (except for the trivial points $R_1 = 0$, $R_2 = \frac{1}{2}$ and $R_1 = \frac{1}{2}$, $R_2 = 0$). For $N = 2$, let

$$\mathbf{X}_1 = [x_{11} \quad x_{12}], \qquad \text{and} \qquad \mathbf{X}_2 = [x_{21} \quad x_{22}]. \tag{6.8}$$

Here, $\mathbf{X}_1$ and $\mathbf{X}_2$ are each given joint Gaussian distributions. For $\mathbf{X}_1$, x_{11} and x_{12} are joint Gaussian with variances σ_{11}^2 and σ_{12}^2 respectively and correlation coefficient τ_1. Similarly, the joint Gaussian distribution for $\mathbf{X}_2$ is characterized by σ_{21}^2, σ_{22}^2, and τ_2. Hence, there are six parameters to specify in order to compute a single point in the A_2 region. By setting $\sigma_{11}^2 = \sigma_{12}^2 = \sigma_{21}^2 = \sigma_{22}^2 = 1$ and varying τ_1 and τ_2 independently between -1 and 1, we obtain the shaded region shown in figure 6.2. In particular, we see that A_2 contains a nontrivial point on the boundary of the capacity region. This point is achieved for $(\tau_1 = 1, \tau_2 = -1)$ and also for $(\tau_1 = -1, \tau_2 = 1)$. Thus, it appears that

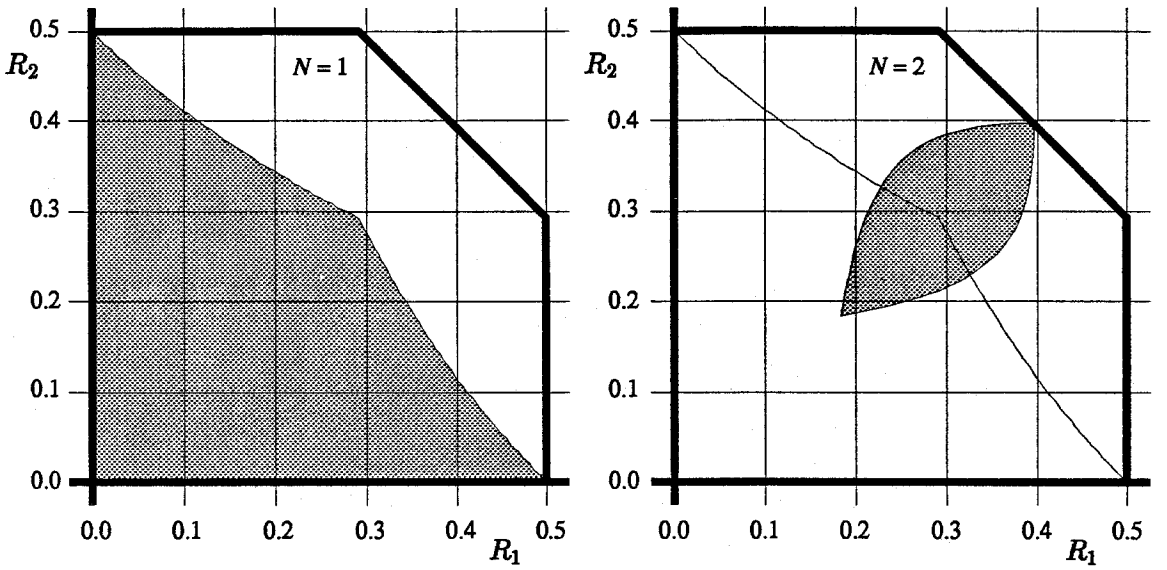

Figure 6.2: *Some achievable points in A_1 and A_2 for the Gaussian interference channel.*

the the expression for capacity given by equation (6.2) does not approach its limit "continuously" as N tends to infinity because this boundary point is achieved for $N = 2$.

6.4 Binary Interference Channel

The binary interference channel is a discrete channel where the channel input symbols and channel output symbols belong to the binary set $\{0, 1\}$. This channel is described as follows. If $x_2 = 0$, there is perfect transmission between x_1 and y_1. That is, if $x_2 = 0$, then $y_1 = x_1$. If $x_2 = 1$, then x_1 and y_1 see a binary symmetric channel with crossover probability ϵ. That is, if $x_2 = 1$, then $y_1 = x_1$ with probability $1 - \epsilon$ and $y_1 \neq x_1$ with probability ϵ. This channel is also symmetric with respect to each input-output pair. Thus, $x_1 = 0$ implies $y_2 = x_2$, and $x_1 = 1$ implies a binary symmetric channel with crossover probability ϵ between x_2 and y_2. Table 6.1 gives a complete description of the conditional probability function $p(y_1, y_2 \,|\, x_1, x_2)$.

There are two special cases, $\epsilon = 0$ and $\epsilon = 1$, for which the capacity region can be determined exactly. For $\epsilon = 0$, there is no interference; $y_1 = x_1$ and $y_2 = x_2$. Thus, the capacity region is the entire square $\{(R_1, R_2) : \ 0 \leq R_1 \leq 1, \text{ and } 0 \leq R_2 \leq 1\}$, as shown in figure 6.3. For $\epsilon = 1$, we have $y_2 = y_1 = x_1 + x_2 \pmod 2$. Since y_1 and y_2 are equal, the channel is reduced to a multiaccess

x_1	x_2	y_1	y_2	$p(y_1, y_2 \mid x_1, x_2)$
0	0	0	0	1
0	0	0	1	0
0	0	1	0	0
0	0	1	1	0
0	1	0	0	0
0	1	0	1	$1-\epsilon$
0	1	1	0	0
0	1	1	1	ϵ
1	0	0	0	0
1	0	0	1	0
1	0	1	0	$1-\epsilon$
1	0	1	1	ϵ
1	1	0	0	ϵ^2
1	1	0	1	$\epsilon(1-\epsilon)$
1	1	1	0	$\epsilon(1-\epsilon)$
1	1	1	1	$(1-\epsilon)^2$

Table 6.1: *Conditional probability function, $p(y_1 y_2 \mid x_1 x_2)$, for the binary interference channel.*

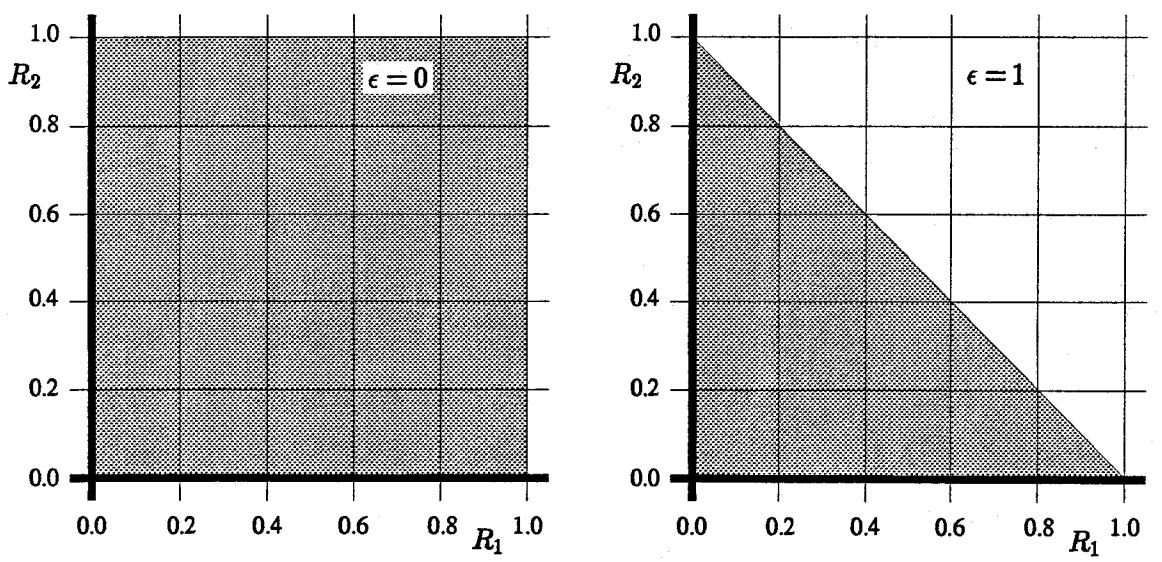

Figure 6.3: *Capacity regions of the binary interference channel for $\epsilon = 0$ and $\epsilon = 1$.*

channel, and the capacity region can be computed using the results of ([11], pg. 334). In this case, the capacity region is given by $\{(R_1, R_2):\ 0 \leq R_1,\ 0 \leq R_2,\ \text{and}\ R_1 + R_2 \leq 1\}$ which is also shown in figure 6.3.

We proceed to compute A_N for $N = 1$ and $N = 2$. For $N = 1$, let

$$\begin{aligned} p_0 &= \Pr\{x_1 = 0\}, \qquad q_0 = \Pr\{x_2 = 0\}, \\ p_1 &= \Pr\{x_1 = 1\}, \qquad q_1 = \Pr\{x_2 = 1\}. \end{aligned} \tag{6.9}$$

Varying these four parameters under the constraints that $p_0 + p_1 = 1$ and $q_0 + q_1 = 1$, we obtain the shaded regions shown in figure 6.4 for $\epsilon = 0.1$ and $\epsilon = 0.7$. For $N = 2$, let

$$\begin{aligned} p_{00} &= \Pr\{\mathbf{X}_1 = [00]\}, \qquad q_{00} = \Pr\{\mathbf{X}_2 = [00]\}, \\ p_{01} &= \Pr\{\mathbf{X}_1 = [01]\}, \qquad q_{01} = \Pr\{\mathbf{X}_2 = [01]\}, \\ p_{10} &= \Pr\{\mathbf{X}_1 = [10]\}, \qquad q_{10} = \Pr\{\mathbf{X}_2 = [10]\}, \\ p_{11} &= \Pr\{\mathbf{X}_1 = [11]\}, \qquad q_{11} = \Pr\{\mathbf{X}_2 = [11]\}. \end{aligned} \tag{6.10}$$

Varying these eight parameters under the constraints that $p_{00} + p_{01} + p_{10} + p_{11} = 1$ and $q_{00} + q_{01} + q_{10} + q_{11} = 1$, we obtain the shaded regions shown in figure 6.4 for $\epsilon = 0.1$ and $\epsilon = 0.7$. For $\epsilon = 0.1$, the regions A_1 and A_2 appear identical. We have not been able to prove this, but within the accuracy and resolution of our numerical calculations and plots, the regions A_1 and A_2 are indistinguishable. For $\epsilon = 0.7$, A_2 appears to be a rate $\frac{1}{2}$ timesharing version of A_1. That is, A_2 appears to be the union of A_1 and all points halfway between two points in A_1. A timesharing argument, similar to the argument in [14], can be used to argue that all such points are in A_2, however, we have not been able to prove that these are the only points in A_2. With respect to these observations, we make the following conjecture.

Conjecture: The capacity region of the binary interference channel defined by table 6.1 is

$$\mathbf{C} = \text{Convex Hull}\{A_1\}. \tag{6.11}$$

The fact that Convex Hull $\{A_1\} \subseteq \mathbf{C}$ follows from a timesharing argument. It only remains to be proven that there are no points outside Convex Hull $\{A_1\}$ that are in $\mathbf{C}$.

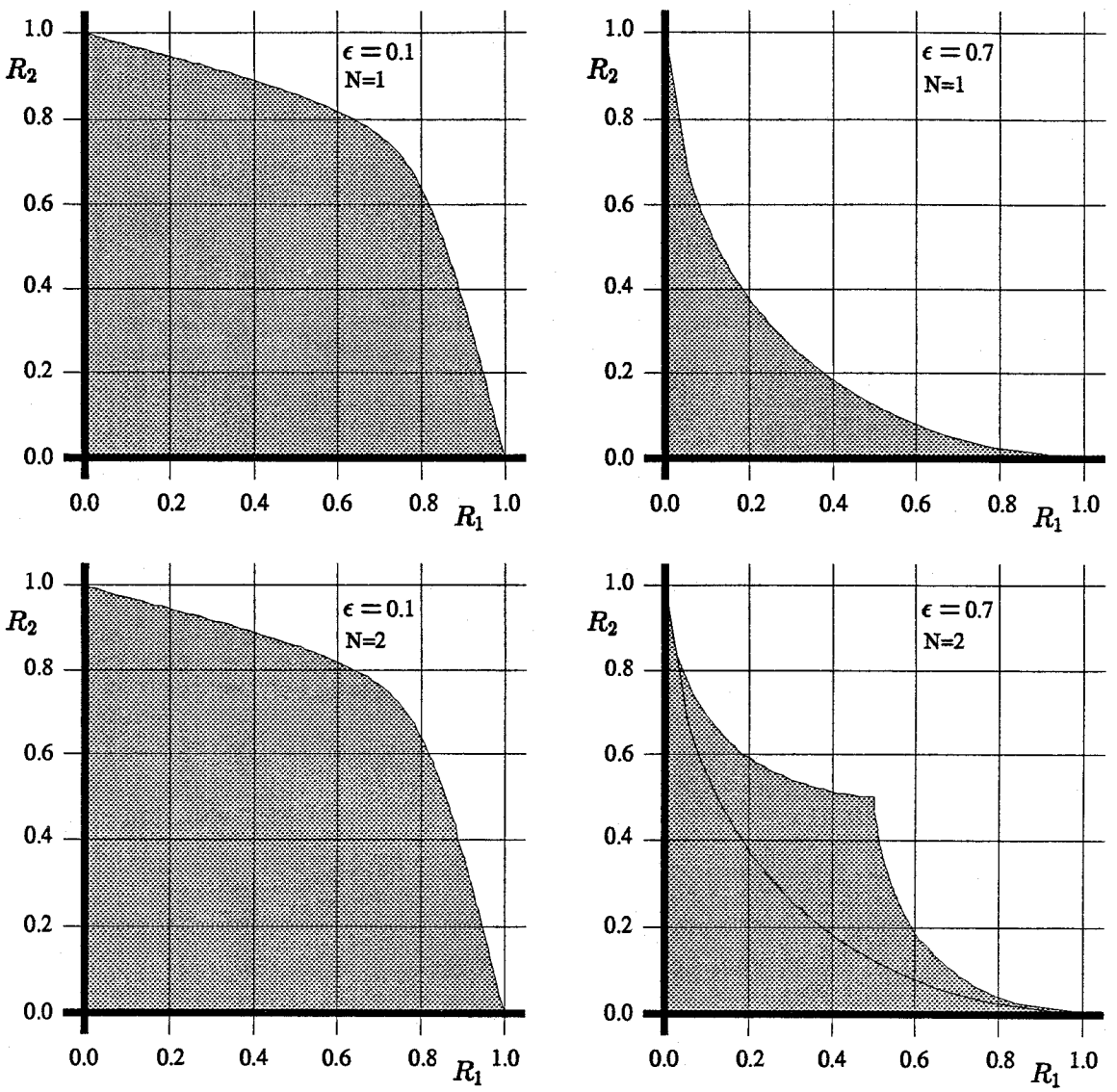

Figure 6.4: *The regions A_1 and A_2 of the binary interference channel are shown for $\epsilon = 0.1$ and $\epsilon = 0.7$.*

7. Conclusions and Future Work

We have seen that an information-theoretic capacity can be defined, and that CDMA has a larger capacity than FH when BPSK modulation is used in a fading environment. This theoretical advantage of CDMA is due to the fact that, unlike the FH system, by not requiring that the users in a sector maintain orthogonality, it is possible for a large amount of traffic to communicate using very low rate codes. However, for the codes we have simulated it is unclear which system performs better because the performance curves cross. There is a tradeoff in performance between the lower interference power in the FH system and the ability to combat frequency selective fading in the CDMA system. There are a number of different ways in which this work can be expanded upon. Probably one of the most important is to try to incorporate the effects of shadowing into the analysis. Shadowing is a function of the actual geometry of the system, i.e., the locations of buildings, mountains, etc. Furthermore, inasmuch as the geometry of a system is fixed and not changing in time, the shadowing parameters are fixed for a given system. It thus seems reasonable to expect that, for a given system, the information-theoretic capacity would be a function of these shadowing parameters, and hence of its geometrical configuration. In this paper, we have solved the problem where the geometry is "flat" so there is no shadowing. Perhaps, given an arbitrary geometrical configuration, it is possible to compute an information-theoretic capacity. If this could be done, then perhaps by considering a random distribution on the geometrical configuration of the system, a probability distribution function could be found for the information-theoretic capacity. Another way in which this work could be improved upon would be to consider other forms of modulation. Finally, it would be interesting to try to simulate more complex codes to see how close the performance curves come to the information-theoretic limits.

A. Appendix

A.1 Geometrical Properties of a Hexagonal Grid

It is assumed without loss of generality that the dimensions of the hexagonal grid are normalized such that the distance between the centers of adjacent cells is unity.

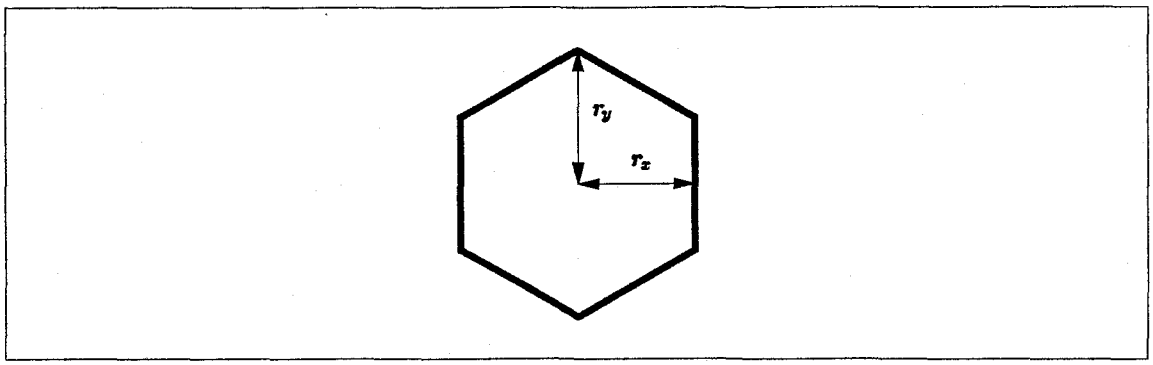

Figure A.1: *Single cell in a normalized hexagonal grid.*

Thus, each cell in the system has the following geometrical measurements:

$$r_x = \frac{1}{2}, \tag{A.1}$$

$$r_y = \frac{\sqrt{3}}{3}, \tag{A.2}$$

$$A_{\text{cell}} = \text{Cell Area} = \frac{\sqrt{3}}{2}, \tag{A.3}$$

$$A_{\text{sec}} = \text{Sector Area} = \frac{\sqrt{3}}{6} = \frac{1}{2\sqrt{3}}. \tag{A.4}$$

If a rectangular coordinate system with origin at the center of cell $(0,0)$ is imposed on this geometry, as shown in figure A.2, the center of cell (i,j) has coordinates (x_{ij}, y_{ij}) given by

$$x_{ij} = i + \frac{1}{2}j, \tag{A.5}$$

$$y_{ij} = \frac{\sqrt{3}}{2}j. \tag{A.6}$$

The distance between the center of cell $(0,0)$ and the center of cell (i,j), denoted by R_{ij}, is then given by

$$R_{ij}^2 = x_{ij}^2 + y_{ij}^2 = i^2 + j^2 + ij. \tag{A.7}$$

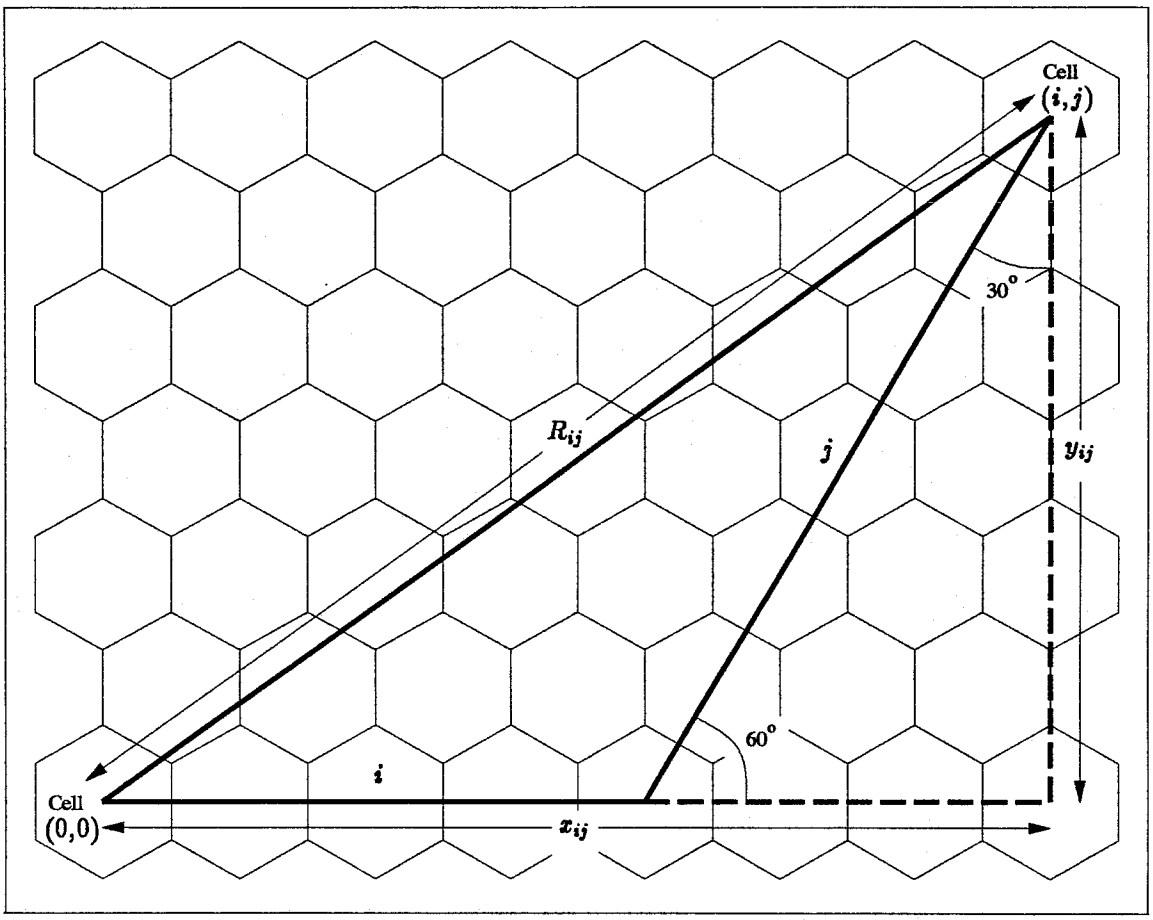

Figure A.2: *Cellular geometry for computing the (x, y) coordinates of the center of cell (i, j).*

A.2 Computation of Interference Parameter, a

In equation (2.7), the interference parameter, a, is defined as

$$a = \sum_{\Delta \neq \bar{0}} \mathrm{E}\{P(\bar{r}(\Delta))\}. \tag{A.8}$$

Consider an interfering user at position $\bar{r}$ in an arbitrary sector Δ as shown in figure A.3. The function $P(\bar{r}(\Delta))$ is the power received in sector $\bar{0}$ from this interfering user divided by the power received in sector $\bar{0}$ from a user that is actually in sector $\bar{0}$.

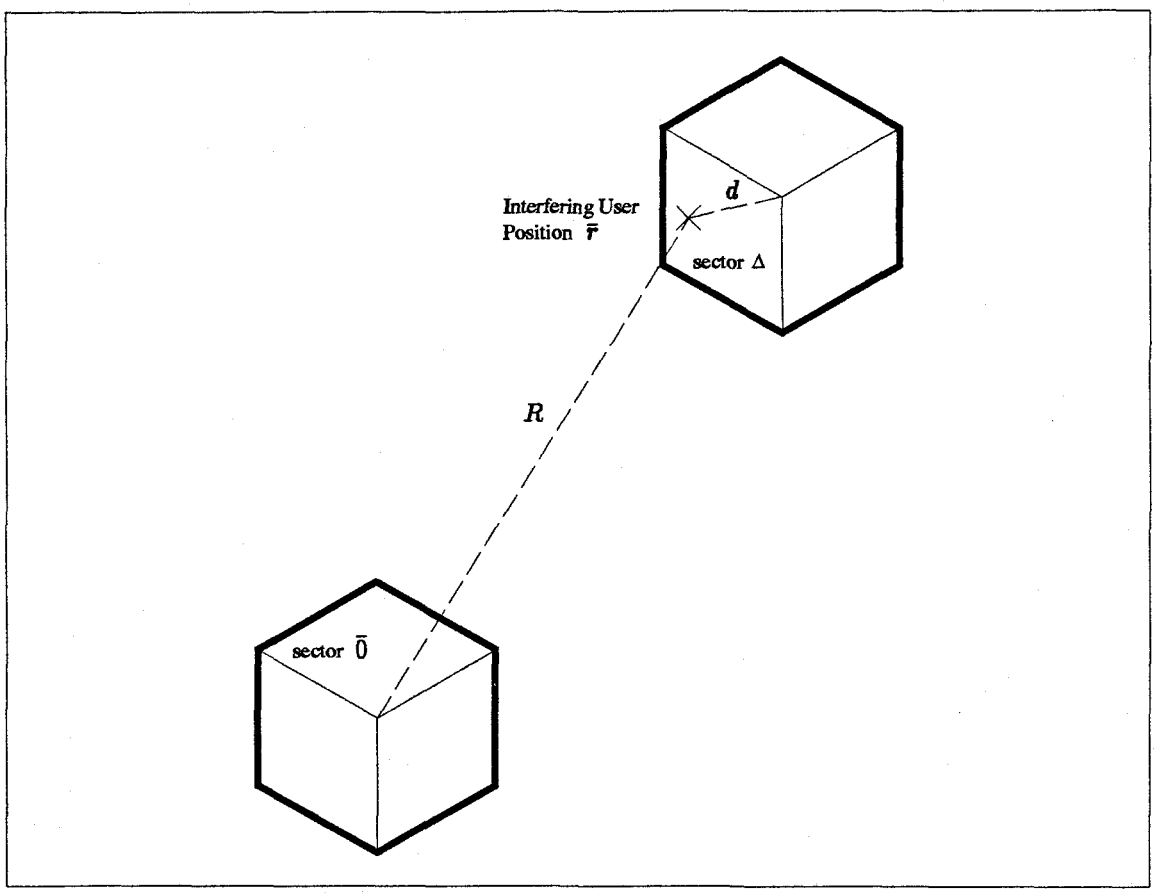

Figure A.3: *Interfering user at position $\bar{r}$ in an arbitrary sector Δ.*

Let P_t be the power transmitted by this user in sector Δ. Under the assumption of fourth power propagation loss in power, the interference power received in sector $\bar{0}$ from this interfering user is given by

$$P_{\mathrm{int}} = kP_t \left(\frac{1}{R}\right)^4 G(\phi), \tag{A.9}$$

where k is some constant, and $G(\phi)$ is the antenna gain for the base station antenna in sector $\bar{0}$ in the direction of the interfering user. Since power control is maintained, the power received in sector $\bar{0}$ from a user that is actually in sector $\bar{0}$ is equal to the power received in sector Δ from the interfering user in sector Δ. This value is thus given by

$$P_0 = kP_t \left(\frac{1}{d}\right)^4, \tag{A.10}$$

Thus,

$$P(\bar{r}(\Delta)) = \frac{P_{\text{int}}}{P_0} = \left(\frac{d}{R}\right)^4 G(\phi). \tag{A.11}$$

Since we are considering uniformly distributed traffic over each sector, the position $\bar{r}$ is a random variable and is uniformly distributed over sector Δ. The expected value of the random variable $P(\bar{r}(\Delta))$ is thus given by

$$\mathrm{E}\{P(\bar{r}(\Delta))\} = \int\int_{\bar{r}\in\Delta} \frac{1}{A_{\text{sec}}} P(\bar{r}) d\bar{r}, \tag{A.12}$$

where A_{sec} is the area of a sector equal to $\sqrt{3}/6$ for a normalized hexagonal grid. For an antenna gain, $G(\phi)$, that is equal to one if the position $\bar{r}$ is in the 120° beam width of sector $\bar{0}$ and 20dB below this at other angles, numerical computation over a cluster of 2883 sectors gives the value $a = 0.46708$.

A.3 Characterization of Additive Noise in the FH System

In this appendix, we compute the exact distribution of the additive noise in the FH system. This additive noise is given by equation (3.20) as

$$Z = r_{\text{noise}} = \sum_{\Delta \neq \bar{0}} \chi(\Delta) d(\Delta) \sqrt{P(\bar{r}(\Delta))} A(\Delta) \cos(\theta(\Delta)). \tag{A.13}$$

First, note that the product $A(\Delta)\cos(\theta(\Delta))$ has a zero-mean Gaussian distribution. This is because $A(\Delta)$ is Rayleigh distributed, $\theta(\Delta)$ is uniformly distributed on $(0, 2\pi)$, and these random variables are independent. Thus, if we let

$$z(\Delta) = A(\Delta)\cos(\theta(\Delta)), \tag{A.14}$$

then $z(\Delta)$ has a Gaussian distributed with mean zero and variance

$$\mathrm{E}\{z^2(\Delta)\} = \underbrace{\mathrm{E}\{A^2(\Delta)\}}_{1} \underbrace{\mathrm{E}\{\cos^2(\theta)\}}_{\frac{1}{2}} = \frac{1}{2}. \tag{A.15}$$

Thus, Z can be written as

$$Z = \sum_{\Delta \neq \bar{0}} \chi(\Delta) d(\Delta) \sqrt{P(\bar{r}(\Delta))} z(\Delta). \tag{A.16}$$

Consider the distribution of Z conditioned on the random variables $\chi(\Delta)$, $d(\Delta)$, and $P(\bar{r}(\Delta))$. This conditional random variable is then a sum of terms in which each term is a constant times an independent Gaussian. Thus, the conditional distribution is Gaussian and has variance given by

$$\mathrm{Var}\left[Z \mid \chi(\Delta), d(\Delta), P(\bar{r}(\Delta))\right] = \sum_{\Delta \neq \bar{0}} \chi^2(\Delta) d^2(\Delta) P(\bar{r}(\Delta)) \,\mathrm{Var}(z(\Delta)). \tag{A.17}$$

Since $d(\Delta)$ is ± 1, $d^2(\Delta) = 1$, and also since $\chi(\Delta)$ is equal to zero or one, $\chi^2(\Delta) = \chi(\Delta)$. Equation (A.17) thus simplifies to

$$\mathrm{Var}\left[Z \mid \chi(\Delta), d(\Delta), P(\bar{r}(\Delta))\right] = \frac{1}{2} \sum_{\Delta \neq \bar{0}} \chi(\Delta) P(\bar{r}(\Delta)) = \frac{1}{2} V^2, \tag{A.18}$$

where

$$V = \sqrt{\sum_{\Delta \neq \bar{0}} \chi(\Delta) P(\bar{r}(\Delta))}. \tag{A.19}$$

It follows that there exists a Gaussian random variable, W, with mean zero and variance one such that

$$Z = \frac{1}{\sqrt{2}} V W. \tag{A.20}$$

At this point, to characterize the distribution of Z, it only remains to characterize the distribution of V, defined by equation (A.19). Consider the random variable $u = \sqrt{P(\bar{r}(\Delta))}$. In appendix A.4, we show the rather unintuitive fact that it is possible to compute, admittedly complicated but nevertheless *analytic*, expressions for the cumulative distribution function and the probability density function of u, denoted $H_\Delta(u)$ and $h_\Delta(u)$, respectively. Using this result, the probability density function of the product, $y = \chi(\Delta)P(\bar{r}(\Delta))$, is

$$p_Y(y) = p\delta(y) + (1-p)h_\Delta(y). \tag{A.21}$$

The probability density function of V can be obtained by convolving these functions over sectors $\Delta \neq \bar{0}$. Figure A.4 shows the resulting cumulative distribution function of V for various values of normalized traffic, p. The conditional probability density function of Z given V is Gaussian with variance $V^2/2$, and thus given by

$$p_{Z|V}(z \mid v) = \frac{1}{\sqrt{\pi v^2}} e^{-z^2/v^2}. \tag{A.22}$$

Finally, having computed the probability density function of V, $p_V(v)$, the probability density function of Z can be written as

$$p_Z(z) = \int_v p_V(v) \frac{1}{\sqrt{\pi v^2}} e^{-z^2/v^2} dv. \tag{A.23}$$

Figure A.5 shows plots of the upper tail probabilities (one minus the cumulative distribution function) of Z for several values of normalized traffic, p. Each curve has been normalized by its standard deviation, $\sqrt{ap/2}$. The corresponding curve for a Gaussian distribution is also shown. Note that not only do these curves differ from Gaussian, the shape of the distribution changes for different values of normalized traffic, p. If each curve were simply a scaled version of a common underlying distribution, then normalizing each to its variance would remove this scale factor and the normalized curves would appear the same for all values of normalized traffic. This, however, is not the case as observed in figure A.5. The tails of the distributions change shape rather significantly for different values of normalized traffic, p.

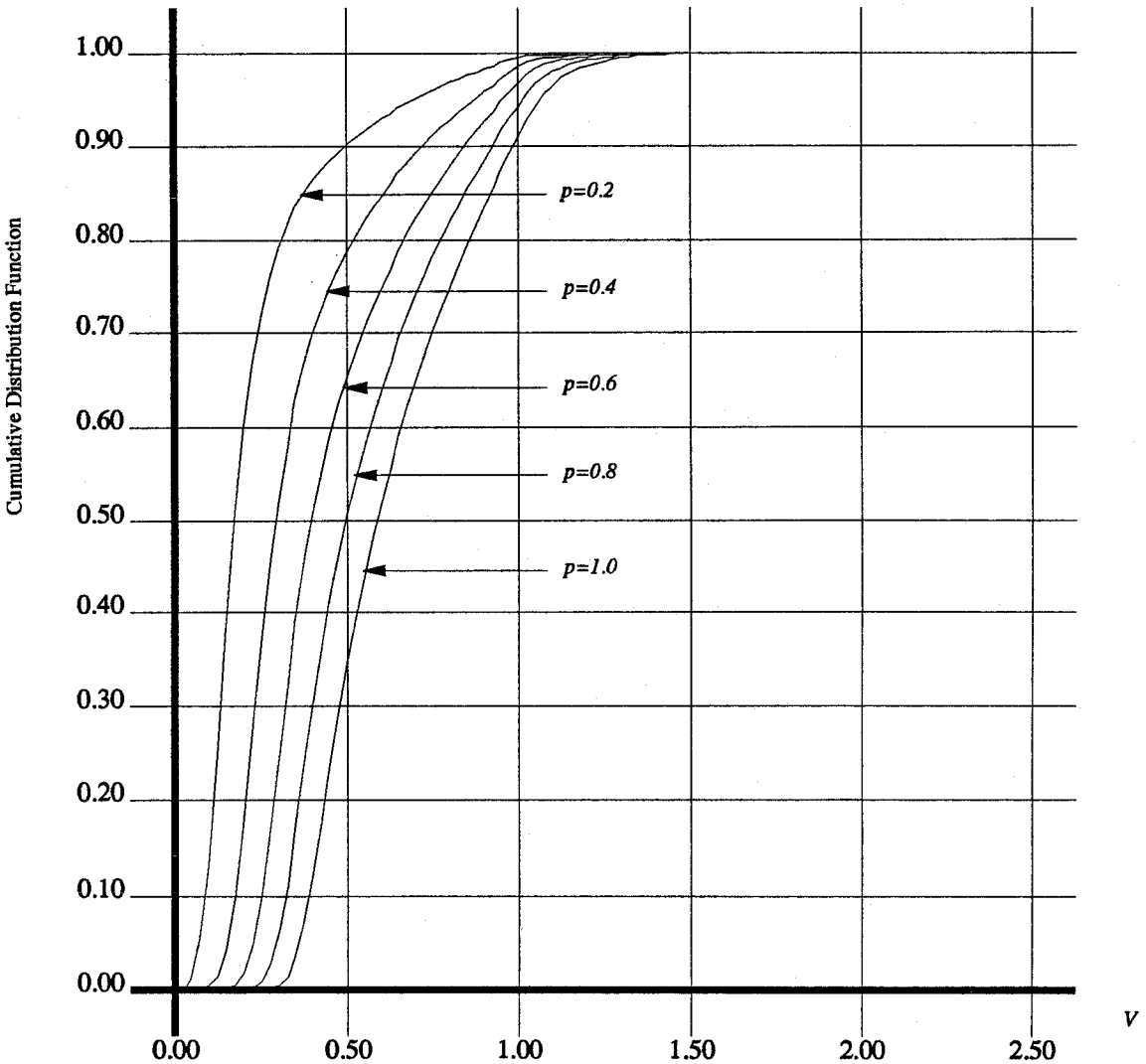

Figure A.4: *Cumulative distribution function of V for various values of normalized traffic, p.*

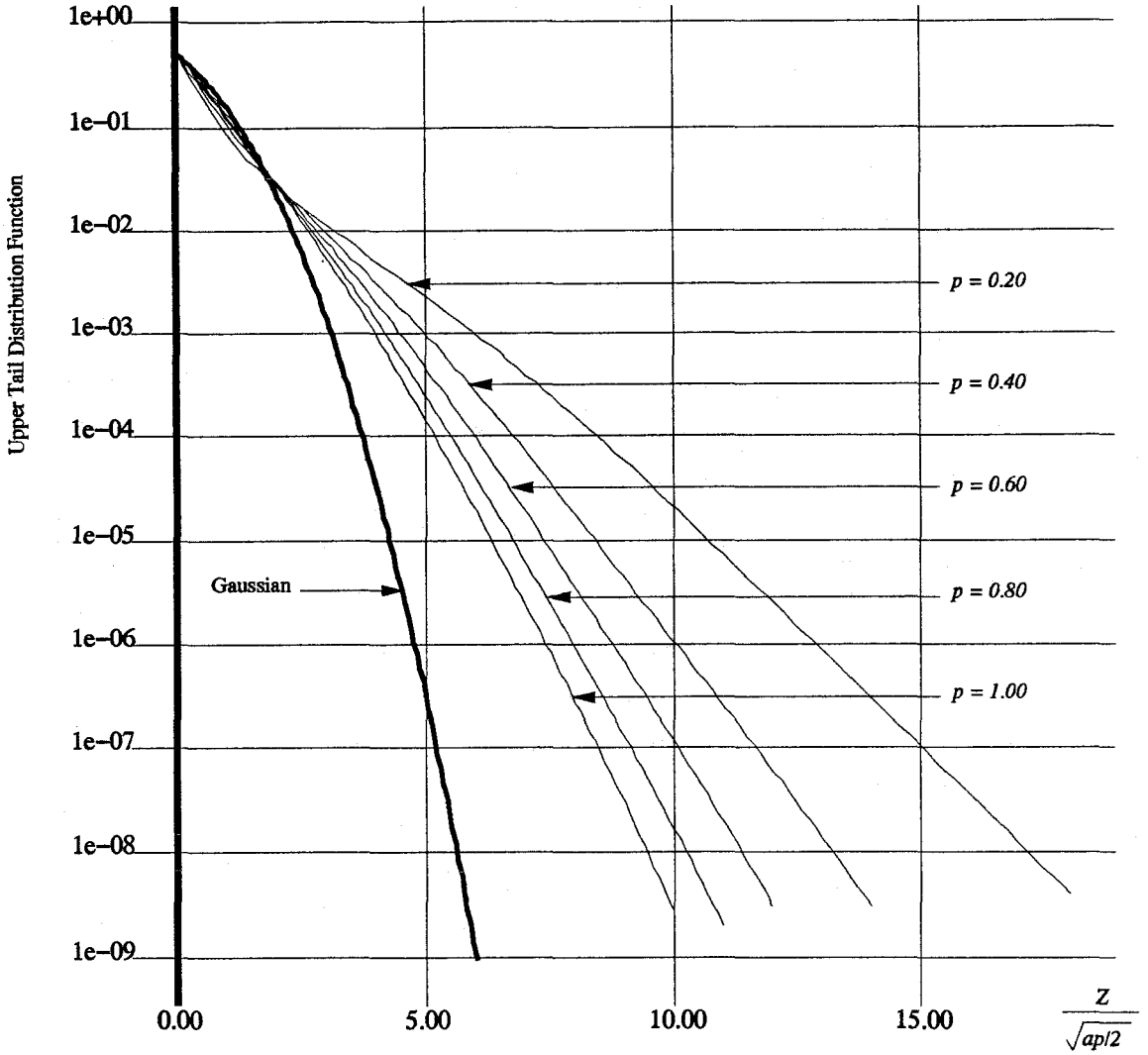

Figure A.5: *Upper tail distribution function of the additive noise, Z, normalized by its standard deviation. Curves are shown for various levels of normalized traffic, p. The corresponding upper tail distribution of a normalized Gaussian is also shown.*

A.4 Probability distribution of $\sqrt{P(\bar{r}(\Delta))}$

For an arbitrary sector, Δ, consider the random variable

$$U = \sqrt{P(\bar{r}(\Delta))}. \tag{A.24}$$

In this appendix, we compute analytic expressions for the cumulative distribution function and the probability density function of U. We begin by considering an arbitrary sector $\Delta = (i, j, s)$ that lies in the 120° beam width of the antenna in sector $\bar{0}$, and thus sees an antenna gain $G(\phi) = 1$. Let u be a constant and consider the locus of points where the random variable U is equal to the constant value u. Note that by the definition of $P(\bar{r}(\Delta))$, it only makes sense to consider values $u \leq 1$. Referring to figure A.3 and equation (A.11), we require that

$$\frac{d^2}{R^2} = u. \tag{A.25}$$

If a rectangular coordinate system with origin at the center of cell $(0, 0)$ is imposed on this geometry, d^2 and R^2 can be written as

$$R^2 = x^2 + y^2, \tag{A.26}$$

$$d^2 = (x_{ij} - x)^2 + (y_{ij} - y)^2, \tag{A.27}$$

where (x_{ij}, y_{ij}) are the coordinates of the center of cell (i, j) and given by equations (A.5) and (A.6). Inserting equations (A.26) and (A.27) into equation (A.25) gives

$$(x_{ij} - x)^2 + (y_{ij} - y)^2 = u(x^2 + y^2). \tag{A.28}$$

Expanding equation (A.28) and collecting terms gives

$$(1 - u)x^2 - (2x_{ij})x + (1 - u)y^2 - (2y_{ij})y + R_{ij}^2 = 0, \tag{A.29}$$

where R_{ij}^2 is given by equation (A.7). Finally, dividing through by $(1-u)$ and completing the square gives the result

$$\left(x - \frac{x_{ij}}{1-u}\right)^2 + \left(y - \frac{y_{ij}}{1-u}\right)^2 = \left[\frac{u}{(1-u)^2}\right] R_{ij}^2. \tag{A.30}$$

This is an equation for a circle with a center and radius given by

$$\text{Center} = \left(\frac{x_{ij}}{1-u}, \frac{y_{ij}}{1-u}\right), \tag{A.31}$$

$$\text{Radius} = d_{\text{rad}} = \left[\frac{\sqrt{u}}{(1-u)}\right] R_{ij}. \tag{A.32}$$

The distance from the center of cell (i,j) to the center of the circle $U = u$, d_{offset}, is given by

$$d_{\text{offset}} = \sqrt{\left(\frac{x_{ij}}{1-u} - x_{ij}\right)^2 + \left(\frac{y_{ij}}{1-u} - y_{ij}\right)^2} = \left[\frac{u}{1-u}\right] R_{ij}. \tag{A.33}$$

Figure A.6 shows some of these circles for different values of u. Note that in general these circles have the following properties.

(1) For $u = 0$, the center is (x_{ij}, y_{ij}), the center of cell (i,j), and the radius is zero leaving only the single point (x_{ij}, y_{ij}) where $u = 0$.

(2) As u increases, the radius increases and the center of the circle moves away from the point $(0,0)$ along the line joining the points $(0,0)$ and (x_{ij}, y_{ij}). That is, the three points $(0,0)$, (x_{ij}, y_{ij}), and $(x_{ij}/(1-u), y_{ij}/(1-u))$ are collinear.

(3) As $u \to 1$, we can refer back to equation (A.29) to see that this circle approaches the line, $(2x_{ij})x + (2y_{ij})y = R_{ij}^2$. This line passes through the point $(x_{ij}/2, y_{ij}, 2)$ and is perpendicular to the line joining the points $(0,0)$ and (x_{ij}, y_{ij}).

(4) For distinct values, u_1 and u_2, that satisfy $u_1 < u_2 < 1$, the circle $U = u_2$ encloses the circle $U = u_1$. This fact follows from the following argument.

   a) The two circles can't be disjoint because both enclose the point (x_{ij}, y_{ij}).
   b) The circle $U = u_1$ can't enclose the circle $U = u_2$ because it has a smaller radius.
   c) The circles can't intersect because u_1 and u_2 are distinct and an intersection would imply the existence of a point where $U = u_1 = u_2$.
   d) The only remaining possibility is that the circle $U = u_2$ encloses the circle $U = u_1$ as stated.

Using these facts and the fact that the traffic is uniformly distributed, we can state that $H_\Delta(u)$, the probability that the random variable U satisfies $U \leq u$, is equal to *the fraction of the area of sector* Δ *that lies inside the circle* $U = u$.

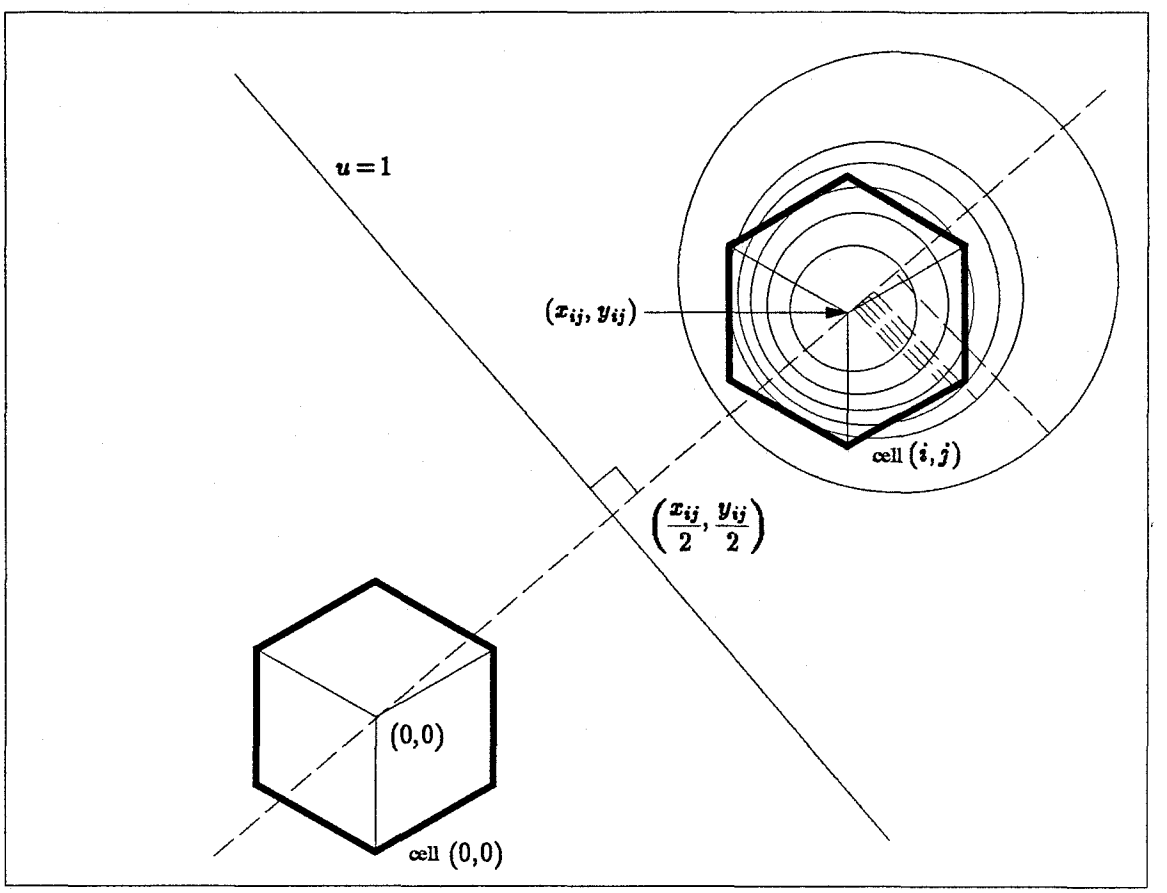

Figure A.6: *Circles on which the the random variable, U, assumes a constant value.*

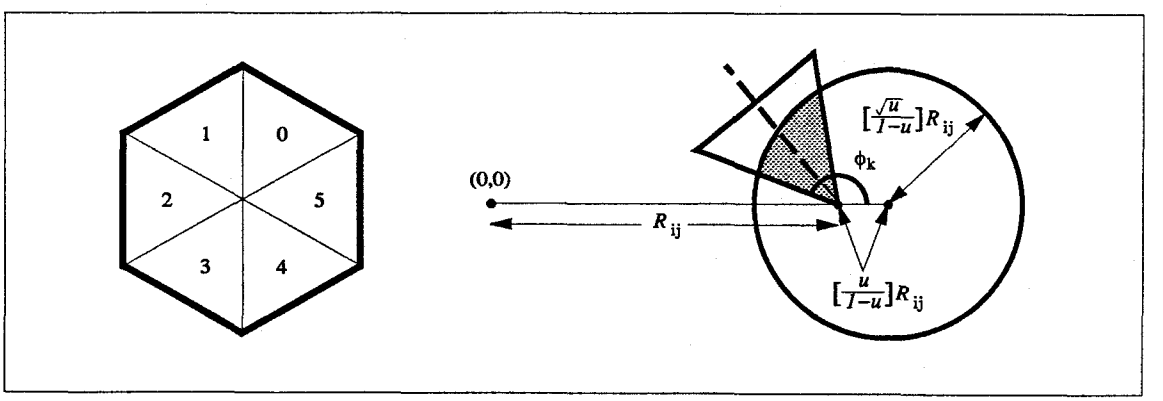

Figure A.7: *Division of each hexagonal cell into six equilateral triangles. For triangle k the angle ϕ_k is defined as shown.*

We proceed by breaking each cell into six equilateral triangles, numbered zero to five, as shown in figure A.7. Each sector is composed of two such triangles, so it suffices to be able to compute the area of an arbitrary one of these triangles that lies inside the circle $U = u$. We now view triangle k of cell (i, j) by rotating the geometry such that the line joining the center of cell $(0, 0)$ and the center of cell (i, j) is horizontal, and define the angle ϕ_k as shown in figure A.7. By the vertical symmetry of the problem, the angles $-\phi_k$ and ϕ_k are equivalent so we can take ϕ_k to be between zero and π. By applying a trigonometric analysis of this geometry, it can be shown that the ϕ_k's are given by

$$\cos(\phi_0) = -\cos(\phi_3) = \frac{i+2j}{2R_{ij}}, \tag{A.34}$$

$$\cos(\phi_1) = -\cos(\phi_4) = \frac{-i+j}{2R_{ij}}, \tag{A.35}$$

$$\cos(\phi_2) = -\cos(\phi_5) = \frac{-2i-j}{2R_{ij}}. \tag{A.36}$$

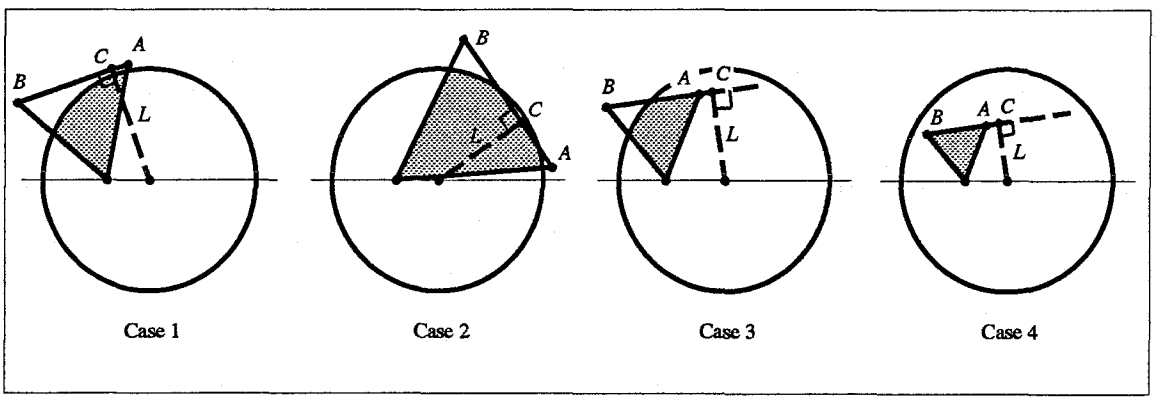

Figure A.8: *Four possible cases to consider for each equilateral triangle.*

For each equilateral triangle, there are four cases to consider as shown in figure A.8. Two corners of the triangle are labeled A and B, as shown in the figure and, also, the parameter L is defined as shown. By a geometrical analysis, the value of L is found to be

$$L = \frac{1}{2} - \left[\frac{u}{1-u}\right] R_{ij} \cos(\phi_k). \tag{A.37}$$

To determine which case is applicable requires knowledge of whether or not point A is in the circle, whether or not point B is in the circle, and whether or not point C lies between points A and B.

These three conditions are determined by

$$\text{point } A \text{ in circle} \iff \frac{1}{3} - \frac{R_{ij}u}{1-u}\left[R_{ij} + \cos(\phi_k) + \frac{\sin(\phi_k)}{\sqrt{3}}\right] < 0, \tag{A.38}$$

$$\text{point } B \text{ in circle} \iff \frac{1}{3} - \frac{R_{ij}u}{1-u}\left[R_{ij} + \cos(\phi_k) - \frac{\sin(\phi_k)}{\sqrt{3}}\right] < 0, \tag{A.39}$$

$$\text{point } C \text{ between } A \text{ and } B \iff \frac{1}{2}\left[\cos(\phi_k) + \frac{\sin(\phi_k)}{\sqrt{3}}\right] - \frac{R_{ij}u}{1-u} < L\cos(\phi_k). \tag{A.40}$$

The determination of which case is applicable is then

Case 1 $\iff$ ($L > d_{\text{rad}}$) OR (point A NOT in circle AND point C NOT between A and B),

Case 2 $\iff$ ($L < d_{\text{rad}}$) AND (point A NOT in circle) AND (point C between A and B),

Case 3 $\iff$ (point A in circle) AND (point B NOT in circle),

Case 4 $\iff$ (point A in circle) AND (point B in circle).

Having determined the applicable case, the area of the triangle that lies in the circle can be found from a geometrical analysis. These areas can be used to find the cumulative distribution function. To find the probability density function, these expressions are differentiated with respect to u. The results are as follows.

For case 1,

$$\text{Area}(u) = \frac{R_{ij}^2 u}{2(1-u)^2}\left[\begin{array}{l} \dfrac{\pi}{3} + \sqrt{3}\left(\cos^2(\phi_k) - \dfrac{1}{2}\right)u \\ \quad + \sin^{-1}\left(\sqrt{u}\sin\left(\phi_k + \dfrac{\pi}{6}\right)\right) - \sin^{-1}\left(\sqrt{u}\sin\left(\phi_k - \dfrac{\pi}{6}\right)\right) \\ \quad + \sin\left(\phi_k + \dfrac{\pi}{6}\right)\sqrt{u - u^2\sin^2\left(\phi_k + \dfrac{\pi}{6}\right)} \\ \quad - \sin\left(\phi_k - \dfrac{\pi}{6}\right)\sqrt{u - u^2\sin^2\left(\phi_k - \dfrac{\pi}{6}\right)} \end{array}\right], \tag{A.41}$$

$$\text{Area}'(u) = \frac{R_{ij}^2}{(1-u)^3}\left[\begin{array}{l} \dfrac{1+u}{2}\left[\begin{array}{l} \dfrac{\pi}{3} + \sin^{-1}\left(\sqrt{u}\sin\left(\phi_k + \dfrac{\pi}{6}\right)\right) \\ \quad - \sin^{-1}\left(\sqrt{u}\sin\left(\phi_k - \dfrac{\pi}{6}\right)\right) \end{array}\right] \\ \quad + \sqrt{3}\left(\cos^2(\phi_k) - \dfrac{1}{2}\right)u \\ \quad + \sin\left(\phi_k + \dfrac{\pi}{6}\right)\sqrt{u - u^2\sin^2\left(\phi_k + \dfrac{\pi}{6}\right)} \\ \quad - \sin\left(\phi_k - \dfrac{\pi}{6}\right)\sqrt{u - u^2\sin^2\left(\phi_k - \dfrac{\pi}{6}\right)} \end{array}\right]. \tag{A.42}$$

For case 2,

$$\text{Area}(u) = \left(\begin{array}{c}\text{Area}(u) \\ \text{for case 1}\end{array}\right) - \frac{R_{ij}^2 u}{(1-u)^2}\left[\cos^{-1}\left(\frac{L}{d_{\text{rad}}}\right) - \frac{L}{d_{\text{rad}}}\sqrt{1 - \left(\frac{L}{d_{\text{rad}}}\right)^2}\right], \tag{A.43}$$

$$\text{Area}'(u) = \begin{pmatrix} \text{Area}'(u) \\ \text{for case 1} \end{pmatrix} - \frac{R_{ij}^2}{(1-u)^3}\left[(1+u)\cos^{-1}\left(\frac{L}{d_{\text{rad}}}\right) + 2\sqrt{u - u\left(\frac{L}{d_{\text{rad}}}\right)^2}\cos(\phi_k)\right]. \quad \text{(A.44)}$$

For case 3,

$$\text{Area}(u) = \frac{1}{2} - \left[\frac{\sqrt{3}}{4}S_1S_2 - d_{\text{rad}}^2\left(\sin^{-1}\left(\frac{S_3}{2d_{\text{rad}}}\right) - \left(\frac{S_3}{2d_{\text{rad}}}\right)\sqrt{1-\left(\frac{S_3}{2d_{\text{rad}}}\right)^2}\right)\right], \quad \text{(A.45)}$$

$$\text{Area}'(u) = \left[\begin{array}{l} (S_1\dot{S}_1 + S_2\dot{S}_2)\dfrac{S_3}{4d_{\text{rad}}\sqrt{1-\left(\frac{S_3}{2d_{\text{rad}}}\right)^2}} \\ -(S_1\dot{S}_2 + S_2\dot{S}_1)\left[\dfrac{\sqrt{3}}{4} + \dfrac{S_3}{8d_{\text{rad}}\sqrt{1-\left(\frac{S_3}{2d_{\text{rad}}}\right)^2}}\right] \\ -\dfrac{(1+u)d_{\text{rad}}}{2u(1-u)}\left[\dfrac{S_3}{\sqrt{1-\left(\frac{S_3}{2d_{\text{rad}}}\right)^2}} - 2d_{\text{rad}}\sin^{-1}\left(\dfrac{S_3}{2d_{\text{rad}}}\right)\right] \end{array}\right], \quad \text{(A.46)}$$

where

$$S_1 = \frac{\sqrt{3}}{6} + \frac{R_{ij}u}{1-u}\sin(\phi_k) - \sqrt{\frac{R_{ij}^2u}{(1-u)^2} - \left(\frac{1}{2} - \frac{R_{ij}u}{1-u}\cos(\phi_k)\right)^2}, \quad \text{(A.47)}$$

$$S_2 = \frac{1}{\sqrt{3}} - \frac{R_{ij}u}{1-u}\left[\cos\left(\phi_k + \frac{\pi}{6}\right) + \sqrt{\frac{1}{u} - \sin^2\left(\phi_k + \frac{\pi}{6}\right)}\right], \quad \text{(A.48)}$$

$$S_3 = \sqrt{S_1^2 + S_2^2 - S_1S_2}, \quad \text{(A.49)}$$

$$\dot{S}_1 = \frac{R_{ij}\sin(\phi_k)}{(1-u)^2} - \frac{R_{ij}^2 + R_{ij}\cos(\phi_k) + 2(1-u)d_{\text{rad}}^2\sin^2(\phi_k)}{2(1-u)^2\sqrt{\frac{R_{ij}^2u}{(1-u)^2} - \left(\frac{1}{2} - \frac{R_{ij}u}{1-u}\cos(\phi_k)\right)^2}}, \quad \text{(A.50)}$$

$$\dot{S}_2 = -\frac{R_{ij}\cos\left(\phi_k + \frac{\pi}{6}\right)}{(1-u)^2} - \frac{R_{ij} + \frac{2R_{ij}u}{1-u}\cos^2\left(\phi_k + \frac{\pi}{6}\right)}{2u(1-u)\sqrt{\frac{1}{u} - \sin^2\left(\phi_k + \frac{\pi}{6}\right)}}. \quad \text{(A.51)}$$

Finally, for case 4,

$$\text{Area}(u) = \frac{1}{4\sqrt{3}}, \quad \text{(A.52)}$$

$$\text{Area}'(u) = 0. \quad \text{(A.53)}$$

Hence, given an arbitrary sector, Δ, the area of Δ that lies inside the circle $U = u$ is obtained by adding the Area(u) terms for the two equilateral triangles corresponding to sector Δ. The cumulative distribution function of U, $H_\Delta(u)$, is then computed by dividing by the area of the entire sector which, by equation (A.4), is $1/(2\sqrt{3})$. Similarly, $h_\Delta(u)$ is computed by adding the Area$'(u)$ terms for the two equilateral triangles corresponding to sector Δ and dividing by the area of the entire

sector. For sectors that are not in the 120° beam width of sector $\bar{0}$, these distribution functions are modified by appropriate scaling. Furthermore, for the sectors that have only half their area in the beam width of sector $\bar{0}$, this scaling is applied to only one of the equilateral triangles.

We have assumed throughout that there is an R^{-4} propagation loss in power, but it is worth noting that these results can be generalized for $R^{-\alpha}$ propagation. This is done by noting that the random variable $\hat{U} = U^{(\alpha/4)}$ has a cumulative distribution function given by

$$P_{\hat{U}}(\hat{u}) = H_{\Delta}(\hat{u}^{(4/\alpha)}), \tag{A.54}$$

and a probability density function given by

$$p_{\hat{U}}(\hat{u}) = \frac{4}{\alpha}\hat{u}^{(\frac{4-\alpha}{\alpha})}h_{\Delta}(\hat{u}^{(4/\alpha)}). \tag{A.55}$$

Figure A.9 shows plots of the function $h_{\Delta}(u)$ for the sectors in cells $(0,1)$, $(-1,2)$, and $(0,2)$. Note that, by symmetry, sectors 1 and 2 of cell $(-1,2)$ have the same distribution.

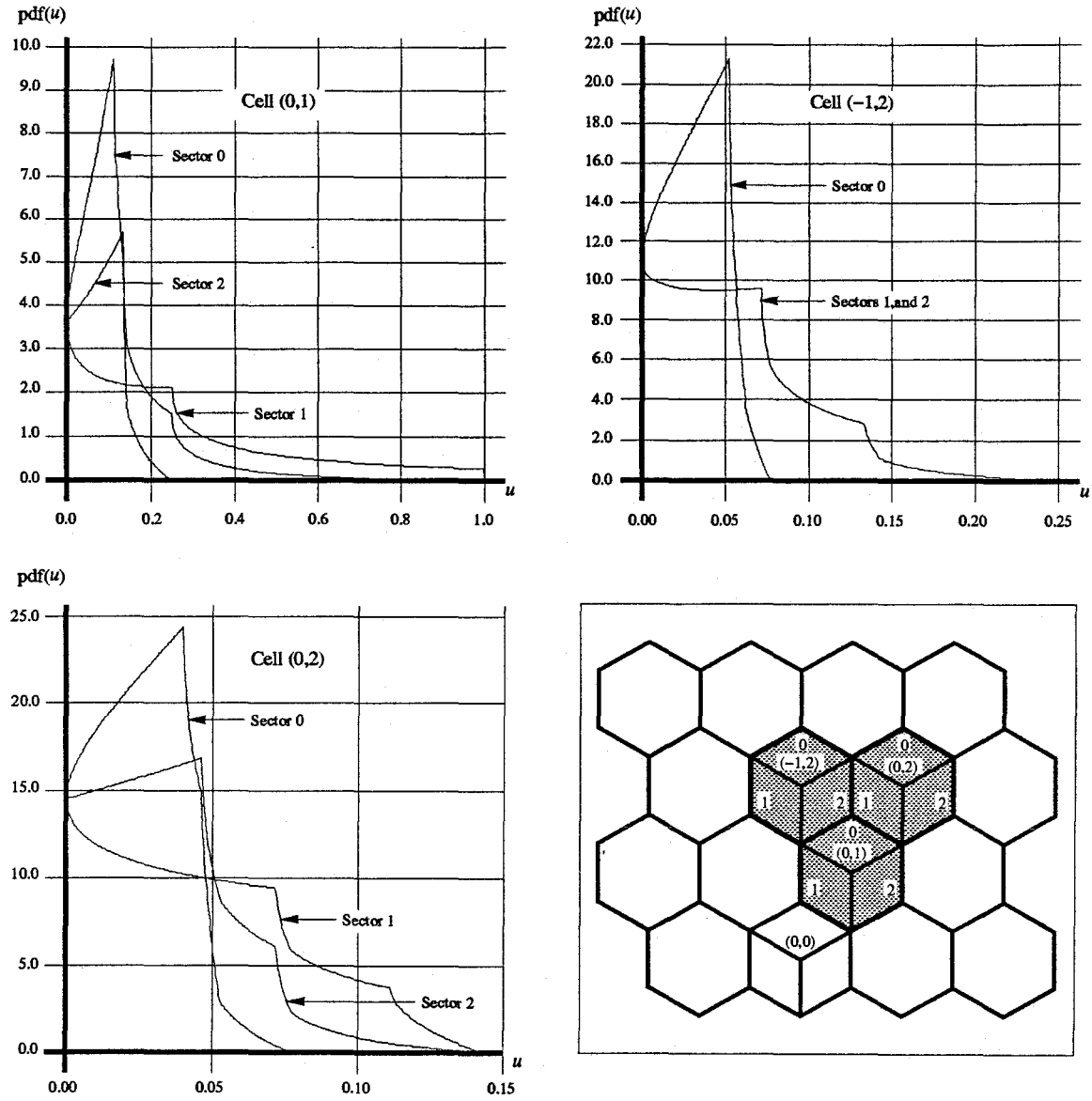

Figure A.9: *Plots of the probability density function,* $h_\Delta(u)$*, are shown for the sectors of cells* $(0,1)$*,* $(-1,2)$*, and* $(0,2)$*.*

A.5 Sum of Dependent Rayleigh-Squared Random Variables

In this appendix, we show that a sum of dependent Rayleigh-squared random variables can be replaced by an equivalent independent sum.

Claim: Let

$$\mathbf{A} = \begin{pmatrix} \mathcal{A}_1 \\ \mathcal{A}_2 \\ \vdots \\ \mathcal{A}_n \end{pmatrix}, \tag{A.56}$$

be a vector of complex valued Gaussian random variables representing the channel parameters defined by equations (3.34) and (3.35). Components of the covariance matrix are computed by equation (3.56). Note that the covariance matrix, ρ, is a real valued symmetric matrix. We claim that there exists a vector

$$\mathbf{B} = \begin{pmatrix} \mathcal{B}_1 \\ \mathcal{B}_2 \\ \vdots \\ \mathcal{B}_n \end{pmatrix}, \tag{A.57}$$

with the following properties.

(1) The real and imaginary parts of each component of $\mathbf{B}$ are *i.i.d.* zero-mean Gaussian random variables.

(2) The covariance matrix of $\mathbf{B}$ is given by

$$\mathrm{E}\{\mathbf{B}\mathbf{B}^\dagger\} = \Lambda, \tag{A.58}$$

where Λ is a diagonal matrix with the eigenvalues of the matrix ρ on the main diagonal.

(3) The vector $\mathbf{B}$ satisfies

$$\mathbf{A}^\dagger\mathbf{A} = \mathbf{B}^\dagger\mathbf{B}, \tag{A.59}$$

which shows that the sum of dependent Rayleigh-squared random variables in equation (3.57) is equivalent to the independent sum shown in equation (3.58).

Note that $X^\dagger$ denotes the complex conjugate transpose of X.

Proof: From the definition of ρ, and the fact that it turns out to be real valued, we can write

$$\mathrm{E}\{\mathbf{A}^*\mathbf{A}^T\} = \mathrm{E}\{\mathbf{A}\mathbf{A}^\dagger\} = \rho. \tag{A.60}$$

Since ρ is real and symmetric, it can be expressed in terms of the real valued matrices M and Λ as ([15], pg. 102)

$$\rho = M^T \Lambda M, \tag{A.61}$$

where

$$M^T M = I, \tag{A.62}$$

and Λ is a diaginal matrix whose entries on the main diaginal are the eigenvalues of ρ. Let

$$\mathbf{Z} = \begin{pmatrix} Z_1 \\ Z_2 \\ \vdots \\ Z_n \end{pmatrix}, \tag{A.63}$$

be a vector of complex valued Gaussian random variables having the following properties.

(1) Each component of the vector $\mathbf{Z}$ is given by $Z_i = Z_{iR} + jZ_{iI}$.

(2) The $2n$ real valued random variables Z_{iR}, Z_{iI} are all *i.i.d.* Gaussian random variables each having mean zero and variance $1/2$.

Then, using the results of appendix A.6, if we write

$$\mathbf{A} = M^T \Lambda^{\frac{1}{2}} Z, \tag{A.64}$$

we have

$$\mathrm{E}\{\mathbf{A}\mathbf{A}^\dagger\} = \rho, \tag{A.65}$$

as desired. Furthermore, the results of appendix A.6 show that for such complex Gaussian random variables, all the statistical properties can be expressed in terms of the covariance matrix ρ. In this respect, this is a valid representation for the vector $\mathbf{A}$. Next, if we let

$$\mathbf{B} = M\mathbf{A} = \Lambda^{\frac{1}{2}} \mathbf{Z}, \tag{A.66}$$

then, using the results of appendix A.6, $\mathbf{B}$ is a vector of complex Gaussian random variables where each component of $\mathbf{B}$ has a real and imaginary part that are *i.i.d.*. The covariance matrix of $\mathbf{B}$ is then

$$\mathrm{E}\{\mathbf{B}\mathbf{B}^\dagger\} = \Lambda. \tag{A.67}$$

That is, the components of $\mathbf{B}$ are *independent* complex Gaussian random variables having variances given by the eigenvalues of the covariance matrix ρ. Finally, we observe that

$$\mathbf{B}^\dagger\mathbf{B} = \mathbf{A}^\dagger M^T M\mathbf{A} = \mathbf{A}^\dagger\mathbf{A}. \quad \blacksquare \tag{A.68}$$

A.6 Characterization of Complex Gaussian Random Variables

Claim 1: Let $\mathcal{C}$ be an $(n \times n)$ complex valued matrix, and let

$$\mathbf{Z} = \begin{pmatrix} Z_1 \\ Z_2 \\ \vdots \\ Z_n \end{pmatrix}, \tag{A.69}$$

be a vector of complex valued Gaussian random variables having the following properties.

(1) Each component of the vector $\mathbf{Z}$ is given by $Z_i = Z_{iR} + jZ_{iI}$.

(2) The $2n$ real valued random variables Z_{iR}, Z_{iI} are all *i.i.d.* Gaussian random variables each having mean zero and variance $1/2$.

If

$$\mathbf{W} = \mathcal{C}\mathbf{Z}, \tag{A.70}$$

then

(1) each component of the vector $\mathbf{W}$, W_i, has real and imaginary parts that are *i.i.d.* zero-mean Gaussian random variables,

(2) the covariance matrix of $\mathbf{W}$ is given by $\mathcal{R} = \mathcal{C}\mathcal{C}^\dagger$,

(3) the joint probability density function of the components of $\mathbf{W}$ is given by

$$p_{\mathbf{W}}(\mathbf{w}) = \left(\frac{1}{\pi}\right)^n \frac{1}{|\det(\mathcal{R})|} e^{-\mathbf{w}^\dagger \mathcal{R}^{-1} \mathbf{w}}. \tag{A.71}$$

The notation $X^\dagger$ denotes the complex conjugate transpose of X. Note that this is a generalization of known results for real valued Gaussian variables in that the statistics of $\mathbf{W}$ are completely determined by its covariance matrix.

Proof: We begin by writing the complex quantities $\mathbf{W}$, $\mathbf{Z}$, and $\mathcal{C}$ in terms of their real and imaginary parts as

$$\mathbf{W} = \mathbf{W}_R + j\mathbf{W}_I, \tag{A.72}$$

$$\mathbf{Z} = \mathbf{Z}_R + j\mathbf{Z}_I, \tag{A.73}$$

$$\mathcal{C} = \mathcal{C}_R + j\mathcal{C}_I. \tag{A.74}$$

Next, we define the *real* valued quantities $\tilde{W}$, $\tilde{Z}$, and $\tilde{C}$ as

$$\tilde{W} = \begin{pmatrix} \mathbf{W}_R \\ \mathbf{W}_I \end{pmatrix}, \qquad (2n \text{ vector}) \tag{A.75}$$

$$\tilde{Z} = \begin{pmatrix} \mathbf{Z}_R \\ \mathbf{Z}_I \end{pmatrix}, \qquad (2n \text{ vector}) \tag{A.76}$$

$$\tilde{C} = \begin{pmatrix} C_R & -C_I \\ C_I & C_R \end{pmatrix}. \qquad (2n \times 2n \text{ matrix}) \tag{A.77}$$

Since

$$\mathbf{W} = C\mathbf{Z}, \tag{A.78}$$

the real and imaginary parts of $\mathbf{W}$ are given by

$$\mathbf{W}_R = C_R\mathbf{Z}_R - C_I\mathbf{Z}_I, \tag{A.79}$$

$$\mathbf{W}_I = C_R\mathbf{Z}_I + C_I\mathbf{Z}_R. \tag{A.80}$$

This can be expressed in terms of the real valued quantities as

$$\tilde{W} = \tilde{C}\tilde{Z}. \tag{A.81}$$

Since, by assumption, the $2n$ components of $\tilde{Z}$ are all *i.i.d.* zero-mean Gaussian random variables each with variance $1/2$, we have

$$\mathrm{E}\{\tilde{Z}\tilde{Z}^T\} = \frac{1}{2}I_{(2n)}, \tag{A.82}$$

where $I_{(2n)}$ is the identity matrix of size $2n$. Furthermore, it also follows that the $2n$ components of $\tilde{W}$ are all zero-mean joint Gaussian random variables. The covariance matrix of $\tilde{W}$, R, can be computed as

$$R = \mathrm{E}\{\tilde{W}\tilde{W}^T\} = \mathrm{E}\{\tilde{C}\tilde{Z}\tilde{Z}^T\tilde{C}^T\} = \frac{1}{2}\tilde{C}\tilde{C}^T. \tag{A.83}$$

Since $\tilde{W}$ is a vector of *real valued* joint Gaussian random variables with covariance matrix R, the probability density function of $\tilde{W}$ can be written as ([1], pg. 32)

$$p(\tilde{W}) = \left(\frac{1}{\sqrt{2\pi}}\right)^{2n} \frac{1}{\sqrt{\det(R)}} e^{-\frac{1}{2}\tilde{W}^T R^{-1}\tilde{W}}. \tag{A.84}$$

The covariance matrix, R, can be expressed in terms of the real and imaginary parts of $\tilde{C}$ as

$$R = \frac{1}{2}\begin{pmatrix} C_R & -C_I \\ C_I & C_R \end{pmatrix}\begin{pmatrix} C_R^T & C_I^T \\ -C_I^T & C_R^T \end{pmatrix} = \frac{1}{2}\begin{pmatrix} D & -E \\ E & D \end{pmatrix}, \tag{A.85}$$

where the $(n \times n)$ matrices D and E are defined as

$$D = C_R C_R^T + C_I C_I^T, \tag{A.86}$$

$$E = C_I C_R^T - C_R C_I^T. \tag{A.87}$$

The covariance matrix, R, can also be expressed in terms of the real and imaginary parts of $\mathbf{W}$ as

$$R = \mathrm{E}\{\tilde{W}\tilde{W}^T\} = \begin{pmatrix} \mathrm{E}\{\mathbf{W}_R\mathbf{W}_R^T\} & \mathrm{E}\{\mathbf{W}_R\mathbf{W}_I^T\} \\ \mathrm{E}\{\mathbf{W}_I\mathbf{W}_R^T\} & \mathrm{E}\{\mathbf{W}_I\mathbf{W}_I^T\} \end{pmatrix}. \tag{A.88}$$

Equating the upper right blocks of equations (A.85) and (A.88), gives

$$\mathrm{E}\{\mathbf{W}_R\mathbf{W}_I^T\} = \frac{1}{2}(C_R C_I^T - C_I C_R^T). \tag{A.89}$$

Note that the matrix $(C_R C_I^T - C_I C_R^T)$ is *antisymmetric* and thus all diagonal terms are zero. Hence,

$$\mathrm{E}\{\mathrm{Re}(W_i)\,\mathrm{Im}(W_i)\} = 0, \qquad (i = 1, 2, \ldots, n), \tag{A.90}$$

so that the real and imaginary parts of each component of the vector $\mathbf{W}$ are uncorrelated joint Gaussian and thus independent. Furthermore, equating the upper left blocks of equations (A.85) and (A.88) and also the lower right blocks gives

$$\mathrm{E}\{\mathbf{W}_R\mathbf{W}_R^T\} = \frac{1}{2}(C_R C_R^T + C_I C_I^T) = \mathrm{E}\{\mathbf{W}_I\mathbf{W}_I^T\}. \tag{A.91}$$

Thus,

$$\mathrm{E}\{\mathrm{Re}(W_i)^2\} = \mathrm{E}\{\mathrm{Im}(W_i)^2\}, \qquad (i = 1, 2, \ldots, n). \tag{A.92}$$

From equations (A.90) and (A.92) we conclude that the real and imaginary parts of each component of the vector $\mathbf{W}$ are in fact *i.i.d.* Gaussian random variables. The complex covariance matrix of $\mathbf{W}$ can be written as

$$\mathcal{R} = \mathrm{E}\{\mathbf{W}\mathbf{W}^\dagger\} = \mathrm{E}\{\mathcal{C}\mathbf{Z}\mathbf{Z}^\dagger\mathcal{C}^\dagger\} = \mathcal{C}\mathcal{C}^\dagger. \tag{A.93}$$

At this point, it only remains to write the probability density function of $\tilde{W}$ in terms of $\mathbf{W}$ and $\mathcal{R}$ as in equation (A.71). This is done in two steps. The first step is to show that $\tilde{W}R^{-1}\tilde{W} = 2\mathbf{W}^\dagger\mathcal{R}^{-1}\mathbf{W}$,

and the second step is to show that $\det(R) = 2^{-2n}|\det(\mathcal{R})|^2$. To show that $\tilde{W}R^{-1}\tilde{W} = 2\mathbf{W}^\dagger\mathcal{R}^{-1}\mathbf{W}$, we begin by expressing $\mathcal{R}$ as

$$\mathcal{R} = \mathcal{C}\mathcal{C}^\dagger = (\mathcal{C}_R + j\mathcal{C}_I)(\mathcal{C}_R^T - j\mathcal{C}_I^T) = D + jE, \tag{A.94}$$

where the matrices D and E are defined in equations (A.86) and (A.87). Next, let F and G be the real and imaginary parts of $\mathcal{R}^{-1}$, so that $\mathcal{R}^{-1}$ can be written as

$$\mathcal{R}^{-1} = F + jG. \tag{A.95}$$

The product of $\mathcal{R}$ and $\mathcal{R}^{-1}$ is thus

$$\mathcal{R}\mathcal{R}^{-1} = (D + jE)(F + jG) = (DF - EG) + j(EF + DG), \tag{A.96}$$

but this must be equal to the identity matrix of size n, $I_{(n)}$. Thus, we have that

$$DF - EG = I_{(n)}, \tag{A.97}$$

$$EF + DG = 0. \tag{A.98}$$

Now consider the following matrix product using the expression for R given by equation (A.85)

$$R\left[2\begin{pmatrix} F & -G \\ G & F \end{pmatrix}\right] = \begin{pmatrix} D & -E \\ E & D \end{pmatrix}\begin{pmatrix} F & -G \\ G & F \end{pmatrix} = \begin{pmatrix} DF - EG & -DG - EF \\ EF + DG & DF - EG \end{pmatrix}. \tag{A.99}$$

Using equations (A.97) and (A.98), this can be written as

$$R\left[2\begin{pmatrix} F & -G \\ G & F \end{pmatrix}\right] = \begin{pmatrix} I_{(n)} & 0 \\ 0 & I_{(n)} \end{pmatrix} = I_{(2n)}. \tag{A.100}$$

Thus, we have shown that the inverse of R is given by

$$R^{-1} = 2\begin{pmatrix} F & -G \\ G & F \end{pmatrix}. \tag{A.101}$$

Now, using equations (A.75) and (A.101), we can compute the product

$$\tilde{W}^T R^{-1}\tilde{W} = 2\left[\mathbf{W}_R^T F\mathbf{W}_R - \mathbf{W}_R^T G\mathbf{W}_I + \mathbf{W}_I^T G\mathbf{W}_R + \mathbf{W}_I^T F\mathbf{W}_I\right]. \tag{A.102}$$

Also, using equation (A.95), we can compute the real part of the product

$$\mathrm{Re}(\mathbf{W}^\dagger\mathcal{R}^{-1}\mathbf{W}) = \mathbf{W}_R^T F\mathbf{W}_R - \mathbf{W}_R^T G\mathbf{W}_I + \mathbf{W}_I^T G\mathbf{W}_R + \mathbf{W}_I^T F\mathbf{W}_I. \tag{A.103}$$

But $\mathbf{W}^\dagger \mathcal{R}^{-1} \mathbf{W}$ must be a positive real number because

$$\mathbf{W}^\dagger \mathcal{R}^{-1} \mathbf{W} = \mathbf{W}^\dagger (\mathcal{C}\mathcal{C}^\dagger)^{-1} \mathbf{W} = (\mathcal{C}^{-1}\mathbf{W})^\dagger (\mathcal{C}^{-1}\mathbf{W}). \tag{A.104}$$

Since this quantity is *real* from equations (A.102) and (A.103), we can conclude that

$$\tilde{W} R^{-1} \tilde{W} = 2\mathbf{W}^\dagger \mathcal{R}^{-1} \mathbf{W}. \tag{A.105}$$

To show that $\det(R) = 2^{-2n} |\det(\mathcal{R})|^2$, we make use of claim 2 which also appears in this appendix and states that since

$$\mathcal{R} = D + jE, \tag{A.106}$$

and

$$2R = \begin{pmatrix} D & -E \\ E & D \end{pmatrix}, \tag{A.107}$$

the determinants of these matrices are related by

$$\det(2R) = |\det(\mathcal{R})|^2. \tag{A.108}$$

Since R is a $(2n \times 2n)$ matrix,

$$\det(2R) = 2^{2n} \det(R). \tag{A.109}$$

It thus follows that

$$\det(R) = 2^{-2n} |\det(\mathcal{R})|^2, \tag{A.110}$$

as advertised. Inserting equations (A.105) and (A.110) into equation (A.84) gives the desired result

$$p_{\mathbf{W}}(\mathbf{w}) = \left(\frac{1}{\pi}\right)^n \frac{1}{|\det(\mathcal{R})|} e^{-\mathbf{W}^\dagger \mathcal{R}^{-1} \mathbf{W}}. \quad \blacksquare \tag{A.111}$$

Claim 2: Let Z by an $(n \times n)$ complex valued matrix with real and imaginary parts X and Y respectively, so that

$$Z = X + jY. \qquad (n \times n \text{ complex matrix}) \tag{A.112}$$

Let M by the $(2n \times 2n)$ real valued matrix given by

$$M = \begin{pmatrix} X & -Y \\ Y & X \end{pmatrix}. \qquad (2n \times 2n \text{ real matrix}) \tag{A.113}$$

Then,

$$\det(M) = |\det(Z)|^2. \tag{A.114}$$

Proof: For any complex number $z = x + jy$, let $[\![z]\!]$ denote the real (2×2) matrix

$$[\![z]\!] = \begin{pmatrix} x & -y \\ y & x \end{pmatrix}. \tag{A.115}$$

Observe that, for complex numbers $z_1 = x_1 + jy_1$ and $z_2 = x_2 + jy_2$, we have the property

$$[\![z_1]\!][\![z_2]\!] = \begin{pmatrix} x_1 & -y_1 \\ y_1 & x_1 \end{pmatrix} \begin{pmatrix} x_2 & -y_2 \\ y_2 & x_2 \end{pmatrix} = \begin{pmatrix} x_1x_2 - y_1y_2 & -x_1y_2 - y_1x_2 \\ y_1x_2 + x_1y_2 & x_1x_2 - y_1y_2 \end{pmatrix} = [\![z_1z_2]\!]. \tag{A.116}$$

Hence, (2×2) matrices of this form have the following properties.

(1) $[\![z_1]\!][\![z_2]\!] = [\![z_2]\!][\![z_1]\!]$ for any complex numbers z_1 and z_2.

(2) $\det[\![z]\!] = \mathrm{Re}(z)^2 + \mathrm{Im}(z)^2 = |z|^2$ for any complex number z.

(3) For any complex number $z \neq 0$, the matrix $[\![z]\!]$ is invertible, and its inverse is given by

$[\![z]\!]^{-1} = [\![1/z]\!]$.

We now proceed to evaluate the determinant of M,

$$\det(M) = \det \begin{pmatrix} X & -Y \\ Y & X \end{pmatrix} = \det \begin{pmatrix} x_{11} & x_{12} & \cdots & x_{1n} & -y_{11} & -y_{12} & \cdots & -y_{1n} \\ x_{21} & x_{22} & \cdots & x_{2n} & -y_{21} & -y_{22} & \cdots & -y_{2n} \\ \vdots & \vdots & \ddots & \vdots & \vdots & \vdots & \ddots & \vdots \\ x_{n1} & x_{n2} & \cdots & x_{nn} & -y_{n1} & -y_{n2} & \cdots & -y_{nn} \\ y_{11} & y_{12} & \cdots & y_{1n} & x_{11} & x_{12} & \cdots & x_{1n} \\ y_{21} & y_{22} & \cdots & y_{2n} & x_{21} & x_{22} & \cdots & x_{2n} \\ \vdots & \vdots & \ddots & \vdots & \vdots & \vdots & \ddots & \vdots \\ y_{n1} & y_{n2} & \cdots & y_{nn} & x_{n1} & x_{n2} & \cdots & x_{nn} \end{pmatrix}. \tag{A.117}$$

At this point, we alternately swap consecutive rows of the matrix until each column alternates in x_{ij} and y_{ij} in the following manner

$$\det(M) = (-1)^k \det \begin{pmatrix} x_{11} & x_{12} & \cdots & x_{1n} & -y_{11} & -y_{12} & \cdots & -y_{1n} \\ y_{11} & y_{12} & \cdots & y_{1n} & x_{11} & x_{12} & \cdots & x_{1n} \\ x_{21} & x_{22} & \cdots & x_{2n} & -y_{21} & -y_{22} & \cdots & -y_{2n} \\ y_{21} & y_{22} & \cdots & y_{2n} & x_{21} & x_{22} & \cdots & x_{2n} \\ \vdots & \vdots & \ddots & \vdots & \vdots & \vdots & \ddots & \vdots \\ x_{n1} & x_{n2} & \cdots & x_{nn} & -y_{n1} & -y_{n2} & \cdots & -y_{nn} \\ y_{n1} & y_{n2} & \cdots & y_{nn} & x_{n1} & x_{n2} & \cdots & x_{nn} \end{pmatrix}, \tag{A.118}$$

where k is the number of times consecutive rows of the matrix are swapped. Next, we perform

exactly the same set of k swaps on the *columns* to express this determinant in the form

$$\det(M) = (-1)^{2k} \det \begin{pmatrix} x_{11} & -y_{11} & x_{12} & -y_{12} & \cdots & x_{1n} & -y_{1n} \\ y_{11} & x_{11} & y_{12} & x_{12} & \cdots & y_{1n} & x_{1n} \\ x_{21} & -y_{21} & x_{22} & -y_{22} & \cdots & x_{2n} & -y_{2n} \\ y_{21} & x_{21} & y_{22} & x_{22} & \cdots & y_{2n} & x_{2n} \\ \vdots & \vdots & \vdots & \vdots & \ddots & \vdots & \vdots \\ x_{n1} & -y_{n1} & x_{n2} & -y_{n2} & \cdots & x_{nn} & -y_{nn} \\ y_{n1} & x_{n1} & y_{n2} & x_{n2} & \cdots & y_{nn} & x_{nn} \end{pmatrix}. \tag{A.119}$$

Thus, this can be expressed as the determinant of a block matrix of the form

$$\det(M) = \det \begin{pmatrix} [\![z_{11}]\!] & [\![z_{12}]\!] & \cdots & [\![z_{1n}]\!] \\ [\![z_{21}]\!] & [\![z_{22}]\!] & \cdots & [\![z_{2n}]\!] \\ \vdots & \vdots & \ddots & \vdots \\ [\![z_{n1}]\!] & [\![z_{n2}]\!] & \cdots & [\![z_{nn}]\!] \end{pmatrix}. \tag{A.120}$$

Since the (2×2) blocks in this matrix are all of the special form that they all commute and their inverses commute, using row reduction techniques, this determinant can be expressed as the determinant of a (2×2) matrix corresponding to the complex determinant of the $(n \times n)$ matrix Z. That is,

$$\det(M) = \det[\![\det(Z)]\!]. \tag{A.121}$$

Finally, since the determinant of these (2×2) matrices gives the squared magnitude of the associated complex number, we obtain the desired result, namely

$$\det(M) = |\det(Z)|^2. \quad \blacksquare \tag{A.122}$$

A.7 Computation of Limit For C_{CDMA}[BPSK, Soft Decision, Fading]

Claim: Let

$$I(\bar{p}) = \int_{\alpha=-\infty}^{\infty} \int_{z=0}^{\infty} p_A(\alpha) p_Z(z) \log_2 \left[\frac{4}{\left(1 + \frac{p_Z(z-2\alpha)}{p_Z(z)}\right)\left(1 + \frac{p_Z(z+2\alpha)}{p_Z(z)}\right)} \right] dz\, d\alpha, \tag{A.123}$$

where A is a random variable with mean square value one, and Z is a Gaussian random variable with variance given by equation (4.4) for CDMA. Thus, $p_A(\alpha)$ satisfies

$$\int_{\alpha=-\infty}^{\infty} p_A(\alpha)\alpha^2 d\,\alpha = 1, \tag{A.124}$$

and $p_Z(z)$ is given by

$$p_Z(z) = \frac{1}{\sqrt{2\pi\sigma^2}} e^{\frac{-z^2}{2\sigma^2}}, \tag{A.125}$$

where

$$\sigma^2 = \frac{1}{2}(a+1)\bar{p}. \tag{A.126}$$

Then

$$\lim_{\bar{p}\to\infty} \bar{p} I(\bar{p}) = \frac{\log_2(e)}{a+1}. \tag{A.127}$$

Remark: In the CDMA analysis, the random variable A is the square root of a sum of Rayleigh-squared random variables, and thus is a nonnegative random variable. Thus the probability density function of A is zero for negative values so the region of integration in equation (4.17) is only over positive values of A. This is not required, however, for equation (A.127) to hold. It suffices to assume that A has mean square value one. In this respect, this claim also treats the nonfading case for which A is equal to the constant value one.

Proof: We begin by defining the random variable X which is a normalized Gaussian random variable. Let

$$X = \frac{Z}{\sigma}. \tag{A.128}$$

The probability density function of X is then given by

$$p_X(x) = \frac{1}{\sqrt{2\pi}} e^{\frac{-x^2}{2}}. \tag{A.129}$$

The mutual information $I(\bar{p})$ can now be expressed as

$$\begin{aligned} I(\bar{p}) &= \int_{\alpha=-\infty}^{\infty}\int_{x=0}^{\infty} p_A(\alpha)p_X(x)\log_2\left[\frac{4}{\left(1+\frac{p_Z(\sigma x-2\alpha)}{p_Z(\sigma x)}\right)\left(1+\frac{p_Z(\sigma x+2\alpha)}{p_Z(\sigma x)}\right)}\right]dx\,d\alpha, \\ &= \log_2(e)\int_{\alpha=-\infty}^{\infty}\int_{x=0}^{\infty} p_A(\alpha)p_X(x)\ln\left[\frac{4}{\left(1+e^{-\frac{(\sigma x-2\alpha)^2}{2\sigma^2}+\frac{(\sigma x)^2}{2\sigma^2}}\right)\left(1+e^{-\frac{(\sigma x+2\alpha)^2}{2\sigma^2}+\frac{(\sigma x)^2}{2\sigma^2}}\right)}\right]dx\,d\alpha, \\ &= \log_2(e)\int_{\alpha=-\infty}^{\infty}\int_{x=0}^{\infty} p_A(\alpha)p_X(x)\ln\left[\frac{4}{\left(1+e^{2x\frac{\alpha}{\sigma}-2\left(\frac{\alpha}{\sigma}\right)^2}\right)\left(1+e^{-2x\frac{\alpha}{\sigma}-2\left(\frac{\alpha}{\sigma}\right)^2}\right)}\right]dx\,d\alpha. \end{aligned} \tag{A.130}$$

Note that the function e^x can be expressed as

$$e^x = 1 + x + \frac{1}{2}x^2 + o(x^2), \tag{A.131}$$

where $o(x^2)$ means

$$\lim_{x\to 0}\frac{o(x^2)}{x^2} = 0. \tag{A.132}$$

Using this fact, we can say

$$\begin{aligned} e^{2x\frac{\alpha}{\sigma}-2\left(\frac{\alpha}{\sigma}\right)^2} &= 1+\left[2x\frac{\alpha}{\sigma}-2\left(\frac{\alpha}{\sigma}\right)^2\right]+\frac{1}{2}\left[2x\frac{\alpha}{\sigma}-2\left(\frac{\alpha}{\sigma}\right)^2\right]^2+o\left(\left[2x\frac{\alpha}{\sigma}-2\left(\frac{\alpha}{\sigma}\right)^2\right]^2\right), \\ &= 1+2x\frac{\alpha}{\sigma}-2\left(\frac{\alpha}{\sigma}\right)^2+2\left(\frac{\alpha x}{\sigma}\right)^2+o\left(\frac{1}{\sigma^2}\right). \end{aligned} \tag{A.133}$$

Similarly, we also have

$$e^{-2x\frac{\alpha}{\sigma}-2\left(\frac{\alpha}{\sigma}\right)^2} = 1-2x\frac{\alpha}{\sigma}-2\left(\frac{\alpha}{\sigma}\right)^2+2\left(\frac{\alpha x}{\sigma}\right)^2+o\left(\frac{1}{\sigma^2}\right). \tag{A.134}$$

The denominator of the argument of the logarithm in equation (A.130) can thus be expressed as

$$\begin{aligned} d(x,\alpha,\sigma) &= \left(1+e^{2x\frac{\alpha}{\sigma}-2\left(\frac{\alpha}{\sigma}\right)^2}\right)\left(1+e^{-2x\frac{\alpha}{\sigma}-2\left(\frac{\alpha}{\sigma}\right)^2}\right), \\ &= \left[2+2x\frac{\alpha}{\sigma}-2\left(\frac{\alpha}{\sigma}\right)^2+2\left(\frac{\alpha x}{\sigma}\right)^2+o\left(\frac{1}{\sigma^2}\right)\right]\left[2-2x\frac{\alpha}{\sigma}-2\left(\frac{\alpha}{\sigma}\right)^2+2\left(\frac{\alpha x}{\sigma}\right)^2+o\left(\frac{1}{\sigma^2}\right)\right], \\ &= 4\left[1+x\frac{\alpha}{\sigma}-\left(\frac{\alpha}{\sigma}\right)^2+\left(\frac{\alpha x}{\sigma}\right)^2+o\left(\frac{1}{\sigma^2}\right)\right]\left[1-x\frac{\alpha}{\sigma}-\left(\frac{\alpha}{\sigma}\right)^2+\left(\frac{\alpha x}{\sigma}\right)^2+o\left(\frac{1}{\sigma^2}\right)\right], \\ &= 4\left[1-2\left(\frac{\alpha}{\sigma}\right)^2+2\left(\frac{\alpha x}{\sigma}\right)^2-\left(\frac{\alpha x}{\sigma}\right)^2+o\left(\frac{1}{\sigma^2}\right)\right], \\ &= 4\left[1-2\left(\frac{\alpha}{\sigma}\right)^2+\left(\frac{\alpha x}{\sigma}\right)^2+o\left(\frac{1}{\sigma^2}\right)\right]. \end{aligned} \tag{A.135}$$

Thus, $I(\bar{p})$ can now be expressed as

$$I(\bar{p}) = \log_2(e) \int_{\alpha=-\infty}^{\infty} \int_{x=0}^{\infty} p_A(\alpha) p_X(x) \ln \left[\frac{1}{1 - 2\left(\frac{\alpha}{\sigma}\right)^2 + \left(\frac{\alpha x}{\sigma}\right)^2 + o\left(\frac{1}{\sigma^2}\right)} \right] dx\, d\alpha. \tag{A.136}$$

Now, note the following property of the natural logarithm which follows directly from its Taylor series expansion about the point $x = 1$, namely that

$$\ln\left(\frac{1}{1-x}\right) = x + o(x). \tag{A.137}$$

Thus,

$$\ln \left[\frac{1}{1 - 2\left(\frac{\alpha}{\sigma}\right)^2 + \left(\frac{\alpha x}{\sigma}\right)^2 + o\left(\frac{1}{\sigma^2}\right)} \right] = 2\left(\frac{\alpha}{\sigma}\right)^2 - \left(\frac{\alpha x}{\sigma}\right)^2 + o\left(\frac{1}{\sigma^2}\right). \tag{A.138}$$

Inserting equation (A.138) into equation (A.136) allows us to write $I(\bar{p})$ as

$$I(\bar{p}) = \log_2(e) \int_{\alpha=-\infty}^{\infty} \int_{x=0}^{\infty} p_A(\alpha) p_X(x) \left[2\left(\frac{\alpha}{\sigma}\right)^2 - \left(\frac{\alpha x}{\sigma}\right)^2 + o\left(\frac{1}{\sigma^2}\right) \right] dx\, d\alpha. \tag{A.139}$$

With respect to equation (A.129), since $p_X(x)$ is the probability density function of a mean zero variance one Gaussian random variable, it follows that

$$\int_0^{\infty} p_X(x) dx = \frac{1}{2}, \qquad \text{and} \qquad \int_0^{\infty} x^2 p_X(x) dx = \frac{1}{2}. \tag{A.140}$$

Applying these relations to equation (A.139) gives

$$\begin{aligned} I(\bar{p}) &= \log_2(e) \int_{\alpha=-\infty}^{\infty} p_A(\alpha) \left[\frac{\alpha^2}{\sigma^2} - \frac{\alpha^2}{2\sigma^2} + o\left(\frac{1}{\sigma^2}\right) \right] d\alpha, \\ &= \frac{\log_2(e)}{2} \int_{\alpha=-\infty}^{\infty} p_A(\alpha) \left[\frac{\alpha^2}{\sigma^2} + o\left(\frac{1}{\sigma^2}\right) \right] d\alpha. \end{aligned} \tag{A.141}$$

Using the fact that $p_A(\alpha)$ is a probability density function and thus integrates to one and also the fact that A has mean square value one so that equation (A.124) is satisfied, $I(\bar{p})$ can be simplified to

$$I(\bar{p}) = \frac{\log_2(e)}{2\sigma^2} + o\left(\frac{1}{\sigma^2}\right). \tag{A.142}$$

Using the expression for σ^2, given by equation (A.126), note that

$$o\left(\frac{1}{\sigma^2}\right) = o\left(\frac{1}{\bar{p}}\right). \tag{A.143}$$

Therefore, we have

$$I(\bar{p}) = \frac{\log_2(e)}{(a+1)\bar{p}} + o\left(\frac{1}{\bar{p}}\right). \tag{A.144}$$

Thus,

$$\bar{p}I(\bar{p}) = \frac{\log_2(e)}{(a+1)} + \frac{o\left(\frac{1}{\bar{p}}\right)}{\left(\frac{1}{\bar{p}}\right)}. \tag{A.145}$$

Finally, letting $\bar{p} \to \infty$ gives the desired result,

$$\lim_{\bar{p}\to\infty} \bar{p}I(\bar{p}) = \frac{\log_2(e)}{a+1}. \quad \blacksquare \tag{A.146}$$

A.8 Computation of Limit For C_{CDMA}[BPSK, Hard Decision, Fading]

Claim: Let

$$P_b(\bar{p}) = \frac{1}{2}\sum_k \pi_k \left(1 - \sqrt{\frac{b_k}{b_k + (a+1)\bar{p}}}\right), \tag{A.147}$$

and

$$I(\bar{p}) = 1 - \mathcal{H}(P_b(\bar{p})), \tag{A.148}$$

where

$$\pi_k = \prod_{i \neq k} \frac{b_k}{b_k - b_i}, \tag{A.149}$$

and $\mathcal{H}(x)$ is the binary entropy function defined by

$$\mathcal{H}(x) = x\log_2\left(\frac{1}{x}\right) + (1-x)\log_2\left(\frac{1}{1-x}\right). \tag{A.150}$$

Then,

$$\lim_{\bar{p}\to\infty} \bar{p}I(\bar{p}) = \frac{\log_2(e)}{2(a+1)}\left(\sum_k \pi_k\sqrt{b_k}\right)^2. \tag{A.151}$$

Proof: First, note that

$$\lim_{\bar{p}\to\infty} P_b(\bar{p}) = \frac{1}{2}. \tag{A.152}$$

This is due to the fact that the π_k's sum to one which is established in appendix A.10 by equation $(A.180)$. Also, note that the derivative of $\mathcal{H}(x)$ is given by

$$\mathcal{H}'(x) = \log_2(e)\ln\left(\frac{1-x}{x}\right). \tag{A.153}$$

We begin by expressing the limit as

$$\lim_{\bar{p}\to\infty} \bar{p}I(\bar{p}) = \lim_{\bar{p}\to\infty} \bar{p}\left[1 - \mathcal{H}(P_b(\bar{p}))\right] = \lim_{\bar{p}\to\infty} \frac{1 - \mathcal{H}(P_b(\bar{p}))}{\frac{1}{\bar{p}}}, \tag{A.154}$$

which is of the form $0/0$. Applying L'Hospital's Rule and making use of equation (A.153) gives

$$\lim_{\bar{p}\to\infty} \bar{p}I(\bar{p}) = \lim_{\bar{p}\to\infty} \log_2(e)\frac{-\ln\left(\frac{1-P_b(\bar{p})}{P_b(\bar{p})}\right)\left[\frac{a+1}{4}\sum_k \pi_k\sqrt{b_k}[b_k + (a+1)\bar{p}]^{-\frac{3}{2}}\right]}{-\frac{1}{\bar{p}^2}}. \tag{A.155}$$

Rearranging equation (A.155) and noting that

$$\lim_{\bar{p}\to\infty} (\bar{p})^{\frac{3}{2}}[b_k + (a+1)\bar{p}]^{-\frac{3}{2}} = (a+1)^{-\frac{3}{2}}, \tag{A.156}$$

gives

$$\lim_{\bar{p}\to\infty} \bar{p}I(\bar{p}) = \frac{\log_2(e)\sum_k \pi_k\sqrt{b_k}}{4\sqrt{a+1}} \lim_{\bar{p}\to\infty} \frac{\ln\left(\frac{1-P_b(\bar{p})}{P_b(\bar{p})}\right)}{\bar{p}^{-\frac{1}{2}}}, \tag{A.157}$$

which is also of the form $0/0$. Applying L'Hospital's Rule again we find

$$\lim_{\bar{p}\to\infty} \bar{p}I(\bar{p}) = \left[\begin{array}{l} \left(\frac{\log_2(e)\sum_k \pi_k\sqrt{b_k}}{4\sqrt{a+1}}\right) \times \\ \qquad \lim_{\bar{p}\to\infty} \frac{\left(\frac{P_b(\bar{p})}{1-P_b(\bar{p})}\right)\left(\frac{-1}{P_b^2(\bar{p})}\right)\left[\frac{a+1}{4}\sum_k \pi_k\sqrt{b_k}[b_k+(a+1)\bar{p}]^{-\frac{3}{2}}\right]}{-\frac{1}{2}\bar{p}^{-\frac{3}{2}}} \end{array} \right]. \tag{A.158}$$

Finally, rearranging equation (A.158) and making use of equations (A.152) and (A.156), we conclude that

$$\lim_{\bar{p}\to\infty} \bar{p}I(\bar{p}) = \frac{\log_2(e)}{2(a+1)} \left(\sum_k \pi_k\sqrt{b_k}\right)^2 . \quad \blacksquare \tag{A.159}$$

A.9 Computation of Limit For C_{CDMA}[BPSK, Hard Decision, No Fading]

Claim: Let

$$P_b(\bar{p}) = \frac{1}{2}\operatorname{erfc}\left(\sqrt{\frac{1}{(a+1)\bar{p}}}\right), \tag{A.160}$$

and

$$I(\bar{p}) = 1 - \mathcal{H}(P_b(\bar{p})), \tag{A.161}$$

where $\mathcal{H}(x)$ is the binary entropy function defined by

$$\mathcal{H}(x) = x\log_2\left(\frac{1}{x}\right) + (1-x)\log_2\left(\frac{1}{1-x}\right). \tag{A.162}$$

Then,

$$\lim_{\bar{p}\to\infty} \bar{p}I(\bar{p}) = \frac{2\log_2(e)}{\pi(a+1)}. \tag{A.163}$$

Proof: First, note that

$$\lim_{\bar{p}\to\infty} P_b(\bar{p}) = \frac{1}{2}. \tag{A.164}$$

Also, note that the derivatives of the functions $\operatorname{erfc}(x)$ and $\mathcal{H}(x)$ are given by

$$\operatorname{erfc}'(x) = -\frac{2}{\sqrt{\pi}}e^{-x^2}, \tag{A.165}$$

$$\mathcal{H}'(x) = \log_2(e)\ln\left(\frac{1-x}{x}\right). \tag{A.166}$$

We begin by expressing the limit as

$$\lim_{\bar{p}\to\infty} \bar{p}I(\bar{p}) = \lim_{\bar{p}\to\infty} \bar{p}\left[1 - \mathcal{H}(P_b(\bar{p}))\right] = \lim_{\bar{p}\to\infty} \frac{1-\mathcal{H}(P_b(\bar{p}))}{\frac{1}{\bar{p}}}, \tag{A.167}$$

which is of the form 0/0. Applying L'Hospital's Rule and making use of equations (A.165) and (A.166) gives

$$\lim_{\bar{p}\to\infty} \bar{p}I(\bar{p}) = \lim_{\bar{p}\to\infty} \log_2(e)\frac{-\ln\left(\frac{1-P_b(\bar{p})}{P_b(\bar{p})}\right)\left[\frac{1}{2\sqrt{\pi}\sqrt{a+1}}e^{-\frac{1}{(a+1)\bar{p}}}\bar{p}^{-\frac{3}{2}}\right]}{-\frac{1}{\bar{p}^2}}. \tag{A.168}$$

Rearranging equation (A.168) and noting that

$$\lim_{\bar{p}\to\infty} e^{-\frac{1}{(a+1)\bar{p}}} = 1, \tag{A.169}$$

gives

$$\lim_{\bar{p}\to\infty} \bar{p}I(\bar{p}) = \frac{\log_2(e)}{2\sqrt{\pi}\sqrt{a+1}} \cdot \lim_{\bar{p}\to\infty} \frac{\ln\left(\frac{1-P_b(\bar{p})}{P_b(\bar{p})}\right)}{\bar{p}^{-\frac{1}{2}}}, \tag{A.170}$$

which is also of the form 0/0. Applying L'Hospital's Rule again we find

$$\lim_{\bar{p}\to\infty} \bar{p}I(\bar{p}) = \frac{\log_2(e)}{2\sqrt{\pi}\sqrt{a+1}} \lim_{\bar{p}\to\infty} \frac{\left(\frac{P_b(\bar{p})}{1-P_b(\bar{p})}\right)\left(-\frac{1}{P_b^2(\bar{p})}\right)\left(\frac{1}{2\sqrt{\pi}\sqrt{a+1}}\right) e^{-\frac{1}{(a+1)\bar{p}}} \bar{p}^{-\frac{3}{2}}}{-\frac{1}{2}\bar{p}^{-\frac{3}{2}}}. \tag{A.171}$$

Finally, rearranging equation (A.171) and making use of equations (A.164) and (A.169), we conclude that

$$\lim_{\bar{p}\to\infty} \bar{p}I(\bar{p}) = \frac{2\log_2(e)}{\pi(a+1)}. \quad \blacksquare \tag{A.172}$$

A.10 Computation of Limit For C_{CDMA}[MASK, Fading]

Claim: Let

$$I(\bar{p}) = -\frac{\log_2(e)}{2}\left[\sum_k \pi_k e^{\frac{(a+1)\bar{p}}{2b_k}} \mathrm{Ei}\left(-\frac{(a+1)\bar{p}}{2b_k}\right)\right], \tag{A.173}$$

where

$$\pi_k = \prod_{i\neq k} \frac{b_k}{b_k - b_i}, \tag{A.174}$$

$\mathrm{Ei}(x)$ is the Exponential integrating function defined by

$$\mathrm{Ei}(x) = \int_{-\infty}^{x} \frac{e^t}{t} dt, \tag{A.175}$$

and the b_k's are positive real numbers that satisfy

$$\sum_k b_k = 1. \tag{A.176}$$

Then,

$$\lim_{\bar{p}\to\infty} \bar{p} I(\bar{p}) = \frac{\log_2(e)}{a+1}. \tag{A.177}$$

Proof: First we establish an important property of the π_k's. Consider the following partial fraction expansion

$$\frac{1}{(1+sb_0)(1+sb_1)\cdots(1+sb_{L-1})} = \frac{\pi_0}{1+sb_0} + \frac{\pi_1}{1+sb_1} + \cdots + \frac{\pi_{L-1}}{1+sb_{L-1}}. \tag{A.178}$$

Differentiating this with respect to s gives

$$\frac{-\frac{b_0}{1+sb_0} - \frac{b_1}{1+sb_1} - \cdots - \frac{b_{L-1}}{1+sb_{L-1}}}{(1+sb_0)(1+sb_1)\cdots(1+sb_{L-1})} = -\frac{\pi_0 b_0}{1+sb_0} - \frac{\pi_1 b_1}{1+sb_1} - \cdots - \frac{\pi_{L-1} b_{L-1}}{1+sb_{L-1}}. \tag{A.179}$$

Now, setting $s = 0$ and letting $L \to \infty$ in equations (A.178) and (A.179) gives

$$\sum_k \pi_k = 1, \qquad \text{and} \qquad \sum_k \pi_k b_k = \sum_k b_k = 1. \tag{A.180}$$

Note that we have made use of equation (A.176). We now proceed to compute the desired limit

$$\begin{aligned}\lim_{\bar{p}\to\infty} \bar{p} I(\bar{p}) &= \frac{\log_2(e)}{2}\left[-\sum_k \pi_k \lim_{\bar{p}\to\infty} \bar{p} e^{\frac{(a+1)\bar{p}}{2b_k}} \mathrm{Ei}\left(-\frac{(a+1)\bar{p}}{2b_k}\right)\right], \\ &= \frac{\log_2(e)}{2}\sum_k \pi_k \lim_{\bar{p}\to\infty} \frac{\int_{\frac{(a+1)\bar{p}}{2b_k}}^{\infty} \frac{e^{-t}}{t} dt}{\frac{1}{\bar{p}} e^{-\frac{(a+1)\bar{p}}{2b_k}}}.\end{aligned} \tag{A.181}$$

This is of the form 0/0. Applying L'Hospital's Rule gives

$$\begin{aligned}
\lim_{\bar{p}\to\infty} \bar{p}I(\bar{p}) &= \frac{\log_2(e)}{2} \sum_k \pi_k \lim_{\bar{p}\to\infty} \frac{-\frac{(a+1)}{2b_k} e^{-\frac{(a+1)\bar{p}}{2b_k}} \frac{2b_k}{(a+1)\bar{p}}}{-\frac{1}{\bar{p}^2} e^{-\frac{(a+1)\bar{p}}{2b_k}} - \frac{(a+1)}{2b_k} \frac{1}{\bar{p}} e^{-\frac{(a+1)\bar{p}}{2b_k}}}, \\
&= \frac{\log_2(e)}{2} \sum_k \pi_k \lim_{\bar{p}\to\infty} \frac{\frac{2b_k}{(a+1)}}{\left(\frac{2b_k}{(a+1)}\right)\frac{1}{\bar{p}} + 1}, \\
&= \frac{\log_2(e)}{a+1} \sum_k \pi_k b_k. \qquad \text{(A.182)}
\end{aligned}$$

Finally, making use of equation (A.180) gives the desired result

$$\lim_{\bar{p}\to\infty} \bar{p}I(\bar{p}) = \frac{\log_2(e)}{a+1}. \quad \blacksquare \qquad \text{(A.183)}$$

A.11 Integration Formula For Repetition Codes

The following integration formula is used in section 5.2 to analyze the probability of bit error performance for both FH and CDMA systems when repetition coding is used.

Claim: Let

$$I_M = \frac{1}{M!c^{M+1}} \int_0^\infty t^M e^{-t/c} \frac{1}{2} \operatorname{erfc}(\sqrt{t})\, dt, \tag{A.184}$$

where c is a positive real number, and M is an integer, $M \geq 0$. Then

$$I_M = \left(\frac{1-\mu}{2}\right)^{M+1} \sum_{l=0}^{M} \binom{M+l}{l} \left(\frac{1+\mu}{2}\right)^l, \tag{A.185}$$

where

$$\mu = \sqrt{\frac{c}{c+1}}. \tag{A.186}$$

Proof: We will make use of the following integration formula. For any integer, $n \geq 0$, and real number, $p > 0$,

$$\int_0^\infty x^{2n} e^{-px^2}\, dx = \frac{(2n)!}{2^n n! 2(2p)^n} \sqrt{\frac{\pi}{p}}. \tag{A.187}$$

This formula appears in [16] as formula 3.461.2. We begin by making the change of variables $y = \sqrt{t}$ to rewrite equation (A.184) as

$$I_M = \frac{1}{M!c^{M+1}} \int_0^\infty y^{2M} e^{-y^2/c} \operatorname{erfc}(y) y\, dy. \tag{A.188}$$

Next, we proceed with a proof by induction on the variable M. For $M = 0$,

$$I_0 = \frac{1}{c} \int_0^\infty e^{-y^2/c} \operatorname{erfc}(y) y\, dy. \tag{A.189}$$

Performing integration by parts where $u = \operatorname{erfc}(y)$ and $dv = ye^{-y^2/c}$ gives

$$I_0 = \frac{1}{2} - \int_0^\infty \frac{1}{\sqrt{\pi}} e^{-y^2\left(\frac{c+1}{c}\right)}\, dy. \tag{A.190}$$

Note that we have made use of equation (A.165) for the derivative of the erfc function. Making use of the integration formula given in equation (A.187) with $n = 0$ and $p = (c+1)/c$, this can be simplified to

$$I_0 = \frac{1-\mu}{2}. \tag{A.191}$$

This agrees with equation (A.185) for $M = 0$. Thus, the claim holds for $M = 0$. Next, we assume that the claim is true for some $(M-1)$, $M \geq 1$, and consider I_M. Performing integration by parts on equation (A.188), where $u = y^{2M}\operatorname{erfc}(y)$ and $dv = ye^{-y^2/c}$, gives

$$I_M = \underbrace{\frac{1}{(M-1)!c^M}\int_0^\infty y^{2M-1}e^{-y^2/c}\operatorname{erfc}(y)\,dy}_{I_{M-1}} - \frac{1}{M!c^M}\int_0^\infty \frac{1}{\sqrt{\pi}}y^{2M}e^{-y^2\left(\frac{c+1}{c}\right)}\,dy. \tag{A.192}$$

Making use of the integration formula given in equation (A.187) with $n = M$ and $p = (c+1)/c$, this can be simplified to

$$I_M = I_{M-1} - \frac{1}{M!c^M}\frac{(2M)!}{2^M M!}\frac{\mu^{2M}}{2^M}\frac{\mu}{2}. \tag{A.193}$$

Using the fact that $\mu^2/c = (1-\mu)(1+\mu)$, this expression can be rearranged as follows

$$\begin{aligned}
I_M &= I_{M-1} - \binom{2M}{M}\left(\frac{1-\mu}{2}\right)^M\left(\frac{1+\mu}{2}\right)^M\left(\frac{1}{2}-\frac{1-\mu}{2}\right),\\
&= I_{M-1} - \frac{1}{2}\binom{2M}{M}\left(\frac{1-\mu}{2}\right)^M\left(\frac{1+\mu}{2}\right)^M + \binom{2M}{M}\left(\frac{1-\mu}{2}\right)^{M+1}\left(\frac{1+\mu}{2}\right)^M,\\
&= I_{M-1} - \binom{2M-1}{M-1}\left(\frac{1-\mu}{2}\right)^M\left(\frac{1+\mu}{2}\right)^{M-1}\left(1-\frac{1-\mu}{2}\right) + \binom{2M}{M}\left(\frac{1-\mu}{2}\right)^{M+1}\left(\frac{1+\mu}{2}\right)^M,\\
&= \left[\begin{array}{l} I_{M-1} - \binom{2M-1}{M-1}\left(\frac{1-\mu}{2}\right)^M\left(\frac{1+\mu}{2}\right)^{M-1} \\ \quad + \binom{2M-1}{M-1}\left(\frac{1-\mu}{2}\right)^{M+1}\left(\frac{1+\mu}{2}\right)^{M-1} \\ \quad + \binom{2M}{M}\left(\frac{1-\mu}{2}\right)^{M+1}\left(\frac{1+\mu}{2}\right)^M \end{array}\right].
\end{aligned} \tag{A.194}$$

By the inductive hypothesis, I_{M-1} is given by

$$I_{M-1} = \left(\frac{1-\mu}{2}\right)^M\sum_{l=0}^{M-1}\binom{M-1+l}{l}\left(\frac{1+\mu}{2}\right)^l. \tag{A.195}$$

Making use of the combinatorial identity

$$\binom{M-1+l}{l} = \binom{M+l}{l} - \binom{M-1+l}{l-1}, \tag{A.196}$$

we can express I_{M-1} as

$$I_{M-1} = \left(\frac{1-\mu}{2}\right)^M\sum_{l=0}^{M-1}\binom{M+l}{l}\left(\frac{1+\mu}{2}\right)^l - \left(\frac{1-\mu}{2}\right)^M\sum_{l=0}^{M-1}\binom{M-1+l}{l-1}\left(\frac{1+\mu}{2}\right)^l. \tag{A.197}$$

Replacing l by $l+1$ in the second summation and using the fact that for any integer k, $\binom{k}{-1} = 0$, gives

$$I_{M-1} = \begin{array}{l} \left[\left(\frac{1-\mu}{2}\right)^M \sum_{l=0}^{M-1} \binom{M+l}{l}\left(\frac{1+\mu}{2}\right)^l\right] \\ -\left[\left(\frac{1-\mu}{2}\right)^M \sum_{l=0}^{M-2} \binom{M+l}{l}\left(\frac{1+\mu}{2}\right)^l\right]\left(\frac{1+\mu}{2}\right) \end{array} \tag{A.198}$$

Rearranging this expression, I_{M-1} can be expressed as

$$I_{M-1} = \left(\frac{1-\mu}{2}\right)^{M+1} \sum_{l=0}^{M-2} \binom{M+l}{l}\left(\frac{1+\mu}{2}\right)^l + \binom{2M-1}{M-1}\left(\frac{1-\mu}{2}\right)^M \left(\frac{1+\mu}{2}\right)^{M-1}. \tag{A.199}$$

Combining equations (A.194) and (A.199), I_M is given by

$$I_M = \left[\begin{array}{l} \left(\frac{1-\mu}{2}\right)^{M+1} \sum_{l=0}^{M-2} \binom{M+l}{l}\left(\frac{1+\mu}{2}\right)^l \\ \qquad + \binom{2M-1}{M-1}\left(\frac{1-\mu}{2}\right)^{M+1}\left(\frac{1+\mu}{2}\right)^{M-1} \\ \qquad + \binom{2M}{M}\left(\frac{1-\mu}{2}\right)^{M+1}\left(\frac{1+\mu}{2}\right)^M \end{array}\right]. \tag{A.200}$$

Incorporating these terms into a single summation gives the result

$$I_M = \left(\frac{1-\mu}{2}\right)^{M+1} \sum_{l=0}^{M} \binom{M+l}{l}\left(\frac{1+\mu}{2}\right)^l. \tag{A.201}$$

This completes the proof. ∎

A.12 Performance of CDMA With Repetition Codes

In this appendix, we derive an expression for the probability density function of the fading parameter, A, defined by equation (5.7) for the CDMA system using D-fold repetition coding. Next, we use this distribution to compute the probablility of bit error by averaging the conditional probability of bit error given by equation (5.15).

For a single Rayleigh random variable, B_q, having mean square value b_q, the random variable B_q^2 has a central chi-squared distribution with 2 degrees of freedom. Thus, it has a characteristic function ([9], pg. 498) given by ([1], pg. 26)

$$\phi_{B_q^2}(s) = \mathrm{E}\{e^{jsB_q^2}\} = \left(\frac{1}{1-jsb_q}\right). \tag{A.202}$$

Since each of the A_m's in equation (5.7) can be expressed as the square root of a sum of independent Rayleigh-squared random variables as in equation (3.58), the characteristic function for A_m^2 is

$$\phi_{A_m^2}(s) = \prod_{q=0}^{L-1}\left(\frac{1}{1-jsb_q}\right). \tag{A.203}$$

We are assuming that a CDMA RAKE receiver with L tap coefficients is being used, and thus each of the A_m^2's is taken to be a sum of L Rayleigh-squared random variables. Since the A_m's are all *i.i.d.*, the random variable A, given by equation (5.7), has characteristic function

$$\phi_A(s) = \prod_{q=0}^{L-1}\left(\frac{1}{1-jsb_q}\right)^D. \tag{A.204}$$

Since the characteristic function is the Fourier transform (with $s = -\omega$ where ω is the standard frequency domain variable) of the probability density function, we search for a function whose transform is equation (A.204). Such a function is the probability density function of A. We will let the symbol $\leftrightarrow$ denote the fact that two functions are related by the Fourier transform (with $s = -\omega$). That is

$$\phi(s) \leftrightarrow f(t) \tag{A.205}$$

means

$$\phi(s) = \int_{-\infty}^{\infty} f(t)e^{jst}\,dt. \tag{A.206}$$

We begin by noting that for a single exponential,

$$\left(\frac{1}{a_q - js}\right) \leftrightarrow e^{-a_q t}u(t), \tag{A.207}$$

where a_q is a constant, and $u(t)$ is a unit step function equal to unity for positive values of t and equal to zero for negative values of t. Using a partial fraction expansion, it then follows that

$$\prod_{q=0}^{L-1}\left(\frac{1}{a_q - js}\right) \leftrightarrow \sum_{q=0}^{L-1} Q_q e^{-a_q t}u(t), \tag{A.208}$$

where

$$Q_q = \prod_{j\neq q}\frac{1}{a_j - a_q}, \tag{A.209}$$

and the a_q's are constants. At this point, we differentiate equation (A.208) with respect to each of the a_q's $(D-1)$ times. This gives

$$[(-1)^{D-1}(D-1)!]^L \prod_{q=0}^{L-1}\left(\frac{1}{a_q - js}\right)^D \leftrightarrow \frac{\partial^{D-1}}{\partial a_0^{D-1}}\frac{\partial^{D-1}}{\partial a_1^{D-1}}\cdots\frac{\partial^{D-1}}{\partial a_{L-1}^{D-1}}\sum_{q=0}^{L-1} Q_q e^{-a_q t}u(t). \tag{A.210}$$

We begin expanding the right hand side of equation (A.210) by considering the single term

$$\frac{\partial^{D-1}}{\partial a_q^{D-1}}(Q_q e^{-a_q t}) = \sum_{k=0}^{D-1}\binom{D-1}{k}\left(\frac{\partial^k}{\partial a_q^k}Q_q\right)(-t)^{D-1-k}e^{-a_q t}. \tag{A.211}$$

Computing the derivatives of Q_q, given by equation (A.209), with respect to a_q gives

$$\frac{\partial^k}{\partial a_q^k}Q_q = \sum_{S(q,k)} k!\prod_{j\neq q}\left[(a_j - a_q)^{-(m_j+1)}\right], \tag{A.212}$$

where

$$S(q,k) = \left\{(m_0, m_1, \ldots, m_{L-1}) : m_j = \text{nonnegative integer}\ ;\quad \sum_{j=0}^{L-1} m_j = k;\quad m_q = 0\right\}. \tag{A.213}$$

For example, if $L = 4$, $q = 2$, and $k = 2$, the set S has six elements of the form (m_0, m_1, m_2, m_3), and is given by $S = \{(2,0,0,0),(1,1,0,0),(1,0,0,1),(0,2,0,0),(0,1,0,1),(0,0,0,2)\}$. In this case, equation (A.212) states that

$$\begin{aligned}\frac{\partial^2}{\partial a_2^2}Q_2 &= \frac{\partial^2}{\partial a_2^2}\left[\left(\frac{1}{a_0 - a_2}\right)\left(\frac{1}{a_1 - a_2}\right)\left(\frac{1}{a_3 - a_2}\right)\right], \\ &= 2\begin{bmatrix} (a_0-a_2)^{-3}(a_1-a_2)^{-1}(a_3-a_2)^{-1} + (a_0-a_2)^{-2}(a_1-a_2)^{-2}(a_3-a_2)^{-1} \\ +(a_0-a_2)^{-2}(a_1-a_2)^{-1}(a_3-a_2)^{-2} + (a_0-a_2)^{-1}(a_1-a_2)^{-3}(a_3-a_2)^{-1} \\ +(a_0-a_2)^{-1}(a_1-a_2)^{-2}(a_3-a_2)^{-2} + (a_0-a_2)^{-1}(a_1-a_2)^{-1}(a_3-a_2)^{-3}\end{bmatrix}.\end{aligned} \tag{A.214}$$

Note that, in general, the number of elements in the set $S(q,k)$ is equal to the number of ways the integer k can be partitioned into $L-1$ nonnegative pieces, which is $\binom{k+L-2}{k}$.

Inserting equation (A.212) into equation (A.211), we have

$$\frac{\partial^{D-1}}{\partial a_q^{D-1}}(Q_q e^{-a_q t}) = \sum_{k=0}^{D-1} \binom{D-1}{k} \sum_{S(q,k)} k! \left[\prod_{j\neq q}(a_j - a_q)^{-(m_j+1)}\right] (-t)^{D-1-k} e^{-a_q t}. \tag{A.215}$$

Now, computing the partial derivatives with respect to the a_j's, where $j \neq q$, gives

$$\frac{\partial^{D-1}}{\partial a_0^{D-1}} \frac{\partial^{D-1}}{\partial a_1^{D-1}} \cdots \frac{\partial^{D-1}}{\partial a_{L-1}^{D-1}} Q_q e^{-a_q t} \tag{A.216}$$
$$= \sum_{k=0}^{D-1} \binom{D-1}{k} \sum_{S(q,k)} k! \left[\prod_{j\neq q}(-1)^{D-1} \frac{(m_j+D-1)!}{m_j!}(a_j - a_q)^{-(m_j+D)}\right] (-t)^{D-1-k} e^{-a_q t}.$$

Note that

$$\binom{D-1}{k} k! \prod_{j\neq q} \frac{(m_j+D-1)!}{m_j!} = \frac{(D-1)!}{k!(D-k-1)!} k! \prod_{j\neq q} \frac{(m_j+D-1)!}{m_j!},$$
$$= \frac{[(D-1)!]^L}{(D-k-1)!} \prod_{j\neq q} \binom{m_j+D-1}{D-1}. \tag{A.217}$$

Also note that

$$(-t)^{D-1-k} \prod_{j\neq q}(-1)^{D-1} = (-1)^{L(D-1)-k} t^{D-1-k} = (-1)^{L(D-1)+k} t^{D-1-k}. \tag{A.218}$$

Inserting equations (A.217) and (A.218) into equation (A.216) gives

$$\frac{\partial^{D-1}}{\partial a_0^{D-1}} \frac{\partial^{D-1}}{\partial a_1^{D-1}} \cdots \frac{\partial^{D-1}}{\partial a_{L-1}^{D-1}} Q_q e^{-a_q t} \tag{A.219}$$
$$= \sum_{k=0}^{D-1} \frac{[(D-1)!]^L}{(D-k-1)!} (-1)^{L(D-1)+k} \sum_{S(q,k)} \left[\prod_{j\neq q} \binom{m_j+D-1}{D-1}(a_j - a_q)^{-(m_j+D)}\right] t^{D-1-k} e^{-a_q t}.$$

Now, summing over q and inserting this into equation (A.210) gives

$$[(-1)^{D-1}(D-1)!]^L \prod_{q=0}^{L-1} \left(\frac{1}{a_q - js}\right)^D \leftrightarrow \tag{A.220}$$
$$\sum_{q=0}^{L-1} \sum_{k=0}^{D-1} \frac{[(D-1)!]^L}{(D-k-1)!} (-1)^{L(D-1)+k} \sum_{S(q,k)} \left[\prod_{j\neq q} \binom{m_j+D-1}{D-1}(a_j - a_q)^{-(m_j+D)}\right] t^{D-1-k} e^{-a_q t} u(t).$$

Dividing through by $[(-1)^{D-1}(D-1)!]^L$ then gives

$$\prod_{q=0}^{L-1} \left(\frac{1}{a_q - js}\right)^D \leftrightarrow \tag{A.221}$$
$$\sum_{q=0}^{L-1} \sum_{k=0}^{D-1} \frac{(-1)^k}{(D-k-1)!} \sum_{S(q,k)} \left[\prod_{j\neq q} \binom{m_j+D-1}{D-1}(a_j - a_q)^{-(m_j+D)}\right] t^{D-1-k} e^{-a_q t} u(t).$$

Now we set $a_q = 1/b_q$ which gives

$$\prod_{q=0}^{L-1}\left(\frac{1}{1-jsb_q}\right)^D \leftrightarrow \sum_{q=0}^{L-1}\sum_{k=0}^{D-1}\frac{\frac{(-1)^k}{(D-k-1)!}\sum_{S(q,k)}\left[\prod_{j\neq q}\binom{m_j+D-1}{D-1}\left(\frac{b_j b_q}{b_q-b_j}\right)^{m_j+D}\right]}{\left[\prod_{q=0}^{L-1}b_q\right]^D}t^{D-1-k}e^{-t/b_q}u(t). \tag{A.222}$$

Note that the left hand side of this equation is equal to the characteristic function of the fading random variable, A, given by equation (A.204). Thus, the right hand side must be the probability density function of the random variable A. Making use of the definition of π_q which appears in equation (3.60), and performing some additional rearrangement, the probability density function of A, $p_A(\alpha)$, can be expressed as

$$p_A(\alpha) = \sum_{q=0}^{L-1}\pi_q^D\sum_{k=0}^{D-1}\frac{1}{(D-k-1)!b_q^{D-k}}F(q,k)\alpha^{D-1-k}e^{-\alpha/b_q}u(\alpha), \tag{A.223}$$

where

$$F(q,k) = (-1)^k\sum_{S(q,k)}\left[\prod_{j=0}^{L-1}\binom{m_j+D-1}{D-1}\left(\frac{b_j}{b_q-b_j}\right)^{m_j}\right]. \tag{A.224}$$

Since each element of $S(q,k)$ has $m_q = 0$, the value of the product in equation (A.224) is not changed by including the term for $j = q$.

The probability of bit error can now be found by computing

$$P_b = \int_0^\infty p_A(\alpha)\frac{1}{2}\operatorname{erfc}\left(\sqrt{\frac{\alpha}{(a+1)Dp}}\right)d\alpha. \tag{A.225}$$

Thus,

$$P_b = \sum_{q=0}^{L-1}\pi_q^D\sum_{k=0}^{D-1}F(q,k)\frac{1}{(D-k-1)!b_q^{D-k}}\int_0^\infty \alpha^{D-1-k}e^{-\alpha/b_q}\frac{1}{2}\operatorname{erfc}\left(\sqrt{\frac{\alpha}{(a+1)Dp}}\right)d\alpha. \tag{A.226}$$

Making the change of variables $t = \alpha/[(a+1)Dp]$, we can rewrite this as

$$P_b = \sum_{q=0}^{L-1}\pi_q^D\sum_{k=0}^{D-1}F(q,k)\frac{1}{(D-k-1)!\left(\frac{b_q}{(a+1)Dp}\right)^{D-k}}\int_0^\infty t^{D-1-k}e^{-t\frac{(a+1)Dp}{b_q}}\frac{1}{2}\operatorname{erfc}(\sqrt{t})\,dt. \tag{A.227}$$

Finally, we make use of the integration formula in appendix A.11 with $M = D-k-1$ and $c = b_q/[(a+1)Dp]$, and obtain the result

$$P_b = \sum_{q=0}^{L-1}\pi_q^D\sum_{k=0}^{D-1}F(q,k)\left(\frac{1-\mu_q}{2}\right)^{(D-k)}\sum_{l=0}^{(D-k-1)}\binom{D-k-1+l}{l}\left(\frac{1+\mu_q}{2}\right)^l, \tag{A.228}$$

where

$$\mu_q = \sqrt{\frac{b_q}{(a+1)Dp+b_q}}. \tag{A.229}$$

8. References.

[1] Proakis, John G., "Digital Communications," New York: McGraw Hill, 1989.

[2] Simon, M.K., J. K. Omura, R. A. Scholtz, and B. K. Levitt, "Spread Spectrum Communications," Vol. 2, MD: Computer Science Press, 1985.

[3] Verhulst, D., M. Mouley, and J. Szpirglas, "Slow Frequency Hopping Multiple Access for Digital Cellular Radiotelephone," IEEE Journal on Selected Areas in Communications, vol. SAC-2, no. 4 pp. 563–574, July 1984.

[4] Wallace, Mark S., "High Capacity Digital Cellular Communications Through Slow Frequency Hopping CDMA," Proc. 29th Annual Allerton Conference on Communication, Control, and Computing, pg. 21, 1991.

[5] Feller, William, "An Introduction to Probability Theory and Its Applications," vol. I, New York: John Wiley & Sons, 1968.

[6] Gilhousen, K. S., I. M. Jacobs, R. Padovani, A. J. Viterbi, L. A. Weaver, and C. E. Wheatley, "On The Capacity Of A Cellular CDMA System," IEEE Trans. Veh. Tech., vol. 40, no. 2, May 1991, pp. 303–312.

[7] Oppenheim, Alan V., Alan S. Willsky, Ian T. Young, "Signals and Systems," New Jersey: Prentice-Hall, Inc., 1983.

[8] Jakes, W. C. Jr., "Microwave Mobile Communications," New York: Wiley, 1974.

[9] Feller, William, "An Introduction to Probability Theory and Its Applications," vol. II, New York: John Wiley & Sons, 1971.

[10] Blahut, Richard E., "Theory and Practice of Error Control Codes," Reading, Mass.: Addison Wesley, 1984.

[11] Blahut, Richard E., "Principles and Practice of Information Theory," Reading, Mass.: Addison Wesley, 1990.

[12] Viterbi, Andrew J, "Spread Spectrum Communications – Myths and Realities," in IEEE Communications Magazine, May 1979, pp. 11–18.

[13] Carleial, Aydano, "Interference Channels," in IEEE Transactions on Information Theory,

Vol. IT-24, No. 1, January 1978, pp. 60–70.

[14] Bergmans, Patrick P., Thomas M. Cover, "Cooperative Broadcasting," in IEEE Transactions on Information Theory, Vol. IT-20, No. 3, May 1974, pp. 317–324.

[15] Franklin, Joel N., "Matrix Theory," New Jersey: Prentice-Hall, Inc., 1968.

[16] Gradshteyn, I. S., I. M. Ryzhik, "Table of Integrals Series and Products," Corrected and Enlarged Edition, California: Academic Press, Inc., 1980.

[17] Cover, T. M., "Some Advances In Broadcast Channels," in Advances in Communication Systems, vol. 4., New York: Academic Press, 1975, pp. 229–260.